

Technische Universität München
Max-Planck-Institut für Biochemie

Abteilung Strukturforschung
Biologische NMR-Arbeitsgruppe

Small molecule inhibitors of the p53-Mdm2 interaction

Arkadiusz Eugeniusz Sikora

Vollständiger Abdruck der von der Fakultät für Chemie der Technischen Universität München zur Erlangung des akademischen Grades eines

Doktors der Naturwissenschaften

genehmigten Dissertation.

Vorsitzender: Univ.-Prof. Dr. Steffen J. Glaser
Prüfer der Dissertation: 1. Univ.-Prof. Dr. Christian F. W. Becker
2. Priv.-Doz. Dr. Gerd Gemmecker

Die Dissertation wurde am 18.04.2011 bei der Technischen Universität München eingereicht und durch die Fakultät für Chemie am 14.06.2011 angenommen.

Acknowledgement

This PHD thesis was done in the Max Planck Institute for Biochemistry. I would like to thank everyone who contributed to this work.

I would like to thank my supervisor Dr. Tad A. Holak, for his support, discussions, patience and help with the experiments and to Prof. Dr. Christian Becker for being my Doktorvater.

Especially I would like to thank Tomasz Sitar for help with protein expression and purification, Grzegorz Popowicz for help with molecular docking, Michał Bišta for providing help with NMR and Siglinde Wolf for help with FP measurements. I would like to thank Anna Ducka, Weronika Janczyk, Marcelino Castro, Kaja Kowalska, Michał Grzejszczyk, Dr. Gerd Hübener and Sonja Golla for support and discussion.

Manuscripts submitted and under preparation:

Spiro[oxindole-3,4'-(4'*H*-pyran)] and 3,4-dihydropyrimidin-2(1H)-ones as the MDM2-p53 binding inhibitors. Arkadiusz E. Sikora, Siglinde Wolf, Weronika Janczyk, Kaja Kowalska, Tad A. Holak, Grzegorz M. Popowicz

Bioorganic & Medicinal Chemistry (2011) submitted.

The multicomponent synthesis of spiro[oxindole-3,4'-(4'*H*-pyrane)]s. Arkadiusz E. Sikora, Tad A. Holak, Alexander Dömling, Grzegorz M. Popowicz

Manuscript in preparation (2011).

Table of contents

Chapter 1. Introduction	1
1.1. p53	1
1.2. Mdm2	2
1.2.1. Structural domains of Mdm2 and their functions	2
1.2.2. Controlling the activity of MDM2 and p53	3
1.2.3. The structure of the p53 binding domain of Mdm2	3
1.3. The inhibitors of p53-Mdm2 interaction	4
1.3.1. Chalcones	4
1.3.2. Nutlins	5
1.3.3. 6-chloroindole-2-carboxylic acid	7
1.3.4. 1,4-benzodiazepine-2,5-diones	8
1.3.5. Chromenotriazolopyrimidines	12
1.3.6. Spiro(oxindole-33'-pyrrolidine)s	14
1.3.7. isoquinolinones	17
1.3.8. Terphenyls	18
1.3.9. Sulphonamides	19
Chapter 2. Goals of the study	20
Chapter 3. Materials and methods	21
3.1. Equipment	21
3.2. Columns	22
3.3. Stock solutions	23
3.4. Cell growth media	24
3.5. Buffers	24
3.5.1. Ion exchange and exclusion chromatography buffers	24
3.5.2. Buffers for immobilized metal-chelate chromatography under native conditions.	25
3.5.3. Buffers for immobilized metal-chelate chromatography Under native conditions	26
3.5.4. Buffer for DNA agarose gel electrophoresis	27
3.6. Reagents and buffers for SDS-Page	27
3.7. E. coli strains and plasmids	29
3.8. Enzymes and other proteins	30

3.9. Kits and reagents	30
3.10. Protein and nucleic acids markers	30
3.11. Substrates for chemical synthesis	31
3.11.1. 6-chloroisatin	31
3.11.2. Cyclopropylurea	34
3.11.3. 4-aminoimidazole	34
3.11.4. 6-chloroindole-3-aldehyde	35
3.11.5. 3-(dicyano)-methyloxindole	37
3.11.6. 4-chloroisatoic anhydride	38
3.11.7. Aliphatic cyanoacetamides	39
3.11.8. The synthesis of methoxyethyl acetoacetamide using 2,2,6-trimethyl-4H-1,3-dioxin-4-one.	39
3.11.8. The microwave synthesis of aromatic acetoacetamides	40
3.11.10. The synthesis of indole-3-carboxylic acid	41
3.12. Proteins	43
3.12.1. Mdm2 preparation and purification	43
3.12.2. The preparation and purification of the complex of Mdm2 and p53	44
3.13. Mdm2's ligands synthesis	46
3.13.1. Synthesis and purification of 3,4-dihydropyrimidin-2(1H)-ones	46
3.13.2. N-3 alkylation of 3,4-dihydropyrimidin-2(1H)-ones	47
3.13.3. Synthesis and purification of spiro[oxindole-3,4'-(4'H-pyran)] Compounds	48
3.13.4. The synthesis and purification of 2,3-dihydroquinazolin-4(1H)-ones and 7-chloro-2,3-dihydroquinazolin-4(1H)-ones	49
3.13.5. The synthesis and purification of 1'H-spiro[6-chloro-isoindole-1,2'- quinazoline]-3,4'(3'H)-diones	50
3.14. Laboratory procedures	51
3.14.1. Preparation of chemically competent cells	51
3.14.2. In silico screening	51
3.14.3. Ligand optimization	51
3.14.4. Fluorescence polarization measurements	52
3.14.4. NMR Measurements	52
3.14.5. Electrophoresis of DNA on agarose gel	52
3.14.6. Transformation of chemically competent cells	53

3.14.7. Sonication	53
3.14.8. Ni affinity chromatography	53
3.14.9. Electrophoresis in SDS polyacrylamide gel	54
3.14.10. Visualization of proteins on polyacrylamide gel	54
Chapter 4. Results and discussion	55
4.1. 3,4-dihydropyrimidin-2(1H)-ones and spiro[oxindole-3,4'-(4'Hpyran)] es	55
4.2. 2,3-dihydroquinazolin-4(1H)-ones	83
4.3. 1'H-spiro[6-chloro-isoindole-1,2'-quinazoline]-3,4'(3'H)-diones	93
Chapter 5. Summary	99
5.1. Summary	99
5.2. Zusammenfassung	101
6. Appendix	103
6.1. Abbreviations	103
6.2. Protein and peptide sequences	105
7. References	106

1.Introduction

1.1. p53

The tumor suppressor protein p53 is involved in many cellular mechanisms, like for example, cell cycle arrest, DNA repair, apoptosis, and aging (Lane 1992). In healthy cells it is maintained at low concentration (Oren 1999), which increases upon cellular stress. Increased concentration of p53 in nucleus can cause the arrest of cell cycle or apoptosis - both prevent proliferation of the cells with defective DNA (Vousden et al., 2002). These processes could prevent the cell from becoming cancerous.

Human p53 consists of 393 aminoacids. It has 5 functional domains (Figure 1).



Figure 1: Schematic organization of functional domains of the p53 protein.

The role of the C-terminal domain of p53 (aminoacids 356-393) is not yet well understood; though it is known that it is a place in which many posttranslational modifications can be made to regulate the protein activity (Joerger et al., 2008). p53 is active as a tetramer and its tetramerization is made through aminoacids 325-356 located near the C-terminus (Okorokov et al., 2006). In the center of the p53 sequence there is a DNA binding domain, which is able to bind specifically to certain DNA sequences (El-Deiry et al., 1992). At the N-terminus of the protein there is transactivation domain, which is a binding site for many proteins responsible for transcription (Lu et al., 1995, Lello et al., 2006, Thut et al., 1995, Gu et al., 1997, Teufel et al., 2007; Joerger et al., 2008, Kussie et al., 1996, Marine et al., 2004). This domain is natively unfolded, but upon binding to one of target proteins a part of it becomes locally ordered; for example, when binding to Mdm2 a short fragment (aminoacids 15-29) adopts a helical structure (Kussie et al., 1996). Between the transactivation domain and DNA binding domain there is a proline rich region which seems to be a linker between these two domains.

Many of human cancers have mutations or deletions in the p53 gene. Most of other cancer cells are capable to express active p53, though the p53 pathway is inactivated by overexpression of Mdm2 and Mdmx (Marine et al., 2004, Wade et al., 2010). Mdm2 and MdmX are structurally related and have similar functions.

1.2. Mdm2

1.2.1. Structural domains of Mdm2 and their functions

The human Mdm2 protein is made of 491 aminoacids, and contains several functional domains, which are shown in Figure 2.

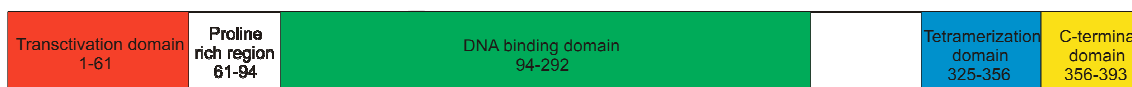


Figure 2: Schematic organization of the Mdm2 protein mapping its functional domains, nuclear localization, and nuclear export signals.

The N-terminal aminoacids 19-108 of Mdm2 bind the transactivation domain of p53 and disablins the transactivation activity of p53 (Joerger et al., 2008, Kussie et al., 1996). Mdm2 has nuclear localization and nuclear export signals (Juven-Gershon et al., 1999) followed by an acidic region (223-247), which contains several aspartic acid and glutamic acid residues, which can bind to the ribosomal L5 protein. Mdm2 has also a zinc finger motif (305-322) and the RING finger domain; the RING domain is able to sequence-specifically bind RNA (Elenbaas et al., 1996) and possesses the E3 ubiquitin ligase activity targeting p53 (Honda et al., 1997).

1.2.2. Controlling the activity of MDM2 and p53

Mdm2 regulates the p53 activity by binding to the p53 transactivation domain and thus blocks the interaction with transcription related proteins and makes p53 inactive (Oliner et al., 1993). Additionally, Mdm2 regulates transcription of the p53 gene (Thut et al., 1997). The Mdm2 protein has the ubiquitin ligase activity targeting p53 for proteosomal degradation and therefore decreases its concentration (Honda et al., 1997; Haupt et al., 1997, Kubbutat et al., 1997).

The transcription of Mdm2 gene is induced by p53 (Perry et al., 1993, Saucedo et al., 1998). Mdm2 protein is quickly cleared through ubiquitination and proteasome degradation (Chang et al., 1998).

1.2.3. The structure of the p53 binding domain of Mdm2

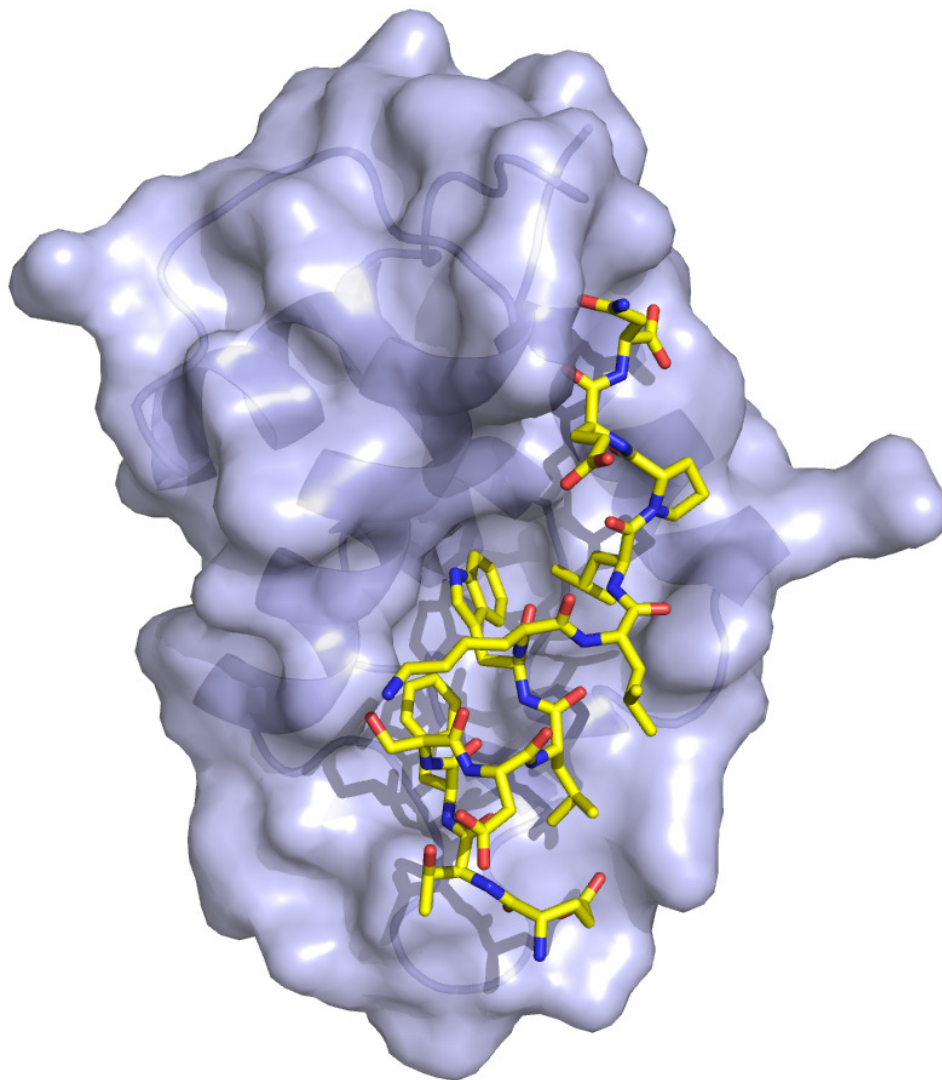


Figure 3: The structure of the complex of the p53 binding domain of Mdm2 with the short p53 peptide.

The crystallographic structure of the p53 binding domain of Mdm2 with a short peptide of the p53 transactivation domain has been solved by Kussie et al. (1996),

which provides detailed information about the interaction between these two proteins. The structure of the complex of Mdm2 construct consisting of aminoacids 17-125 and a peptide of 15-29 aminoacids of p53 is shown in Figure 3.

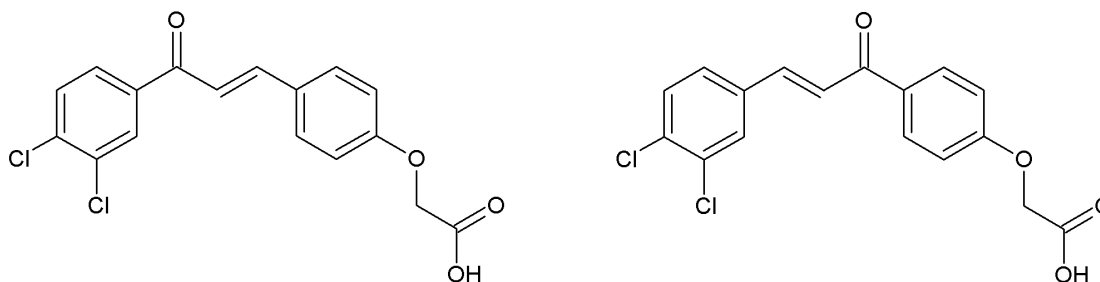
The X-ray structures of these complexes revealed a deep, hydrophobic cleft on the Mdm2's surface which is the place for the p53 binding. The p53 peptide forms an α -helix in most of its length. Three aminoacids of p53: Phe19, Trp23, and Leu26 are crucial for the Mdm2-p53 interaction. Trp23 occupies the deepest part of the binding pocket in Mdm2, its indole group forms a hydrogen bond with the Leu54 carbonyl of Mdm2 and makes hydrophobic interactions inside the Mdm2 protein. The p53 peptide binds to the Mdm2 protein with 450 nM the affinity (Kussie et al., 1996).

Mdm2 was found to be overexpressed in many human cancers (Oliner et al., 1992, Cordon-Cardo et al., 1994, Zhou et al., 2000). Inhibiting the p53 binding to Mdm2 could rescue the active p53 and restore the p53 pathway. The structure shown in Figure 3 suggests that a small organic molecule could possibly mimic the three p53 residues and compete for the Mdm2 binding with p53. The p53 binding cleft of Mdm2 is asymmetric, so whenever the inhibitor is provided as a racemic mixture only one stereoisomer is expected to bind effectively. The presence of the indole group in the deepest region of the p53 binding pocket of Mdm2 suggests designing the small molecules that possess the indole or spiroindole groups in their structures.

1.3. The inhibitors of p53-Mdm2 interaction

1.3.1. Chalcones

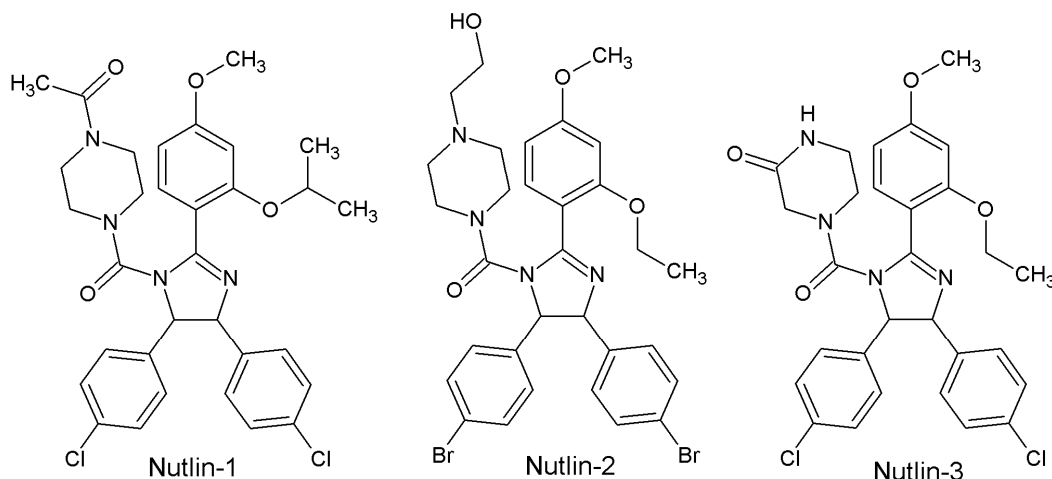
The first inhibitors of the Mdm2-p53 interaction were chalcones (Scheme 1) (Stoll et al., 2001). They bound to the Mdm2 binding pocket, though the binding was weak – the strongest of them had $IC_{50}=49 \mu\text{M}$, and the attempt to improve them led to the increased toxicity through inhibition of other enzymes (Kumar et al., 2003).



Scheme 1: Examples of chalcones capable to interact with Mdm2.

1.3.2. Nutlins.

The first compounds capable of disrupting the Mdm2-p53 interaction *in vivo* were *cis*-imidazolines called nutlins (Scheme 2) (Vassilev et al., 2004). These compounds bind to Mdm2 with IC_{50} between 100 and 300 nM. They were synthesized in multistep reaction as racemats and the enantiomers were separated on chiral columns. There were significant differences in the activities between enantiomers, for Nutlin-3 the difference was 150 times.



Scheme 2: Nutlins.

Nutlin-2 was co-crystallized with Mdm2 and the structure of the complex was determined (Figure 4). Nutlin-2 binds to the p-53 binding pocket of Mdm2 utilizing many hydrophobic interactions. One bromophenyl group is placed inside the Trp23 binding pocket, another bromophenyl moiety is in the Leu26 pocket and the ethyl ether group is in the Phe19 binding pocket.

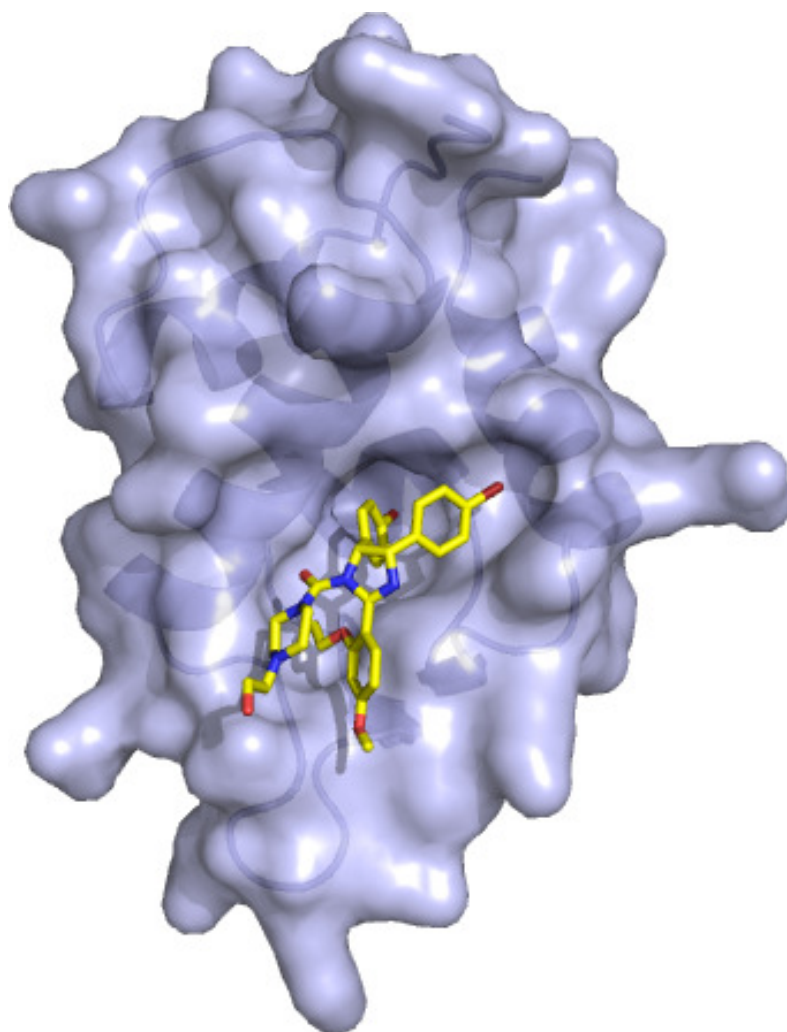
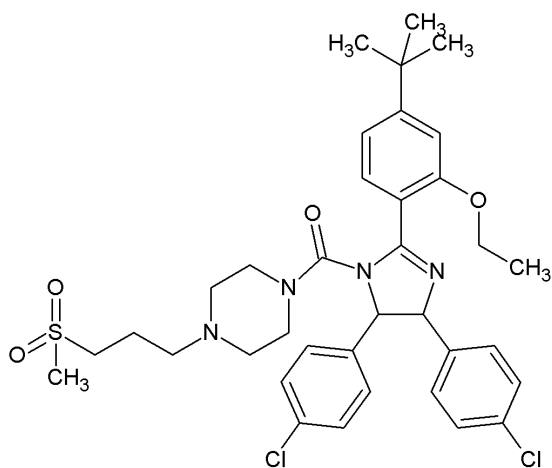


Figure 4: The crystal structure of the complex of Mdm2 with Nutlin-2.

Nutlins were subjected to cell lines experiments, and it was found out that Nutlins indeed stimulated the accumulation of p53. They caused cell cycle arrest or apoptosis in human cancer cell lines with functional p53, and were inactive in cell lines with mutated p53. Nutlin-3 was tested on mice resulting in tumor growth suppression in 90% of cases.

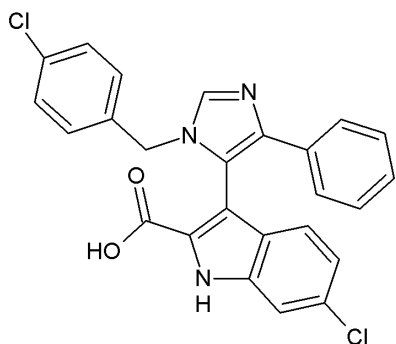
Following the success with Nutlins, Roche optimized them in order to improve the activity in vivo (Kong et al., 2003, Ding et al., 2007, Fotouhi et al., 2007, Kong et al., Kong et al., 2003). One of the compounds from this optimization, called RG7112 (Scheme 3), went to the phase I clinical trials.



Scheme 3: RG7112.

1.3.3. 6-chloroindole-2-carboxylic acid

The Novartis company (Boettcher et al., 2008) and Doemling et al. (Popowicz et al., 2010) independently developed the Mdm2-p53 binding inhibitors, like the one in Scheme 4, which have a 6-chloroindole-2-carboxylic acid or its amide bound to imidazole.



Scheme 4: 6-chloro-3-[1-(4-chlorobenzyl)-4-phenyl-imidazol-5-yl]-indole-2-carboxylic acid.

The crystal structure of the complex of the compound in Scheme 4 with Mdm2 (Figure 5) confirms the expectation that the 6-chloroindole moiety mimics the Trp23 residue from p53 and fills its binding pocket, the chlorine is situated in the deep part of the p53 binding pocket of Mdm2, which is not used while interacting with p53.

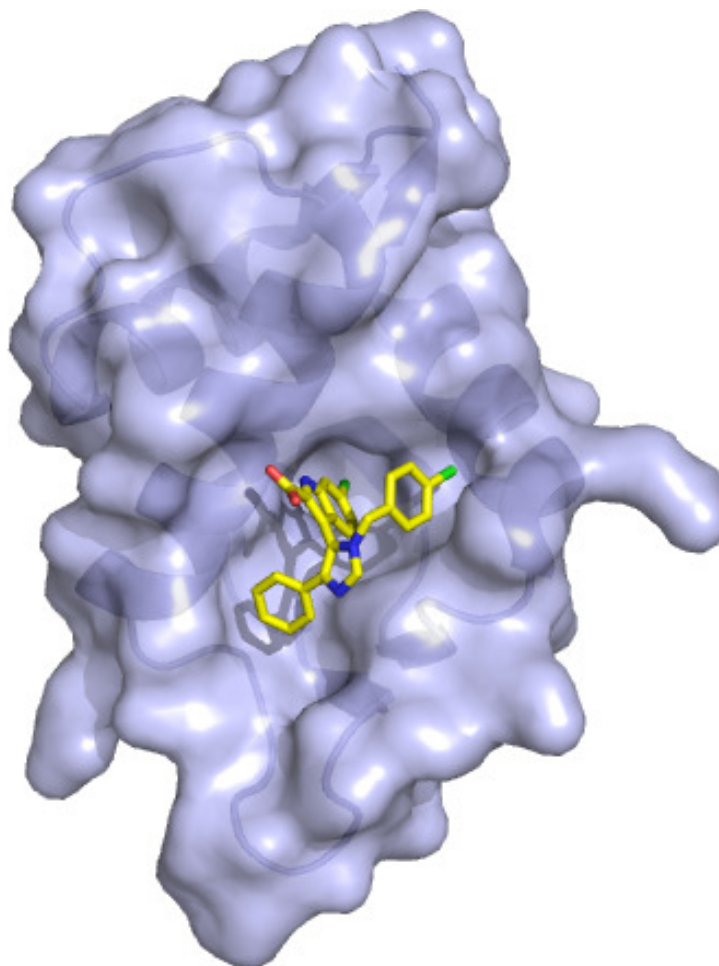
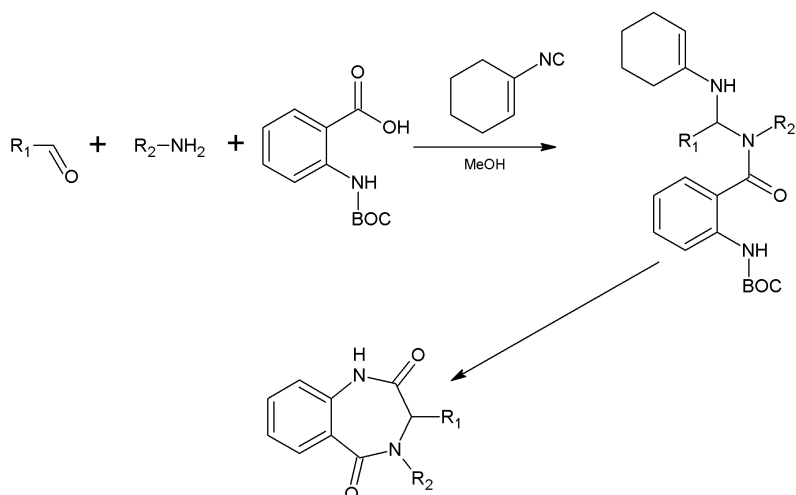


Figure 5: The crystal structure of the complex between compound from Scheme 4 with Mdm2.

1.3.4. 1,4-benzodiazepine-2,5-diones

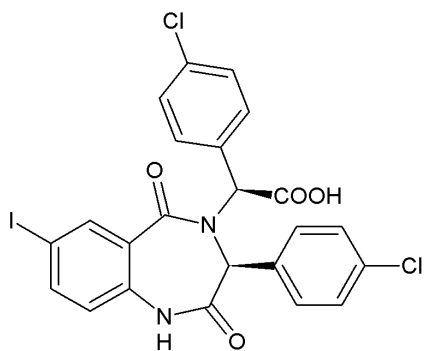
The Jonson & Jonson company developed the inhibitors of the p53-Mdm2 binding based on the 1,4-benzodiazepine-2,5-dione scaffold as small molecule compounds mimicking the Phe19, Trp23 and Leu26 residues of the p53 peptide (Cummings et al., 2006). They were discovered by screening of compounds library using the ThermoFluor technology, in which the melting temperature of a protein is measured in the presence of the compound and compared with a control sample. The hits were identified as the samples in which the protein's melting temperature is 3 times higher than the standard deviation (Parks et al., 2005). The hits obtained by the ThermoFluor technology were confirmed by the fluorescence polarization assay.

The compounds were optimized to improve the binding to Mdm2. The sets of compounds were synthesized using the condensation reaction followed by cyclization (Scheme 5).



Scheme 5: The synthesis of 1,4-benzodiazepine-2,5-diones.

In each set of the compounds one of the moieties was altered while the rest of the compound's structure remained unchanged. Synthesized compounds were then subjected to the Thermofluor and Fluorescence polarization assays. The result of this optimization was compound TDP222669 shown in Scheme 6 (Raboisson et al., 2005).



Scheme 6: 1,4-benzodiazepine-2,5-dione (TDP222669).

The co-crystal of the compound above bound to Mdm2 was solved (Grassberger et al., 2005) and it showed that the predictions of its binding with Mdm2 were correct and the compound occupies the same binding place as the p53 peptide.

The chlorophenyl moieties reside in the Trp23 and Leu26 binding pockets and iodobenzene goes to the Phe19 binding pocket.

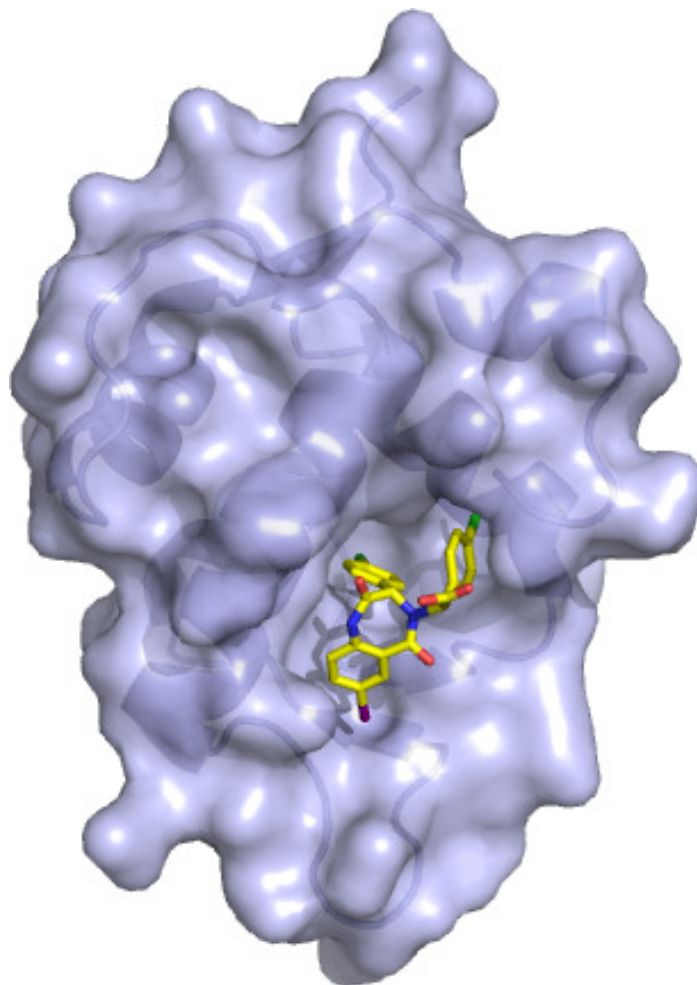
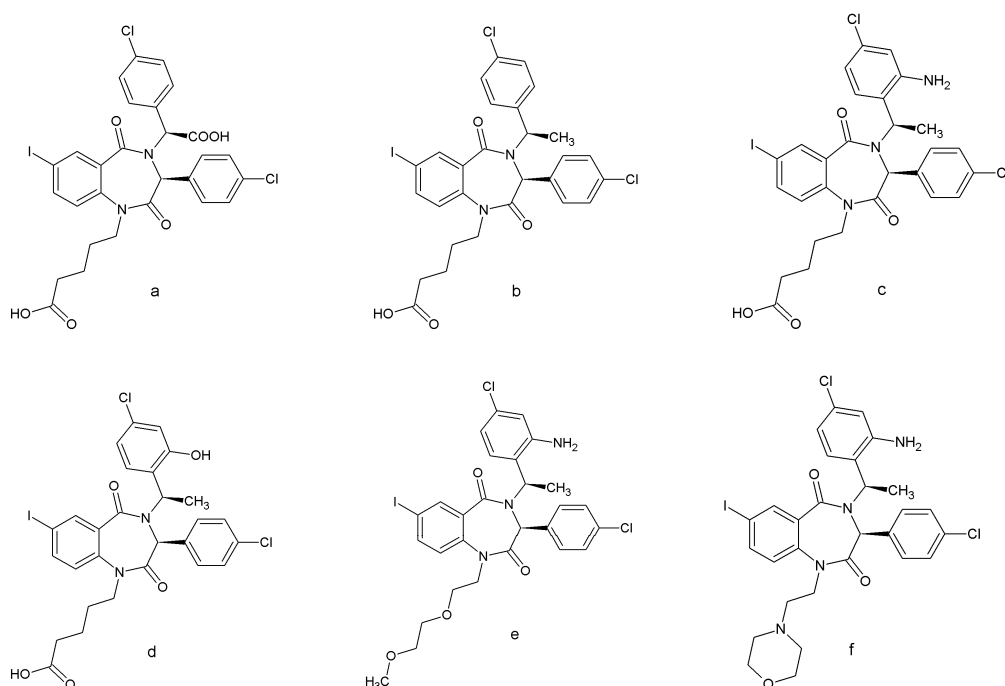


Figure 6: The crystal structure of 1,4-benzodiazepine-2,5-dione shown in Scheme 6 co-crystallized with the Mdm2 protein.

Compound TDP222669 was tested in cell lines. In the cells expressing wild type p53 the decrease of proliferation was observed at $IC_{50} = 30 \mu\text{M}$. The cells which did not express the active p53 were insensitive to the compound (Grassberger et al., 2005).

Tested in vivo, the compound shown poor bioavailability and rapid clearance, its solubility was low and it did not pass the cell membranes well, most probably because of the carboxyl group ionization (Parks et al., 2006), thus detailed

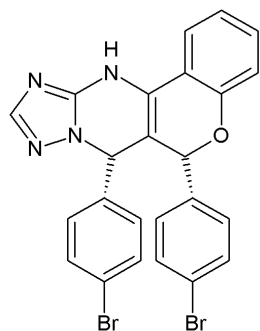
optimization was carried out. Neither amidation nor esterification of the carboxyl group improved cell membrane permeability, and often caused significant loss of potency, finally the carboxylic group was replaced with methyl (Scheme 7b). Attempts to replace iodide with ethyl or chloride of the phenyl group with larger, hydrophobic trifluoromethyl did not lead to any improvement of the compound properties (Parks et al., 2006). Introducing the *o*-amino (Scheme 7c) or *o*-hydroxy (Scheme 7d) group in the benzylic moiety added the extra hydrogen bond between the compound and Val93 of Mdm2, which increased the compound's potency. Alkylation of the N1 nitrogen with solubilizing groups was investigated (Parks et al., 2006, Leonard et al., 2006), valeric acid (Scheme 7a) improved activity in cell lines. Replacing valeric acid with methoxyethoxyethyl (Scheme 7e) decreased the binding in FP assay, but led to better penetration of the cell and increased activity in the cells. N1 alkylation with morpholino moieties with short linkers (Scheme 7f) further increased the potency of the compound, while N-methylpiperazine or dimethylamine moieties caused significant drop in potency (Leonard et al., 2006).



Scheme 7: The optimization of 1,4-benzodiazepine-2,5-diones.

1.3.5. Chromenotriazolopyrimidines

A HTRF high throughput screen of 1 400 000 compounds showed that chromenotriazolopyrimidines interact with Mdm2 (Allen et al., 2009). The synthesis of the compounds includes 4 steps and gives racemic mixtures. Diastereoisomers of the compound in Scheme 8 were separated via chiral chromatography and their configuration was determined using circular dichroism. All diastereoisomers were tested for interaction with Mdm2. Only syn-(6R,7S) compound was active ($IC_{50} = 1.23 \mu\text{M} \pm 0.82 \mu\text{M}$). The diastereoisomers are unstable and when kept in dimethylsulfoxide at room temperature formed mixtures consisting mostly anti stereoisomers, which are more stable. It was found that the N11-methylation prevents racemization of the compounds.



Scheme 8: The active diastereoisomer of chromenotriazolopyrimidine.

The compound was co-crystallized with Mdm2, the structure is shown in Figure 4. The C6 bromophenyl is located in the Trp23 binding pocket, the C6 bromophenyl occupies the Leu26 binding site and the benzene ring of chromenotriazolopyrimidine resides in the Phe19 binding pocket.

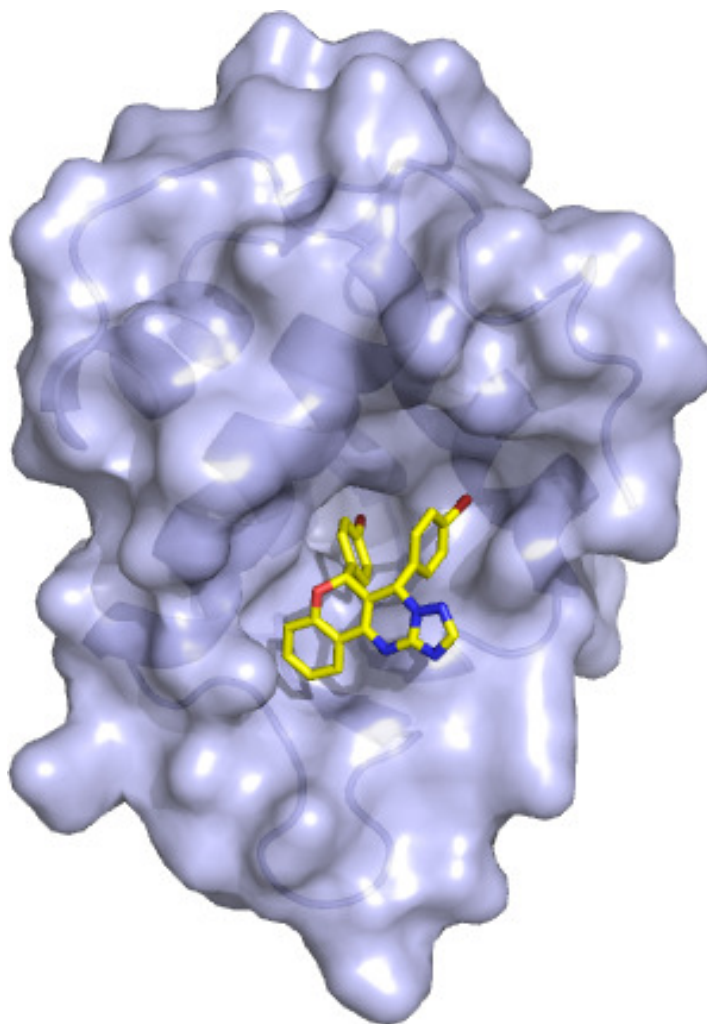
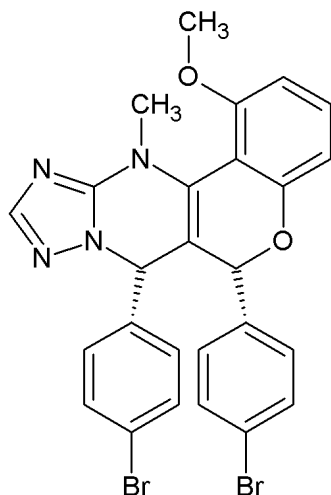


Figure 7: The crystal structure of chromenotriazolopyrimidine (shown in Scheme 8) bound to Mdm2 protein.

The chromenotriazolopyrimidine was optimized to improve its activity. In the optimization racemic mixtures of compounds were used. Changing bromine to chloride in the phenyl ring resulted in better binding to Mdm2 ($IC_{50} = 0.89 \mu\text{M} \pm 0.20 \mu\text{M}$), probing nitrile and ethyl substituents gave the compounds with similar activity as the starting one, fluorine and big substituents diminished the activity. The substitution of chromenotriazolopyrimidine's benzene ring was checked in order to improve the binding in the Phe19 binding pocket. The binding increased after adding methoxy group at position C1 ($IC_{50} = 0.30 \mu\text{M} \pm 0.06 \mu\text{M}$), or methyl at C2 ($IC_{50} = 0.44 \mu\text{M} \pm 0.08 \mu\text{M}$); however, combining these modification decreased potency of the

compound. The compound with methyl at C2 and fluorine at C3 had $IC_{50} = 0.44 \mu\text{M} \pm 0.02 \mu\text{M}$. The syn-(6R, 7S) isomers of the best compounds were tested. The best of the compounds (Scheme 9) had $IC_{50} = 0.20 \mu\text{M} \pm 0.011 \mu\text{M}$.



Scheme 9: The most active chromenotriazolopyrimidine.

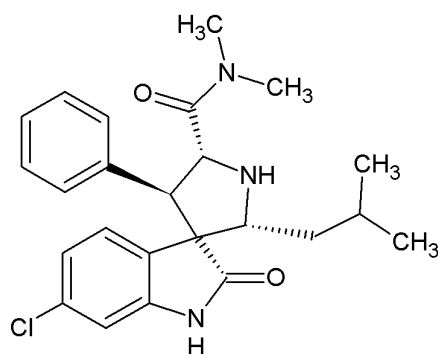
In cancer cell lines the chromenotriazolopyrimidine shown above caused apoptosis, due to the p53 activation.

1.3.6. Spiro(oxindole-3,3'-pyrrolidine)s.

As the Trp23 sidechain of p53 is the most buried in the p53 binding cavity of Mdm2, it seems to be the most crucial element for the p53-Mdm2 interaction. The spirooxindole scaffold was found to perfectly mimic the tryptophan sidechain in the interaction with Mdm2. It forms a hydrogen bond with the carbonyl group of Mdm2 and has a hydrophobic interaction with the binding pocket. Several spirooxindoles were docked to Mdm2 to find the core scaffold, which could be used as a starting point in the design of the inhibitor of the Mdm2-p53 interaction (Ding et al., 2005). The spiro(oxindole-3,3'-pyrrolidine) core was found to be the best, because it provided a rigid scaffold from which the substituents can be projected into the Phe19 and Leu26 binding pockets.

A library of spiro(oxindole-3,3'-pyrrolidine)s with different substituents was designed and docked to Mdm2 resulting in a compound which well fits the p53-binding cavity of Mdm2.

Adding the 6-chloro substituent to spiroxindole helped to fill the small space located deeply in the protein, which is not used by the Trp23 of p53. The designed compound is shown in Scheme 10 (Ding et al., 2005) and its interaction with Mdm2 was tested via fluorescence polarization assay giving the $K_i = 8.46 \mu\text{M}$.



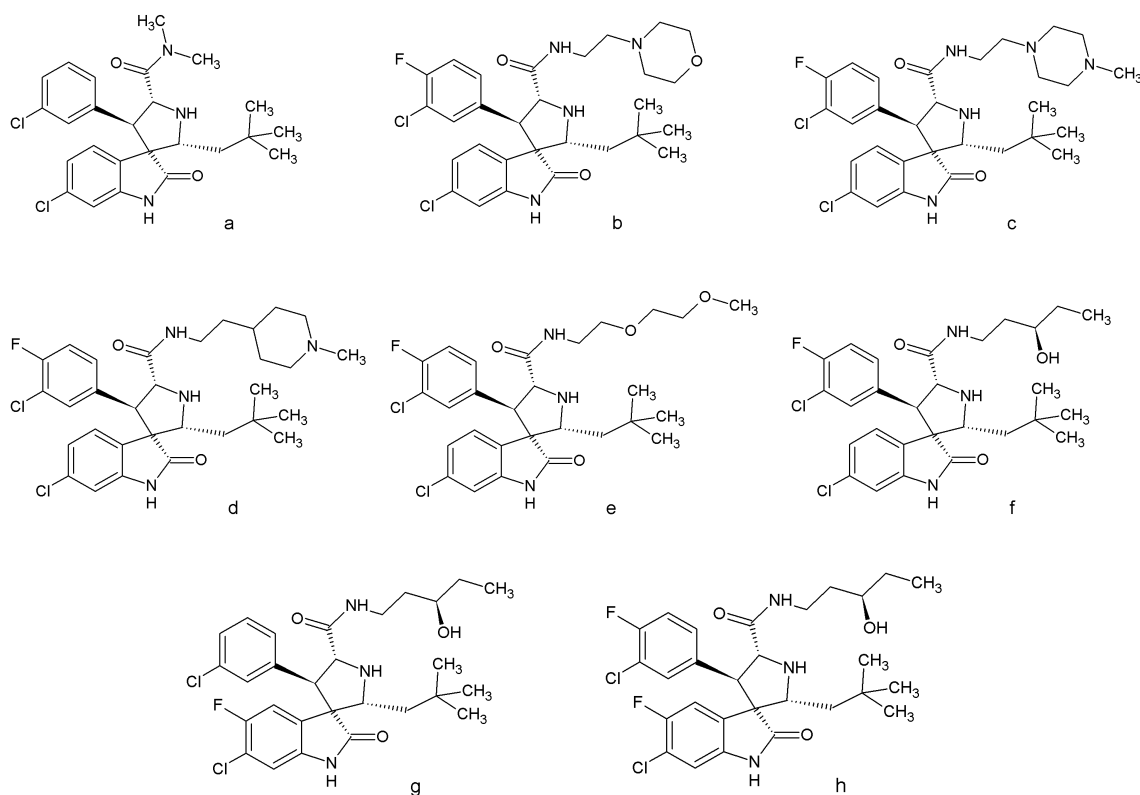
Scheme 10: Spiro(oxindole-3,3'-pyrrolidine) able to interact with the Mdm2 protein.

The compound was optimized by adding a *m*-chloro substituent in the phenyl ring and changing iso-propyl into a larger iso-buthyl group. As these modifications caused the compound better filled the binding cavity of Mdm2, the binding should also improve ($K_i = 300 \text{ nM}$). Despite of this improvement the iso-buthyl group was not optimal and it was replaced with 2,2-dimethylpropyl group (Scheme 11a). That compound had $K_i = 86 \text{ nM}$ (Ding et al., 2005).

The compounds were found to decrease cancer cell growth for the cell line with wild type p53, but they were ineffective on the cell lines with deleted p53, which confirmed that the growth inhibition was caused by activation of the p53 pathway. The compound shown in Scheme 10 had $IC_{50} = 9.7 \mu\text{M}$ and the optimized compound shown in Scheme 11a had $IC_{50} = 1.9 \mu\text{M}$. The compounds were also tested for toxicity against the healthy cells and they were much less toxic to them than to cancer cells (Ding et al., 2005).

The researchers noticed that the Mdm2 binding peptides utilize the Leu22 binding pocket which was not exploited by the small organic molecule inhibitors. The Leu22 binding pocket is shallow and exposed to water, so more hydrophilic moiety is

needed to mimic this aminoacid sidechain, which would additionally improve the compounds solubility (Ding et al., 2006). The 2-morpholinyl-4-yl-ethylamine group was introduced (Scheme 11b). According to the docking such a moiety fills the Leu22 binding pocket and additionally forms the electrostatic interaction with Lys90 of Mdm2, which interacts with Glu17 of p53. The compound was synthesized and tested via fluorescence polarization assay ($K_i = 13\text{nM}$). For further improvement of this compound, the fluorine was introduced to the m-chlorophenyl ring, this modification raised K_i value twice. The compound shown in Scheme 11b inhibited the cancer cell growth with $\text{IC}_{50} = 800\text{ nM}$.



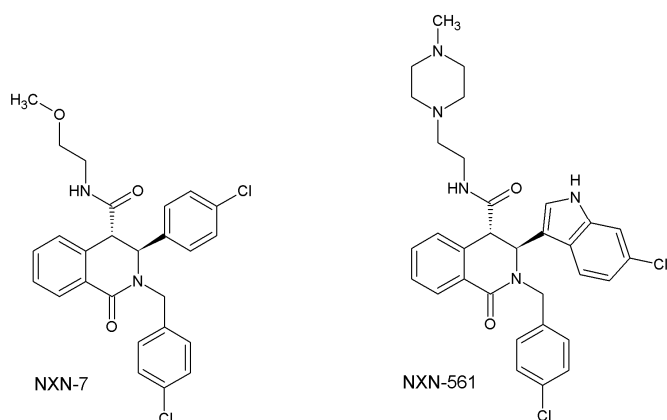
Scheme 11: Optimization of the spiro(oxindole-3,3'-pyrrolidine) scaffold.

The compounds were further optimized for better oral availability: The researchers synthesized the compounds which had different groups than 2-morpholinyl-4-yl-ethylamine and tested the interaction in the Mdm2 binding assay and their influence on the cell lines growth (Yu et al., 2009). The compound MI-126, with methylpiperazyl group (Scheme 11c) had $K_i = 1.5\text{ nM}$, and MI-122 - with

methyloperidiyl (Scheme 11d) - $K_i = 2.0$ nM. Both of them inhibited the growth of cancer cells with the wild type p53 and shown good selectivity over the cells without the functional p53. However, compounds MI-126 and MI-122 are protonated at physiological conditions and it was necessary to design a compound which would stay neutral. The compounds MI-142 (Scheme 11e) and MI-147 (Scheme 11f) were synthesized. They were also very potent in the MDM2 binding assay MI-142 had $K_i = 0.8$ nM while MI-147 had $K_i = 0.6$ nM, furthermore they were very selective in cell lines; MI-147 inhibited the growth of the cells with wild type p53 91 times better than the growth of the cells with the deleted p53. The compound MI-142 had better pharmacokinetic profile and the fluoride substitution was investigated revealing that that the 4-fluoro substituent in the spiroindole ring (Scheme 11g,f) caused the loss of potency, but the improvement of pharmacokinetic profile. Further modification of the butanediol sidechain and chiral carbons configuration did not lead to any improvement of the compound. The compounds MI-147, MI-219 (Scheme 11g), and MI-319 (Scheme 11f) were tested on mice, both inhibited tumor growth.

1.3.7. Isoquinolinones

Isoquinolinones were discovered using the in-silico screening, and tested with the NMR-based binary titration and the AIDA-NMR assay (Rothweiler et al., 2008). The strongest of these compounds, named NXN-7 (Scheme 7), showed the $K_D = 5$ μ M in the NMR binary titration and $K_D = 2$ μ M in the AIDA-NMR assay. In cells lines NXN-7 decreased proliferation of the cancer cells expressing the wild type p53, and with an $IC_{50} = 27.1$ μ M, it caused some antiproliferative effects in the cells which did not expressed the wild type p53, but with $IC_{50} = 62.5$ μ M. The compound caused apoptosis of the cancer cells expressing the wild type p53 when applied at concentration of 40 μ M.

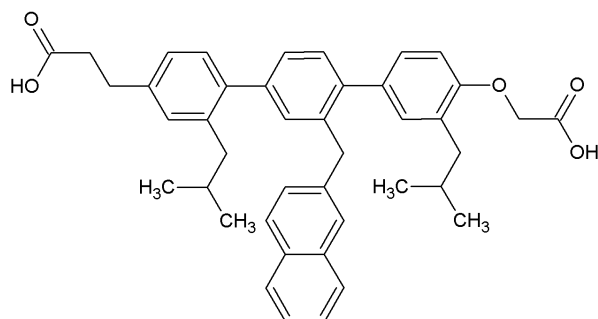


Scheme 12: NXN 7 and NXN-561.

NXN-7 had been optimized in order to increase the solubility and activity in the cells, resulting in compound NXN-561 (Figure 7). This compound shown better activity in the cells.

1.3.8. Terphenyls

The terphenyl scaffold was used to design the substances mimicking the α -helix and hydrophobic residues of p53 and thus interact with Mdm2. The designed compounds were synthesized and tested (Chen et al., 2005). They bound to Mdm2 ($IC_{50} = 10$ to $20 \mu\text{M}$) and stimulated p53 accumulation in cancer cells. The investigation of the structure-activity relationship revealed that the active compounds possessed a hydrophobic substituents at 2, 2', 6' 2'' positions of the phenyls, and the 1-carboxy group was necessary for p53 accumulation in cancer cells.

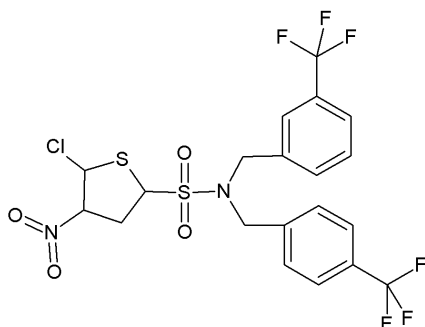


Scheme 13: The best terphenyl Mdm2-p53 inhibitor.

The compounds were optimized to improve their Mdm2 affinity (Yin et al., 2005). It was found that the compound shown in Scheme 13 with isobuthyls at 2 and 2'' and β -methyl-naphatalene at 2' was the most potent, it gave $K_i = 182$ nM in the fluorescence polarization assay.

1.3.9. Sulphonamides.

A common pharmacophore of sulphonamide was used to design the Mdm2 binding molecules (Galatin et al., 2004). The researchers from the Cyclacel company investigated the Mdm2 binding sulphonamides (Wang et al., 4004). The best of their sulphinamide compounds had $IC_{50} = 3.5$ μ M (Scheme 14). The compounds, however, did not have good selectivity between the cells expressing the wild type p53 and the cells without the functional p53.



Scheme 14: Mdm2 binding sulphonamide.

2. Goals of the study.

In many human cancers the tumor suppressor protein p53 retains its native structure and could potentially inhibit tumor growth, though it is inactivated through the binding to Mdm2 and Mdmx proteins. Small molecular weight organic molecules capable to disrupt the complex of p53 with these proteins would release the active wild type p53, which would prevent the cancer cells form uncontrolled proliferation.

The goal of this work was to develop novel, small molecule inhibitors of the interaction between p53 and Mdm2/x proteins. The p53 binding pocket of Mdm2 was chosen as a target for the designed molecules. The basic scaffolds of the molecules were identified by the computer based approach and the hits were tested, and if successful, further optimization was undertaken.

3. Materials and methods

3.1. Equipment

Integral 100Q Multidimensional Biospecific HPLC System	PerSeptive Biosystems
HPLC Pump 2248	Pharmacia
VWM 2141 HPLC Flow detector	Pharmacia
High pressure mixer	Pharmacia
REC 102 recorder	Pharmacia
ÄKTA explorer 10	Amersham Pharmacia
Peristaltic pump P-1	Amersham Pharmacia
Fraction collector RediFrac	Amersham Pharmacia
Recorder REC-1	Amersham Pharmacia
UV flow through detector UV-1	Amersham Pharmacia
BioLogic LP System	Biorad
Hei-VAP Value rotary evaporator	Heidolph
Two step rotary vacuum pump	Edwards
2110 Fraction collector	Biorad
J2-21M Centrifuge	Beckman
Avanti J-30I Centrifuge	Beckman
j-6ME Centrifuge	Beckman
5804 R Centrifuge	Eppendorf
5415 R Centrifuge	Eppendorf
3k15 Centrifuge	Sigma

3.2. Columns

250/10mm 5 μ HyPurity Advance	Hypersil
VP 250/21 NUCLEODUR C18 ec	Macherey-Nagel
Phusion-RP 80-A	Phenomenex
Source 5RPC ST4,6/150	Pharmacia
Supelcosil LC-18	Supelco
HiLoad 26/60 Superdex S75pg	Amersham Pharmacia
HiLoad 16/60 Superdex S75pg	Amersham Pharmacia
HiLoad 16/60 Superdex S200pg	Amersham Pharmacia
HiLoad 10/300 Superdex S75pg	Amersham Pharmacia
HiLoad 10/300 Superdex S200pg	Amersham Pharmacia
Mono Q HR 5/5, 10/10	Amersham Pharmacia
Mono S HR 5/5, 10/10	Amersham Pharmacia
NiNTA-agarose	Qiagen
ProBond Resin	Invitrogen
NTA Superflow	Qiagen
Glutathione Sepharose 4 Fast Flow	GE Healthcare
Octadecyl-Si100	Serva
μ Bondpack Phenyl	Waters

3.3. Stock solutions

Ampicillin: 100 mg/ml of ampicillin dissolved in H₂O, sterilized by filtration, stored in aliquots at -20°C until used. Working concentration: 150 µg/ml.

Chloramphenicol: 34 mg/ml dissolved in ethanol (0.34 g/10 ml). Working concentration: 34 µg/ml.

Streptomycin: 60 mg/ml of streptomycin dissolved in H₂O, sterile filtered and stored in aliquots at -20°C until usage. Working concentration 60 µg/ml.

Kanamycin: 100 mg/ml of kanamycin dissolved in H₂O, sterile filtrated and stored in aliquots at -20°C until used. Working concentration: 100 µg/ml.

IPTG: A sterile filtered 1 M stock of IPTG in dissolved distilled water was prepared and stored in aliquots at -20°C until used.

Glucose: 20% solution in H₂O, autoclaved.

Thiamin: 1% solution in H₂O, sterilized by filtration.

MgSO₄: 1 M solution in H₂O, sterilized by filtration.

Zn-EDTA solution: 5 mg/ml EDTA

8.4 mg/ml Zn(CH₃COO)₂

Trace elements solution:

2.5 g/l H₃BO₃

2.0 g/l CoCl₂ x H₂O

1.13 g/l CuCl₂ x H₂O

9.8 g/l MnCl₂ x 2H₂O

2.0 g/l Na₂MoO₄ x 2H₂O

pH lowered with citric acid or HCl.

3.4. Cell growth media

LB medium:	10 g/l tryptone
	5 g/l yeast extract
	10 g/l NaCl

pH was adjusted to 7.0. For the preparation of agar plates the medium was supplemented with 15 g agar.

Minimal medium (MM) for uniform enrichment with ^{15}N :

0.5 g/l NaCl
1.3 ml/l trace elements solution
1 g/l citric acid monohydrate
36 mg/l ferrous citrate
4.02 g/l KH_2PO_4
7.82 g/l $\text{K}_2\text{HPO}_4 \times 3\text{H}_2\text{O}$
1 ml/l Zn-EDTA solution
1 g/l NH_4Cl or $^{15}\text{NH}_4\text{Cl}$

pH was adjusted to 7.0 with NaOH, the mixture was autoclaved, upon cooling separately sterilized solutions were added: 25 ml/l glucose, 560 $\mu\text{l/l}$ thiamin, antibiotics, 2 ml/l MgSO_4 stock.

3.5. Buffers

3.5.1 Ion exchange and exclusion chromatography buffers

Buffer P(0)	8 mM KH_2PO_4
	6 mM Na_2HPO_4
	0.05% NaN_3

	pH 7.2
Buffer P(1000)	8 mM KH_2PO_4
	16 mM Na_2HPO_4
	1 M NaCl
	0.05% NaN_3
	pH 7.2
PBS	140 mM NaCl
	2.7 mM KCl
	10 mM Na_2HPO_4
	1.8 mM KH_2PO_4
	0.05% NaN_3
	pH 7.3

3.5.2. Buffers for immobilized metal-chelate chromatography under native conditions

Binding buffer	50 mM NaH_2PO_4
	300 mM NaCl
	10 mM imidazole
	pH 8.0
Wash buffer	50 mM NaH_2PO_4
	300 mM NaCl
	20 mM imidazole
	pH 8.0

Elution buffer	50 mM NaH_2PO_4
	300 mM NaCl
	250 mM imidazole
	pH 8.0

3.5.3. Buffers for immobilized metal-chelate chromatography under native conditions

Biding buffer	6 M guanidinium chloride
	100 mM $\text{NaH}_2\text{PO}_4 \times \text{H}_2\text{O}$
	10 mM Tris
	10 mM β -mercaptoethanol
	pH 8.0

Wash buffer	6 M guanidinium chloride
	100 mM $\text{NaH}_2\text{PO}_4 \times \text{H}_2\text{O}$
	10 mM Tris
	10 mM β -mercaptoethanol
	pH 6.5

Elution buffer	6 M guanidinium chloride
	100 mM $\text{CH}_3\text{COONa} \times 3\text{H}_2\text{O}$
	10 mM β -mercaptoethanol
	pH 4.0

Dialysis buffer	6 M guanidinium chloride
------------------------	--------------------------

	pH 3.0
Refolding buffer	200 mM arginine HCl
	1 mM EDTA
	100 mM Tris
	2 mM reduced GSH
	2 mM oxidized GSH
	10% glycerol
	0.05% NaN ₃
	pH 8.4

3.5.4. Buffer for DNA agarose gel electrophoresis

50X TAE buffer

40 mM Tris-acetate	242 g/l of Tris base
1 mM EDTA	100 ml/l of 0.5 M EDTA (pH 8.0)
acetic acid	57.1 ml/l

2.5.5 Dyes for DNA electrophoresis

6x DNA Loading Dye	Fermentas
SYBR ® Safe DNA gel stain	Invitrogen

3.6. Reagents and buffers for the SDS-PAGE

Anode buffer	200 mM Tris pH 8.9
Cathode buffer	100 mM Tris pH 8.25
	100 mM tricine
	0.1% SDS

Separation buffer	1 M Tris pH 8.8 0.3% SDS
Stacking buffer	1 M Tris pH 6.8 0.3% SDS
Separation acrylamide	48% acrylamide 1.5% bis-acrylamide
Stacking acrylamide	30% acrylamide 0.8% bis-acrylamide
Separation gel	1.675 ml H ₂ O 2.5 ml separation buffer 2.5 ml separation acrylamide 0.8 ml glycerol 25 µl 10% (NH ₄) ₂ S ₂ O ₈ 2.5 µl TEMED
Intermediate gel	1.725 ml H ₂ O 1.25 ml separation buffer 0.75 ml separation acrylamide 12.5 µl 10% (NH ₄) ₂ S ₂ O ₈ 1.25 µl TEMED
Stacking gel	2.575 ml H ₂ O 0.475 ml stacking buffer 0.625 ml stacking acrylamide 12.5 µl 0.5 M EDTA, pH 8.0

37.5 μ l 10% $(\text{NH}_4)_2\text{S}_2\text{O}_8$

1.9 μ l TEMED

Protein visualization

Coomassie-blue solution

45% ethanol

10% acetic acid

1% Coomassie Brilliant Blue R

Destaining solution

5% ethanol

10% acetic acid

5x protein loading dye:

0.225 M Tris-HCl, pH 6.8

50% glycerol

5% SDS

0.05% bromophenol blue

0.25 M DTT

3.7. E. coli strains and plasmids

Cloning strains

One Shot TOP10

Invitrogen

GigaSingles

Novagen

Protein expression strains

BL21 Star

Invitrogen

BL21 Star(DE3)

Invitrogen

Plasmids

pET 41 Ek/LIC	Novagen
pET 46 Ek/LIC	Novagen

3.8. Enzymes and other proteins

Pfu DNA Polymerase	Fermentas
Phusion HF DNA Polymerase	BioCat
Enterokinase	Novagen
Anti His antibodies (mouse)	Santa Cruz biotech
Goat anti mouse antibodies	Santa Cruz biotech

3.9. Kits and reagents

QIAquick PCR Purification Kit	Qiagen
QIAprep Spin Miniprep Kit	Qiagen
Pre-Crystallization Test (PCT)	Hampton Research
Rapid Ligation Kit	Roche
Complete Protease Inhibitor Cocktail	Roche
pET LIC cloning Kits	Novagen

3.10. Protein and nucleic acids markers

Page Ruler™ Prestained Protein Ladder	Fermentas
Spectra Multicolor™	Fermentas
Precision Plus Protein Kaleidoscope	BioRad

Gene Ruler™ DNA Ladder	Fermentas
100 BP DNA marker	New England BioLabs
1Kb DNA marker	New England BioLabs

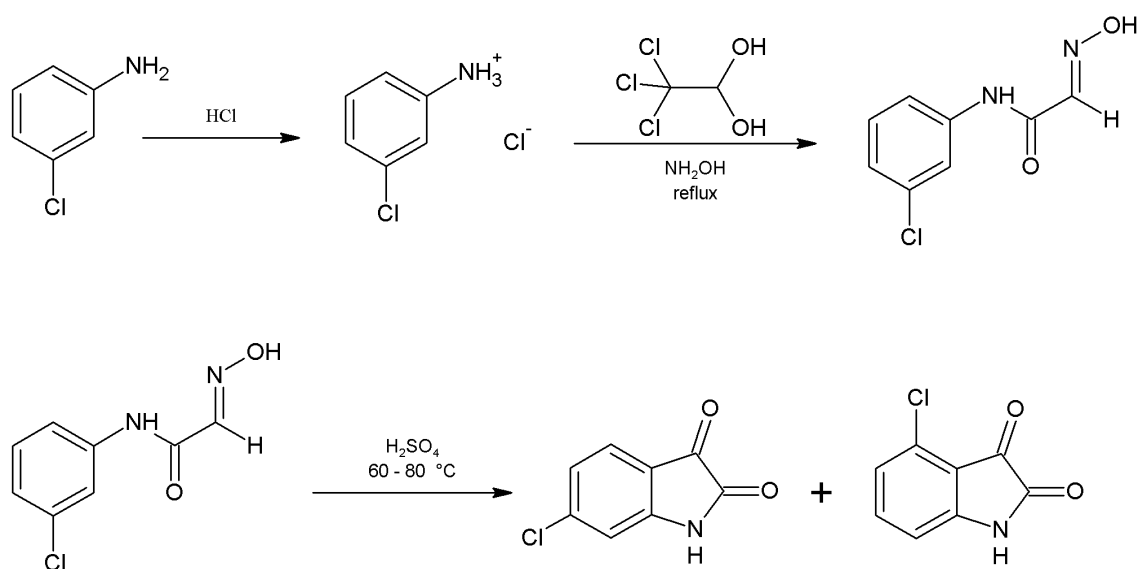
3.11. Substrates for chemical synthesis

3.11.1. 6-chloroisatin

6-chloroisatin was prepared in two step synthesis as it is shown on Scheme 15 analogously to the published synthesis of isatin (Marvel and Hiers, 1925). In a 20 l. round-bottomed flask were placed 180 g (1.08 mol) of chloral hydrate, 4 l of water and 1.5 kg of anhydrous sodium sulfate. Obtained mixture was stirred for 1 h to dissolve sodium sulfate. In 1 l beaker equipped with magnetic stirrer 86 ml (1.04 mol) of concentrated hydrochloric acid was diluted with 600 ml water and added stepwise 127 g (1 mol) of 3-chloroaniline. Obtained solution was added to the reaction mixture in 20 l flask and stirred. Finally a solution of 220 g (3.16 mol) of hydroxylamine hydrochloride in 1 l of water was added. The solution was refluxed 20 min on the heating mushroom. After one to two minutes of vigorous boiling the reaction is complete. The 3-chloro-isonitrosoacetanilide precipitated as a porous yellow-brown substance. The mixture was cooled to room temperature.

The 3-chloro-isonitrosoacetanilide was filtered off, washed with 1 l of water and dried for a week under vacuum.

652 ml of concentrated sulfuric acid was warmed to 50°C in a 2 l round-bottomed flask equipped with magnetic stirrer and, 3-chloro-isonitrosoacetanilide obtained in the previous step was added gradually while the flask was ice-cooled to keep the temperature below 70°C. After the compound was added, the solution was heated to 80°C for 15 minutes.



Scheme 15: The synthesis of 6-chloroisatin.

The mixture was poured into a 2 l beaker with ice and stirred. The product was filtered, washed with 1 l of water and dried under vacuum for 2 days. Except of the desired 6-chloroisatin, some 4-chloroisatin was expected to form, the purity amount of 6-chloroisatin was checked on the silica TLC with solvent mixture of ethyl acetate/heptan in ratios: 1/5, 1/1, 5/1 . The photos of the TLC plates in the UV light are shown in Figure 8.

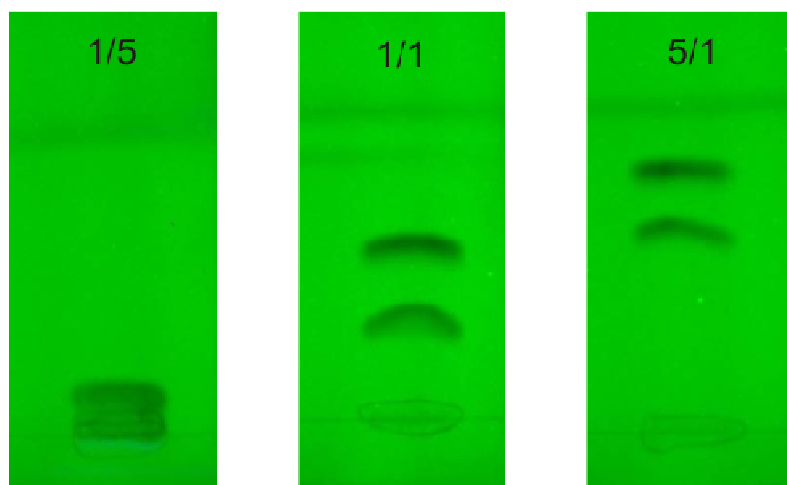


Figure 8: TLC plates with separated products of the reaction of Scheme 15.

The reaction produced approximately 50% of 6-chloroisatin and 50% of 4-chloroisatin. The isomers of chloroisatin were separated on a silica column with mixture of ethyl acetate/heptane 5/1 as a solvent. 6-chloroisatin was eluted as the first yellow band. The identity of 6-chloroisatin was confirmed by mass spectrometry and NMR. The 1D ^1H NMR spectrum and the peak assignment is shown in Figure 9.

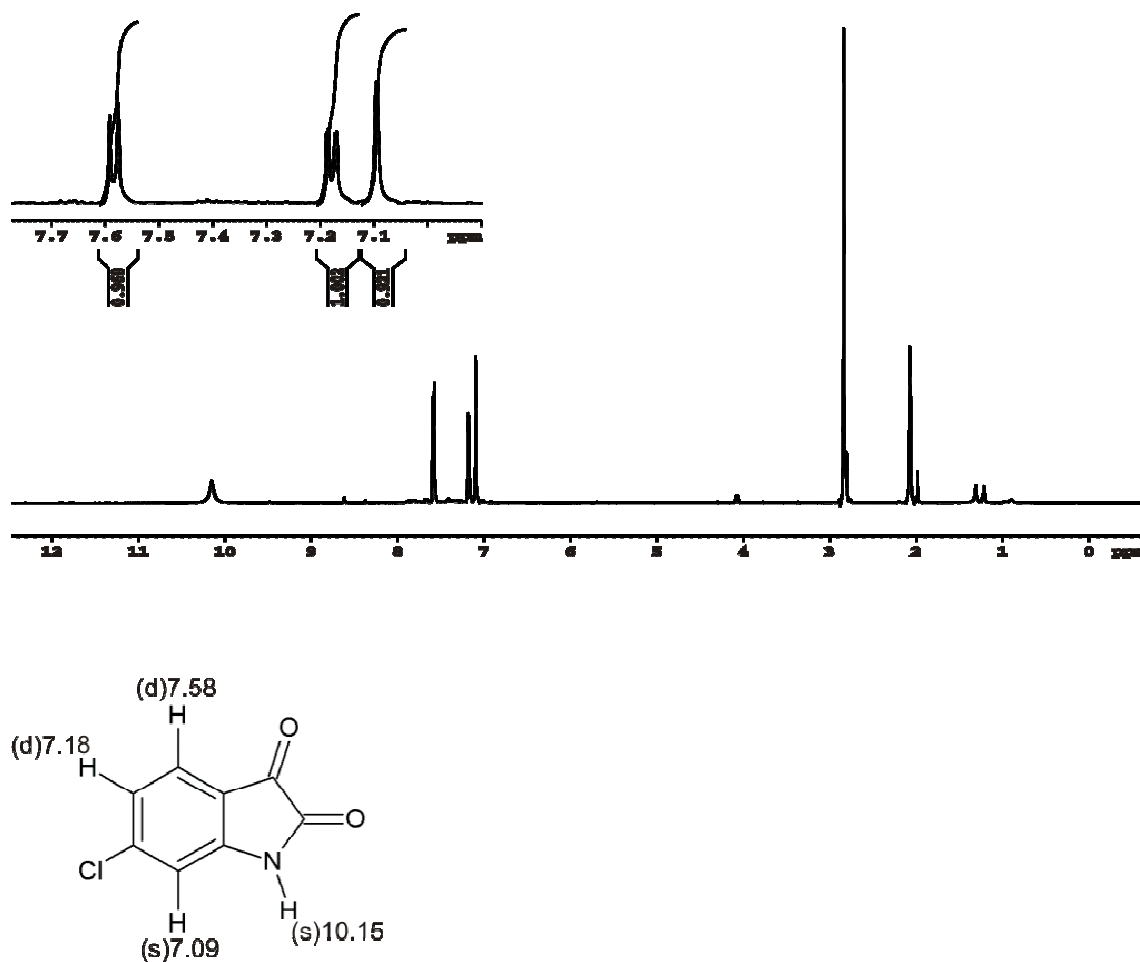


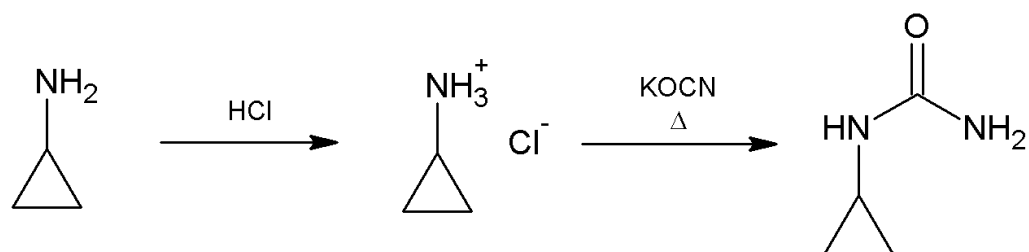
Figure 9: The NMR 1D proton spectrum of 6-chloroisatin and the NMR peak assignment, the peak positions are in ppm. The peak at 2.07 ppm comes from the residual acetone, and the one at 2.84 ppm from water.

3.11.2. Cyclopropylurea

Cyclopropylureas was prepared analogously to described protocol for cyclohexylurea (Kehm et al., 1963). In a 250 ml round bottomed flask equipped with magnetic stirrer 15 ml of concentrated hydrochloric acid was dissolved in 150ml water. 10 ml (0.15 mol) of cyclopropylamine was added stepwise while stirring. After the addition of whole cyclopropylamine the solution was heated to 60°C. While slowly stirred 15 g (0.185 mol) of potassium cyanate was added in small steps to avoid releasing a gas bubbles.

After adding potassium cyanate the reaction was heated for 1 h to complete the reaction.

The product was extracted into three volumes of ethyl acetate 500 ml each. The solvent was evaporated on rotary evaporator and the product was dried on air for 2 days.



Scheme 16: The synthesis of cyclopropylurea.

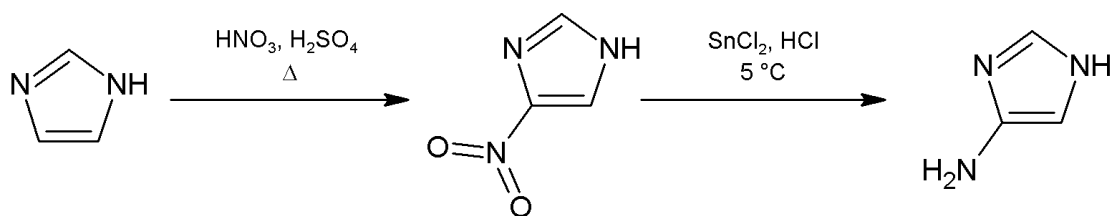
The product's identity was checked by NMR.

3.11.3. 4-aminoimidazole

4-aminoimidazole was supposed to be obtained in two step synthesis shown on Scheme 17. The nitration of imidazole was done as published (Novikov et al., 1970). In 500 ml round bottomed flask 100 ml concentrated nitric acid was mixed with 100 ml concentrated sulfuric acid. 50 g (0.73 mol) imidazole was added stepwise while the mixture was stirred. After the addition of imidazole the solution was refluxed for 1 h to complete the reaction. The mixture was cooled to room temperature and

poured on ice. The product was filtered off, washed with water and dried under vacuum for a day. 4-nitroimidazole was obtained as a white powder.

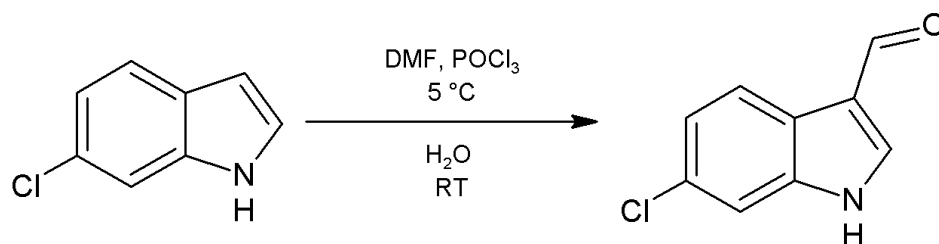
The reduction was done as published (Fargher, 1920). In 500 ml round bottomed ice cooled flask equipped with magnetic stirrer was placed 33 g (0.3 mol) of 4-nitroimidazole and 100 g concentrated hydrochloric acid. The solution of 70 g (0.37 mol) tin(II) chloride in 160 ml concentrated hydrochloric acid was added dropwise while the mixture in the flask was stirred and its temperature was maintained below 5°C. After the complete addition of tin (II) chloride the mixture was stirred and kept in the temperature below 5°C for 1 h. The volume of solution was decreased by evaporation and the crystals of salts were collected. In the remaining dark-brown oil 4-aminoimidazole was detected by mass spectrometry, but the purification was unsuccessful.



Scheme 17: The synthesis of 4-aminoimidazole.

3.11.4. 6-chloroindole-3-aldehyde

6-chloroindole-3-aldehyde was prepared analogously to the indole-3-aldehyde which synthesis was published (James and Snyder, 1959). In a 100 ml round bottomed flask equipped with stirrer 3 g (0.02 mol) of 6-chloroindole was dissolved in N,N-dimethylformamide. The mixture was stirred and the flask was cooled on ice and 4 ml (0.04 mol) of phosphorus (V) oxychloride was added dropwise in such a rate that the temperature of the reaction mixture did not rise over 5°C. The mixture was cooled and stirred for 1 h and stirred at room temperature for 2 h.



Scheme 18: The synthesis of 6-chloroindole-3-aldehyde

After that time the solution was poured into 300 ml of water and was allowed to precipitate for 5 days. The product was filtered, washed with water and dried under vacuum for a day. The purity of the product was checked by TLC, the image of the plate is shown in Figure 10. The product seems to be pure, only a single band is visible in TLC.



Figure 10: TLC of 6-chloroindole-3-aldehyde.

The identity of the product was confirmed by MS and NMR. The 1D NMR proton spectrum and the peak assignments are shown in Figure 11.

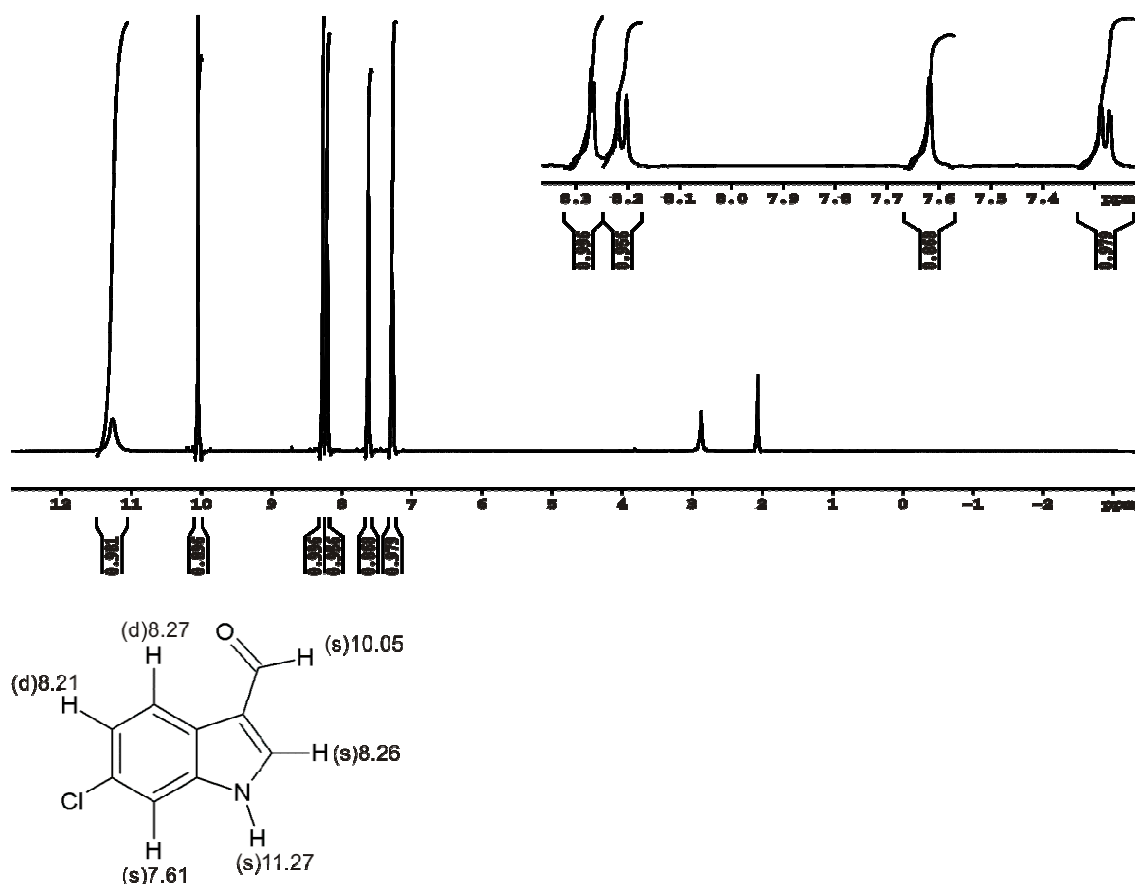


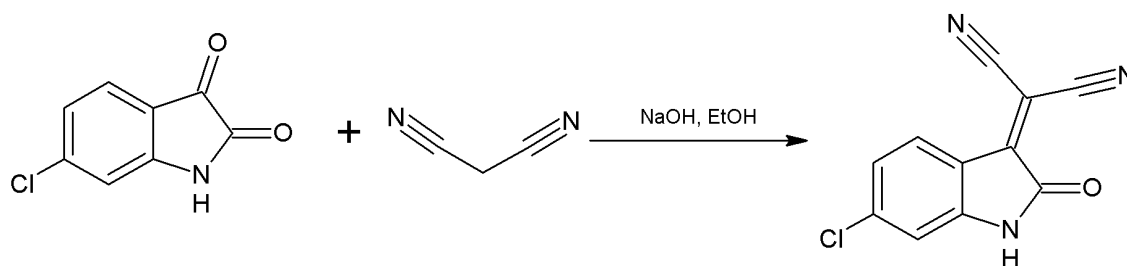
Figure 11: The NMR 1D proton spectrum of 6-chloroisatin and the NMR peak assignments, the peak positions are in ppm. The peak at 2.07 ppm originates from the residual acetone, and the one at 2.88 ppm from water.

3.11.5. 3-(dicyano)-methyloxindole

3-(dicyano)-methylox-6-chloroindole was synthesized as published (Walter 1902). In 400 ml beaker 20 g (0.13 mol) of 6-chloroisatin and 10 g (0.15 mol) of malononitrile were dissolved in 200 ml ethanol. The solution was stirred and 3 drops of 36% sodium hydroxide were added. The solution was stirred for overnight.

After the reaction was completed the solution was boiled to dissolve the substance and slowly cooled. The solution was kept for overnight in refrigerator for product crystallization. 3-(dicyano)-methylox-6-chloroindole formed dark purple crystals which were filtered out, washed with water and dried under vacuum. The identity of the substance was confirmed by mass spectrometry and its purity was

investigated by HPLC on silica, the result suggested that only 6-chloroisatin reacted and 4-chloroisatin which was the impurity did not react or was removed during the crystallization of the product.

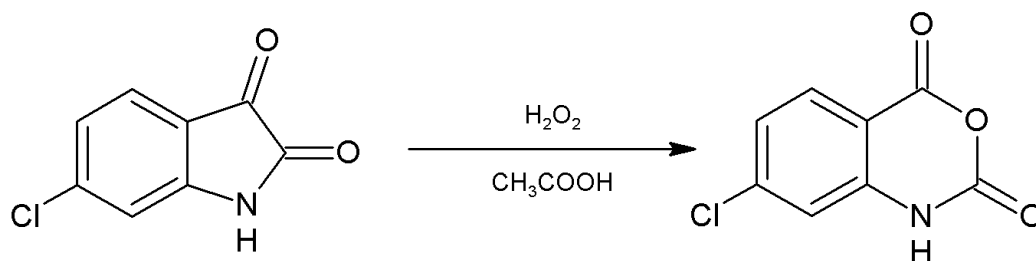


Scheme 19: The synthesis of 3-(dicyano)-methylox-6-chloroindole.

3.11.6. 4-chloroisatoic anhydride

4-chloroisatoic anhydride was prepared from 6-chloroisatin as published (Reissenweber, 1980). In 250 ml round bottomed flask equipped with magnetic stirrer 10 g (0.055 mol) of 6-chloroisatin was dissolved in 100 ml of concentrated acetic acid. The solution was stirred and 10 ml of 30% hydrogen peroxide was added dropwise. The reaction was the stirred for 30 minutes to complete.

The reaction mixture was poured into water and the product was filtered off, washed with water and dried under vacuum. The identity of the compound was checked on mass spectrometry and its purity on analytical RP HPLC.

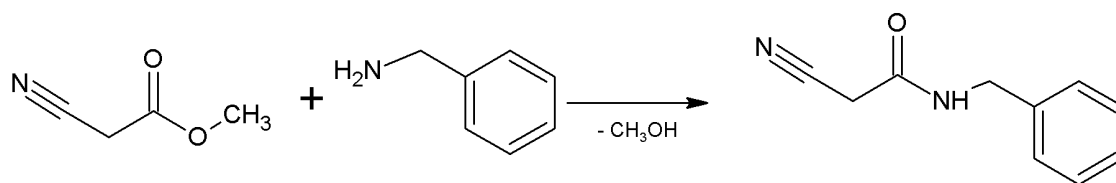


Scheme 20: The synthesis of 4-chloroisatoic anhydride.

3.11.7 Aliphatic cyanoacetamides

Various cyanoacetamides needed for further synthesis were prepared according to the published method (Wang et al., 2009). In 100 ml beaker equipped with stirrer was placed 0.2 mol of primary aliphatic amine and 0.2 mol of methyl cyanoacetate. The mixture was stirred for 3-16 h at room temperature, during this time white crystals of product appeared.

After the reaction was completed the product was filtered off, washed with ethyl ether and dried on air.

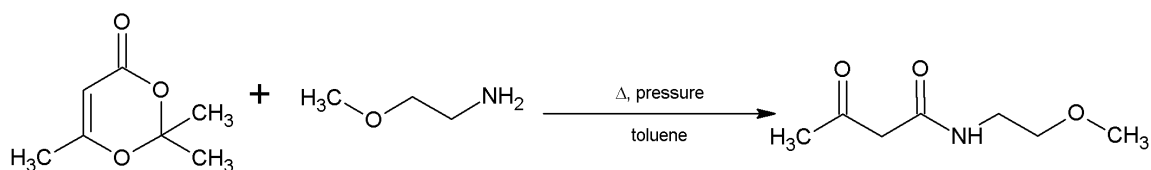


Scheme 21: An example of cyanoacetamide synthesis.

3.11.8. The synthesis of methoxyethyl acetoacetamide using 2,2,6-trimethyl-4H-1,3-dioxin-4-one.

Methoxyethyl acetoacetate was prepared as published (Clemens and Hyatt, 1984). 50 ml of methoxyethylamine, 100 ml of 2,2,6-trimethyl-4H-1,3-dioxin-4-one acetone solution and 100 ml of toluene were placed in a pressure container with magnetic stirrer. The container was placed in a heating coat placed on the magnetic stirrer. The reaction was heated to 140 °C for 6 h. After that time the container was removed from the heating coat and allowed to cool for overnight and when cold it was opened and the inner container with the substance.

The product was purified by fractional distillation under vacuum. The fractions were identified by mass spectrometry, the desired product was found in the fraction boiling at 130 °C. The product was washed with 50 ml water and dried under vacuum for a day.

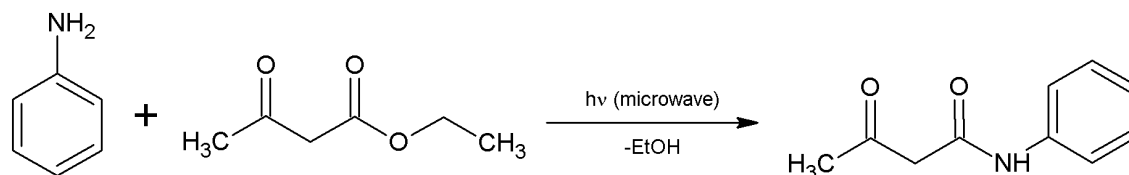


Scheme 22: The synthesis of methoxyethyl acetoacetamide using 2,2,6-trimethyl-4H-1,3-dioxin-4-one as a substrate.

3.11.8. The microwave synthesis of aromatic acetoacetamides

The synthesis of some aromatic acetoacetamides needed for further synthesis was performed as published (Suri et al., 2000). In 1 L flask were placed 0.2 mol of primary aromatic amine and 1 mol of ethyl acetoacetate. The flask was placed opened in a microwave and irradiated for 2-15 min at 800W.

The product was washed with ethyl ether, and dried. The identity of the product was checked on mass spectrometry.



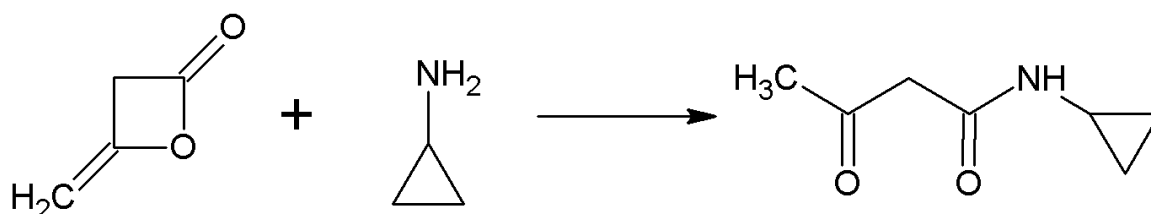
Scheme 23: An example of a microwave synthesis of aromatic acetoacetamide.

3.11.9. The synthesis of acetoacetamides with diketene

Acetoacetamides which could not be easily synthesized and purified using the methods described above were prepared analogously to the published protocol (Williams and Krynitsky 1955). In 250ml round bottomed flask equipped with magnetic stirrer was placed 0.1 mol of amine and 100 ml of dichloromethan or ethyl ether depending of the amine solubility in both of them. The low boiling solvent added in large amount helped to not overheat the reaction and was easy to remove after the reaction was completed. While the amine solution was vigorously stirred under the

fume hood 0.1 mol of diketene was added dropwise, the heat formed by the reaction was removed by boiling solvent.

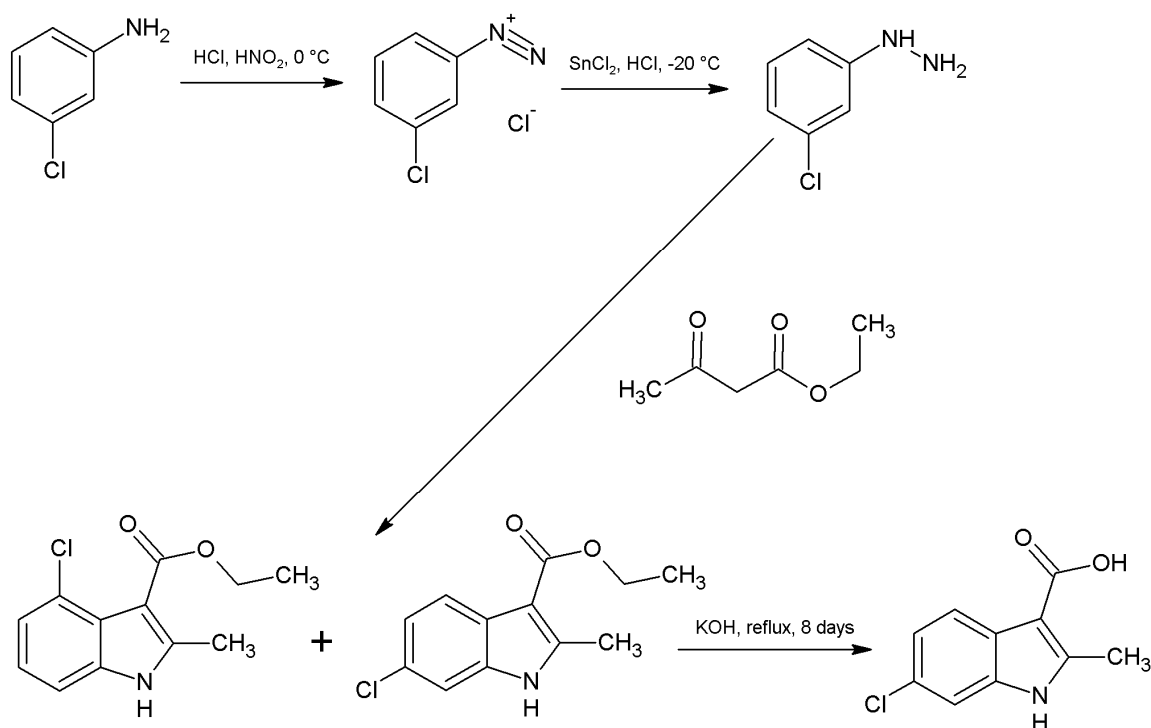
The excess of solvent was removed on rotary evaporator in case of dichloromethane or by slow evaporation on air in case of ethyl ether. The identity of acetoacetamides was confirmed on mass spectrometry.



Scheme 24: An example of a synthesis of acetoacetamide using diketene as a substrate.

3.11.10. The synthesis of indole-3-carboxylic acid

The synthesis was done in 4 steps presented on scheme 25. First the diazonium compound was prepared, then reduced to substituted hydrazine, from which the 2-methyl-6-chloroindole-3-carboxylic acid's ester was prepared and hydrolysed in last step. First 3 steps were done analogously to the published synthesis (Brodfuehrer et al., 1997).



Scheme 25: The synthesis of 2-methylindole-3-carboxylic acid.

In round bottomed 4 L flask equipped with magnetic stirrer, thermometer and dropping funnel were placed; 800 ml (9.4 mol) of concentrated hydrochloric acid, 400 ml of water and 51 g (0.4 mol) of 3-chloroaniline were mixed until the reaction completed. The reaction mixture was stirred and cooled to -5 °C. The solution of 30 g sodium nitrate (III) in 400 ml water was added dropwise while stirred and cooled on ice to not exceed the temperature 5 °C.

The resulting solution was cooled to -20 °C and added dropwise a solution of 227 g (1,2 mol) of tin (II) chloride in 800 ml of concentrated HCl in such a rate that the temperature was between -10 and -20 °C. After this addition the solution was stirred for 2 h to complete the reaction. (3-chlorophenyl)-hydrazine hydrochloride was filtered out, washed with cold ethanol and dried under vacuum for 8 h.

35 g (0,2 mol) of (3-chlorophenyl)-hydrazine hydrochloride was placed in 2 L flask with 500 ml of ethanol and 400 ml of water and the pH was set to 3.5 with 30 % sodium hydroxide solution. The mixture was heated to 60 °C for 4 h.

After the reaction was completed ethanol was removed on rotary evaporator and the product was extracted with ethyl acetate. The organic phase was washed with water, evaporated on rotary evaporator and dried in vacuum for overnight.

In 1 L round bottomed flask equipped with magnetic stirrer 20 g (0.09 mol) of the obtained mixture of esters was placed with 400 ml of water and 160 g (4 mol) of potassium hydroxide. The mixture was vigorously stirred and refluxed for 8 days.

After this time the reaction mixture was cooled to room temperature. The remaining substrate was extracted with chlorophorm. Water phase was moved into 1 L beaker with 500 ml of ethyl acetate. While stirred the excess of acetic acid was added and the product was extracted into organic phase.

The solution of the product was evaporated on rotary evaporator, than the substance was dried in vacuum for a day.

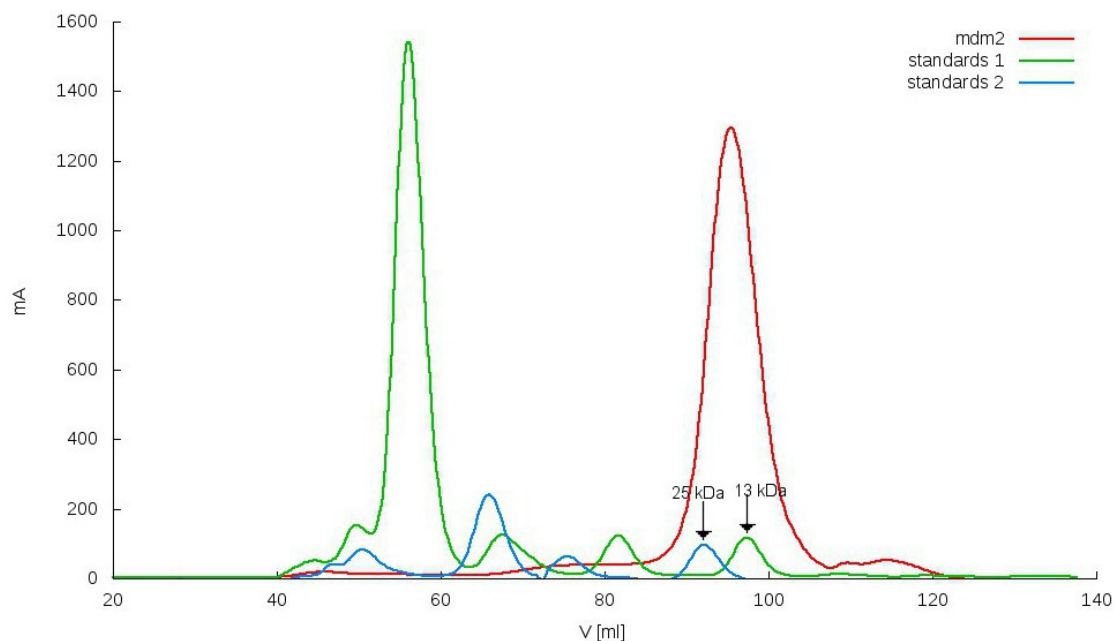
3.12. Proteins

3.12.1. Mdm2 preparation and purification

The recombinant human Mdm2 protein containing the first 118 N-terminal aminoacids was obtained in Escherichia coli BL21(DE3) RIL expression system using a pET46 Ek/LIC vector. The bacteria were grown at 37°C in LB medium with 100 ml/L of ampicillin and 34 mg/L of chloramphenicol for unlabeled protein or in minimal medium for uniform enrichment with ¹⁵N with 50 mg/L of ampicillin and 17 mg/L of chloramphenicol if labeled protein was needed. The bacteria were induced at an OD_{600nm} of 0.7-0.8 for with 1 mM of IPTG. The protein was expressed for 4 h at 37°C.

The cells were centrifuged at 5000 rpm for 15 min and the pelet was suspended in PBS buffer. The bacteria were lysed by sonication at 0°C. The lysat was centrifuged at 12000 rpm for 30 minutes. The protein was expressed into inclusion bodies which were inside the pelet. The inclusion bodies were washed twice with PBS buffer containing 0.05% Triton X-100 with subsequent centrifugation at 12000 rpm for 30 min. The inclusion bodies were dissolved in the buffer with pH 8.0 containing 6 M guanidine hydrochloride, 100 mM tris 1 mM EDTA and 10 mM DTT

and centrifuged at 20000 rpm for 40 min to remove cell membranes. The protein solution was dialysed for overnight into the buffer with pH 3.5 containing 4 M guanidine hydrochloride, 100 mM tris, 1 mM EDTA and 10 mM DTT. The protein was refolded by dropwise dilution 1:100 into the buffer with pH 7.0 containing 10 mM tris, 1 mM EDTA and 10 mM DTT. After dilution the solution was stirred for overnight at 4°C to complete the refolding. $(\text{NH}_4)_2\text{SO}_4$ was added to concentration 1.5 M and the solution was stirred for 1 h, then 7-10 ml Butyl Sepharose 4 Fast Flow was added and the mixture was stirred for 2 h. The refolded protein was eluted with pH 7.2 buffer containing 0.1 M tris and 5 mM DTT. The final step of purification was done by gel filtration on HiLoad 26/60 Superdex 75 pg column with the running buffer containing 50 mM KH_2PO_4 , 50 mM Na_2HPO_4 , 150 mM NaCl 5 mM DTT. The Mdm2's elution volume was compared with the standards, it eluted between 13 kDa and 25 kDa standards, what is expected from 14 kDa protein. The fractions containing monomeric Mdm2 were pooled.



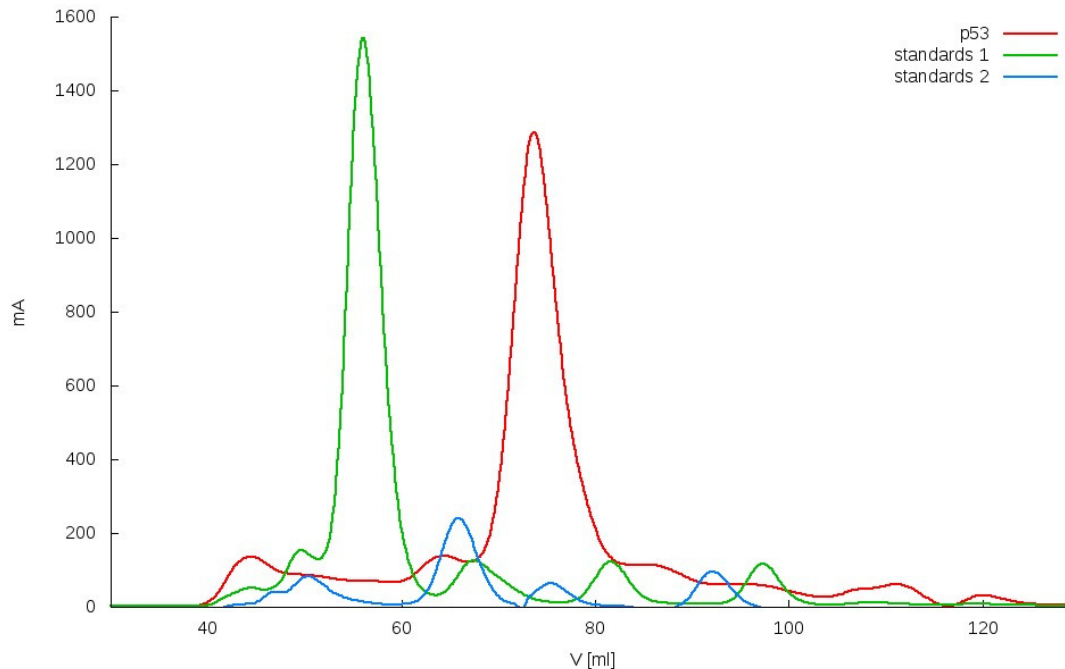
Plot 1: Chromatogram of size exclusion chromatography of MDM2 protein.

The mass of the protein was confirmed by gel electrophoresis in denaturing conditions.

3.12.2. The preparation and purification of the complex of Mdm2 and p53

Human P53 protein containing the first 321 N-terminal aminoacids was obtained in Escherichia coli BL21(DE3) RIL expression system using a pET46 Ek/LIC vector. The bacteria were grown at 37°C in LB medium with 100 mg/L of ampicillin and 34 mg/L of chloramphenicol. They were induced at an OD_{600nm} of 0.7-0.8 for with 1 mM of IPTG. The protein was expressed for 12 h at 20°C.

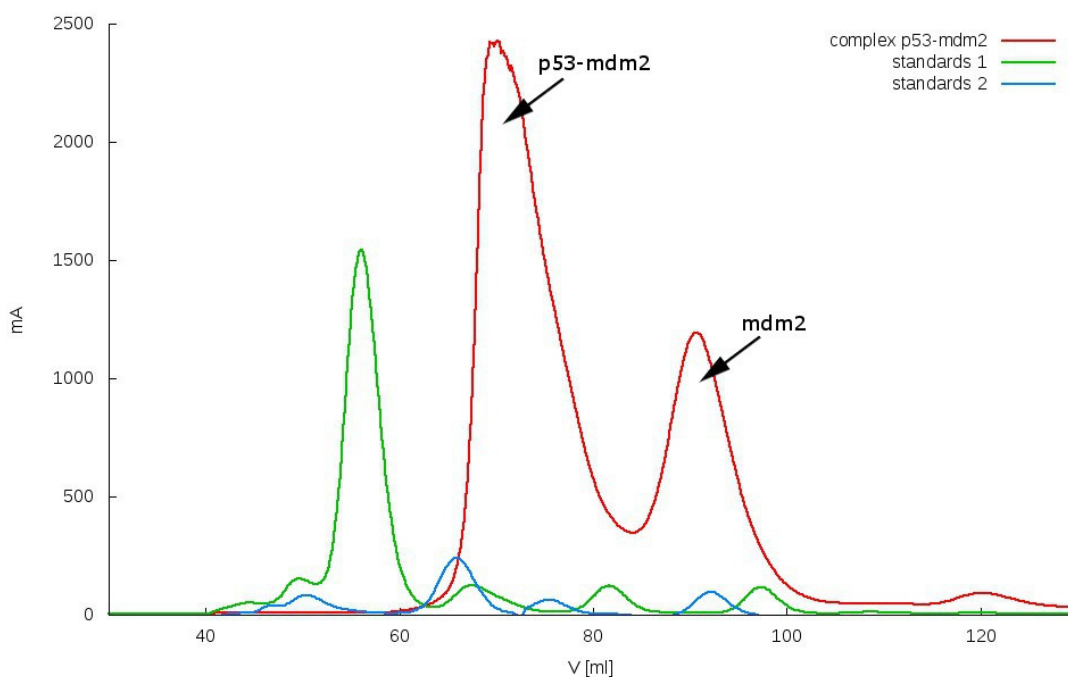
The cells were centrifuged at 5000 rpm for 15 min and the pelet was suspended in binding buffer for immobilized metal-chelate chromatography in native conditions. The bacteria were lysed by sonication at 0°C. The lysat was centrifuged at 20000 rpm for 30 minutes. The protein was bound to Ni-NTA column at 4°C, washed with wash buffer until steady absorbance at 280 nm and then eluted with elution buffer. The final step of purification was done by gel filtration on HiLoad 26/60 Superdex 200 column with the running buffer with pH 0.2 containing 10 mM, Na₂HPO₄, 1.8 mM KH₂PO₄, 140 mM NaCl, 2.7 mM KCl, 0.05% Na₃N, 5 mM DTT.



Plot 2: Chromatogram of size exclusion chromatography of p53 protein.

P53 is eluted earlier than standards with similar mass because it is not folded and can have a different shape than globular.

The Mdm2-p53 complex was prepared by mixing p53 with excess of Mdm2. It was purified by gel filtration on HiLoad 16/60 Superdex 200 column with running buffer containing 10 mM Na₂HPO₄, 1.8 mM KH₂PO₄, 140 mM NaCl, 2.7 mM KCl, 0.05% NaN₃, 5 mM β-mercaptoethanol, pH 7.2. During this step the excess of Mdm2 was removed.



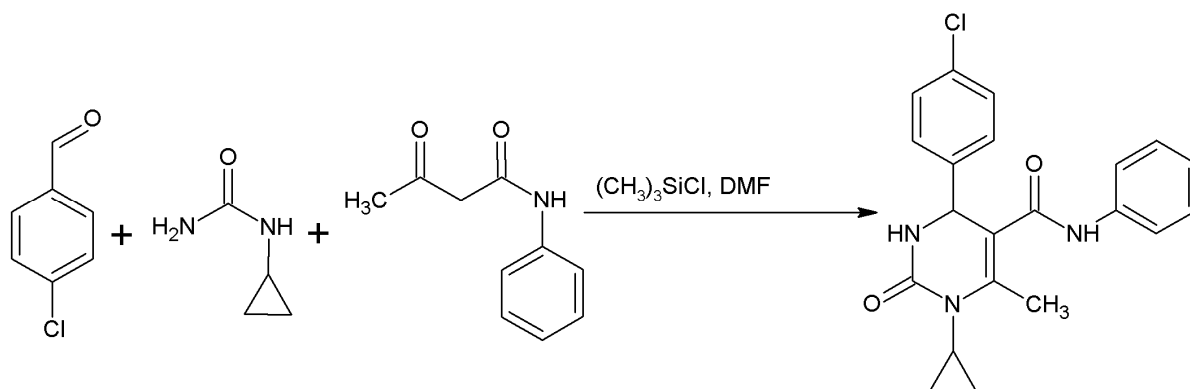
Plot 3: Chromatogram of size exclusion chromatography of p53-Mdm2 complex.

3.13. Mdm2's ligands synthesis

3.13.1. Synthesis and purification of 3,4-dihydropyrimidin-2(1H)-ones

3,4-dihydropyrimidin-2(1H)-ones were prepared accordingly to the method published by (Ryabukhin et al., 2007). 5 mmol p-chlorobenzaldehyde, 5 mmol acetoacetate or acetoacetamide and 5 mmol the N-substituted urea were placed in a 50ml round bottomed flask and dissolved in 20 ml of N,N-dimethylformamide. After obtaining clear solution 20 mmol of trimethylchlorosilane was added dropwise while stirring. The mixture was stirred for 3 days to complete the reaction.

The products were purified by precipitation, followed by extraction between water and chloroform or by the reverse phase high pressure liquid chromatography. The pure product was dried in vacuum.

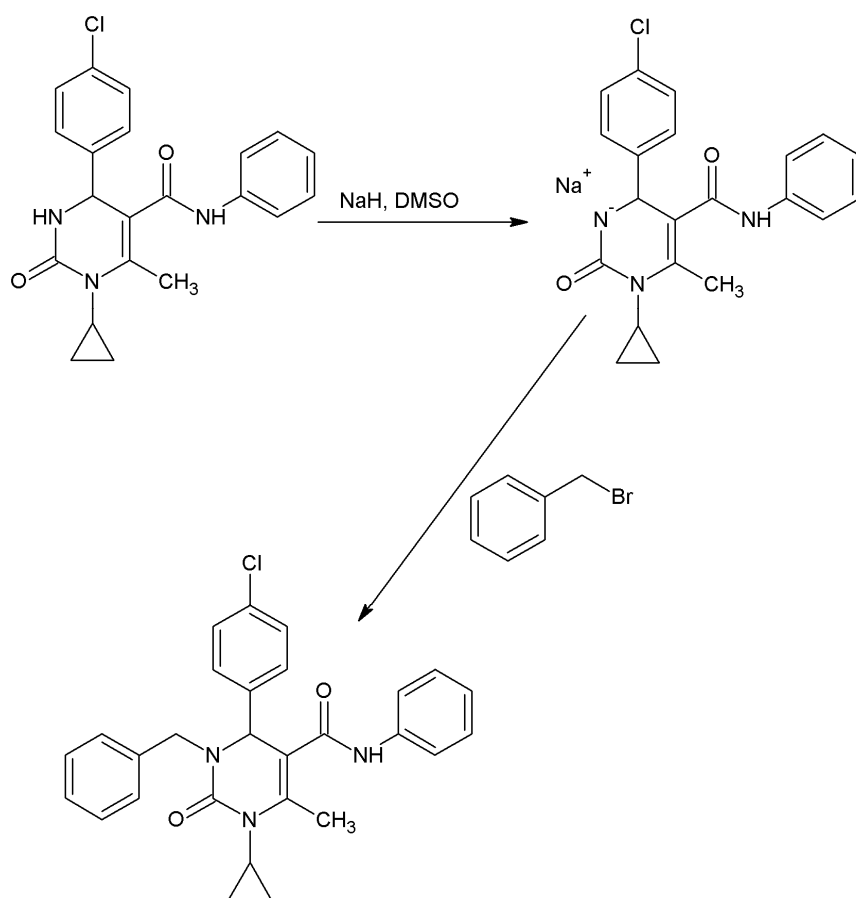


Scheme 26: An example of the synthesis of 3,4-dihydropyrimidin-2(1H)-one.

3.13.2. N-3 alkylation of 3,4-dihydropyrimidin-2(1H)-ones

In a 10 ml pointed flask 1 mmol 3,4-dihydropyrimidin-2(1H)-one was dissolved in 5 ml dimethylsulfoxide. 1.2 mmol NaH was added and the mixture was stirred as long as hydrogen was released. After completion of this step, 1.1 mmol alkyl bromide was added and the reaction mixture was heated up to 150°C for 30 – 120 min depending on the reagents; usually the color changes were observed when the reaction proceeded.

The products was precipitated with water and purified by the RP HPLC, and checked on mass specrometry.

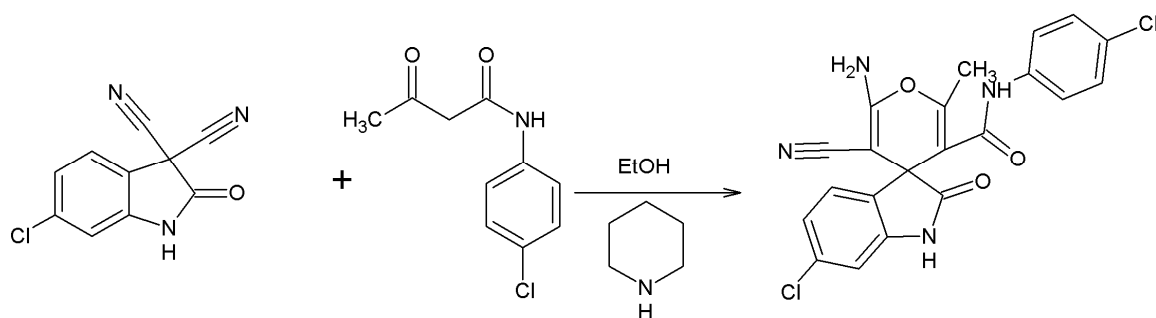


Scheme 27: Alkylation of 3,4-dihydropyrimidin-2(1H)-one.

3.13.3. Synthesis and purification of spiro[oxindole-3,4'-(4'*H*-pyran)] compounds

The synthesis was performed according to the published protocol (Higashiyama et al., 1980). In a 20 ml vial equipped with magnetic stirrer 1 mmol 6-chloro-2-oxo-1,2-dihydro-3*H*-indole-3,3-dicarbonitrile and 1.1 mmol acetoacetamide or acetoacetate were dissolved in 10 ml ethanol and 10 μ l of pyrimidine was added.

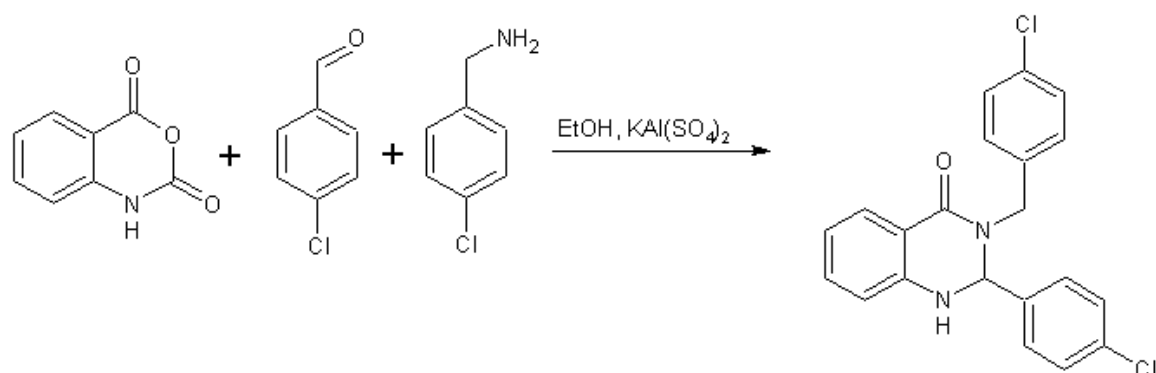
The reaction mixture was stirred until precipitate was formed or otherwise for 4 days. If the precipitate was formed, it was filtered out, washed with ethanol and dried under vacuum. If no precipitation occurred, then the mixture was evaporated in vacuum until dry, and the product was purified by PR HPLC. The identity of the product was confirmed by MS.



Scheme 28: An example synthesis of spiro[oxindole-3,4'-(4'*H*-pyran)].

3.13.4. The synthesis and purification of 2,3-dihydroquinazolin-4(1H)-ones and 7-chloro-2,3-dihydroquinazolin-4(1H)-ones

The substances were prepared analogously to the published protocol (Dabiri et al., 2005). Preparation of 2,3-dihydroquinazolin-4(1H)-ones was carried out in the ethanol solution with $KAl(SO_4)_2$ as a catalyst 20 ml of absolute ethanol was placed in a 50 ml round bottomed flask, 2 mmol of isatoic anhydride or its derivative, 2 mmol of a primary amine, 2 mmol of aryl aldehyde and 200 mg $KAl(SO_4)_2$ were added, and the reaction mixture was stirred and the mixture was refluxed for 6 h for 2,3-dihydroquinazolin-4(1H)-ones and 12h for 7-chloro-2,3-dihydroquinazolin-4(1H)-ones.



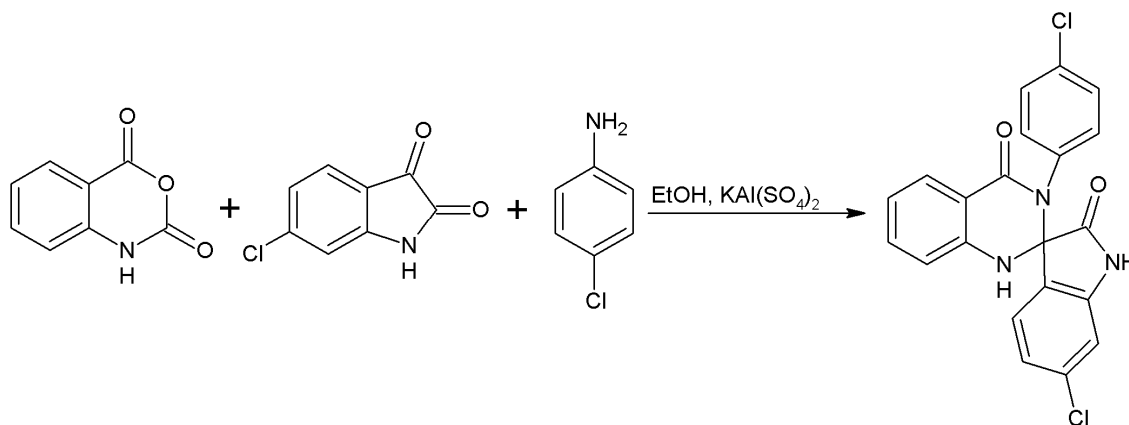
Scheme 29: An example of the synthesis of 2,3-dihydroquinazolin-4(1H)-one.

After the reaction was completed, the mixture was poured into water, and depending on the precipitate's shape, centrifuged or filtered and washed with water. The substance was then either recrystallized from ethanol and dried under vacuum for a day or purified on the RP HPLC and dried.

3.13.5. The synthesis and purification of 1'H-spiro[6-chloro-isoindole-1,2'-quinazoline]-3,4'(3'H)-diones

The substances were prepared analogously to published method (Mohammadi et al., 2009) 5 mmol 6-chloroisatin, 5 mmol isatoic anhydride, 5 mmol primary amine and 500 mg $KAl(SO_4)_2$ were added to 50ml ethanol placed in 250 ml round bottom flask. The mixture was refluxed for 8 h, though in case the 4-chloroisatoic anhydride was used the reaction was slower and the time it was carried out was extended to 24h.

The product was precipitated by the addition of water, dried under vacuum, purified on the RP HPLC and dried.



Scheme 30: An example reaction of synthesis of 1'H-spiro[6-chloro-isoindole-1,2'-quinazoline]-3,4'(3'H)-dione.

3.14. Laboratory procedures

3.14.1. Preparation of chemically competent cells

A single colony of overnight grown bacteria from a LB agar plate was grown in 20 ml of LB media in a 100 ml flask at 37°C until OD ~0.6. The bacteria were transferred to sterile, disposable, ice-cold 50 ml polypropylene tube and cooled down to 4°C on ice for 10 min. they were centrifuged at 5000 rpm for 10 min at 4°C. Supernatant was removed and the pelets were resuspended in 10 ml of the ice-cooled 0.1 M MgCl₂ solution. Again, cells were centrifuged at 5000 rpm for 10 min at 4°C. Supernatant was removed and the cells were resuspended in 5 ml of ice-cooled solution containing 0.1 M CaCl₂ and 15% glycerol. At the end the bacteria were aliquoted of 50 µl into 2ml sterile, polypropylene tubes and frozen in liquid nitrogen. The aliquots were stored at -80°C.

3.14.2. In silico screening

The ZINC database (Irwin and Shoichet, 2005) was filtered to create two subsets. First subset contained compounds with two p-halogenated phenyl rings, second one compounds with indole moiety double substituted at position 3 and unsubstituted at positions 4, 5 and 7. Sets were subsequently docked to Mdm2 receptor protein (PDB ID: 1YCR, Kussie et al.,1996) using DOCK software (Ewing et al.,1997). Docked ligands were inspected manually. Two families of compounds were chosen for *in vitro* testing. One family was based on 3,4-dihydropyrimidin-2(1H)-one scaffold, the second on spiro[oxindole-3,4'-(4'*H*-pyran)].

3.14.3. Ligand optimization

Confirmed in-silico hits were optimized by creating small, virtual derivative libraries that were subsequently docked to the Mdm2 structure (PDB ID: 1RV1 chain B) using eHits software (SimBioSys Inc, Zsolt Zsoldos et al., 2007). Compounds that have good score and probable binding poses were synthesized.

3.14.4. Fluorescence polarization measurements

Compounds were measured for their ability to disrupt Mdm2-p53 complex by fluorescence polarization assay as described previously (Gzarna et al., 2009). Briefly, the fluorescent-labelled peptide was bound to Mdm2 protein. The amount of peptide displaced by a measured compound was measured by observing polarization of emitted light after excitation with polarized beam. For each compound a 12-point measurement curve was prepared for the concentrations ranging from 200 μ M to 100nM. IC50 was calculated by fitting a 4-parameter logistic curve to the measured points. Ki was calculated according to (Huang, 2003).

3.14.4. NMR Measurements

Molecules that were showing good affinity in fluorescence polarization assay were subjected to NMR assay called AIDA (Antagonist-Induced Dissociation Assay) using previously published methodology. (D'Silva et al., 2005). Briefly, all NMR spectra were acquired at 300K on a Bruker DRX 600 MHz spectrometer equipped with a cryoprobe. Typically, protein samples of p53-Mdm2 complex obtained from gel filtration, as described before were concentrated or diluted to the desired concentration of 10 to 30 μ M and mixed with up to 10% (v/v) of D2O. Stock solutions of the compounds used in the titrations were prepared in D6-dimethyl sulfoxide. The spectra were processed with the Topspin software version 1.3. 1D 1 H spectra were recorded using SEI pulse sequence (2) and total 300 ms of acquisition and relaxation period. A total of 4k points were acquired during t1 evolution, zero filled to 32k and subjected to Fourier transform and polynomial baseline correction.

3.14.5. Electrophoresis of DNA on agarose gel

1% agarose in a 30 - 100 ml TAE buffer was heated until agarose dissolved. 3-10 μ l of SYBR stain was added and stirred to get homegenous solution, which was then poured into the electrolyser and allowed to coagulate.

The DNA samples were mixed with the 6x sample buffer prior to loading. DNA samples were run along with the 1 kb DNA ladder (NEB or pEQ lab) at 100-120 V DC. Results were visualized using UV illumination.

3.14.6. Transformation of chemically competent cells

1 - 5 μ l of plasmid DNA solution was added to 50 μ l of chemically competent cells. The mixture was incubated on ice for 30 min followed by a heat shock of 45 s at 42°C and 2 min cooling on ice. After this 250 μ l of LB medium was added and the cells were incubated for 1 h at 37°C. 50-100 μ l of the mixture was spread out on LB agar plates containing the antibiotics on which the bacteria should be resistant after the transformation. The plates were kept for overnight at 37°C.

The plasmid used for transformation contained the gene responsible for an antibiotic resistance and only the bacteria which contained the plasmid grew on the plate forming colonies. Some of the colonies were chosen for further research.

3.14.7. Sonication

Sonication was used to disrupt bacteria's cell membranes. Sonication was carried out on ice, in the sonication flask. It was done in 3 steps, 5 min each, with 5 min intervals between steps, to avoid overheating of the sample.

3.14.8. Ni affinity chromatography

Nickel affinity chromatography was used as a first step of purification of soluble proteins with His-tag. The pH of the solution containing the protein was adjusted to 8.0 with 1 M NaOH, which is optimal for the binding to the Ni-NTA resin. A Ni-NTA slurry was added and the mixture was agitated for 1-2 h. The ratio of the Ni-NTA resin used to the amount of the His-tagged protein is crucial for purity of the protein. It is more efficient to use less resin and perform a stepwise elution, obtaining a pure, concentrated protein in a shorter time.

3.14.9. Electrophoresis in SDS polyacrylamide gel

The SDS polyacrylamide gel electrophoresis was performed at various stages of purification to check the purity and identity of proteins. It was done according to published procedure (Schagger and von Jagow, 1987). The protein samples were prepared by mixing 10 μ l of protein solution with 10 μ l of sample buffer and heating for 5 min at 100°C.

3.14.10. Visualization of proteins on polyacrylamide gel

The gel was stained in a Coomassie-blue solution with microwave irradiation. Background was cleared by boiling the gel in an ethanol - water mixture in the microwave. If not cleared enough the solution was changed to fresh one and boiling was repeated.

4. Results and discussion

4.1. 3,4-dihydropyrimidin-2(1H)-ones and spiro[oxindole-3,4'-(4'*H*-pyran)]es

Two of the highest ranking hits from docking; one 3,4-dihydropyrimidin-2(1H)-one shown in Figure 12 and one spiro[oxindole-3,4'-(4'*H*-pyran)] shown in Figure 13 were chosen for optimization.

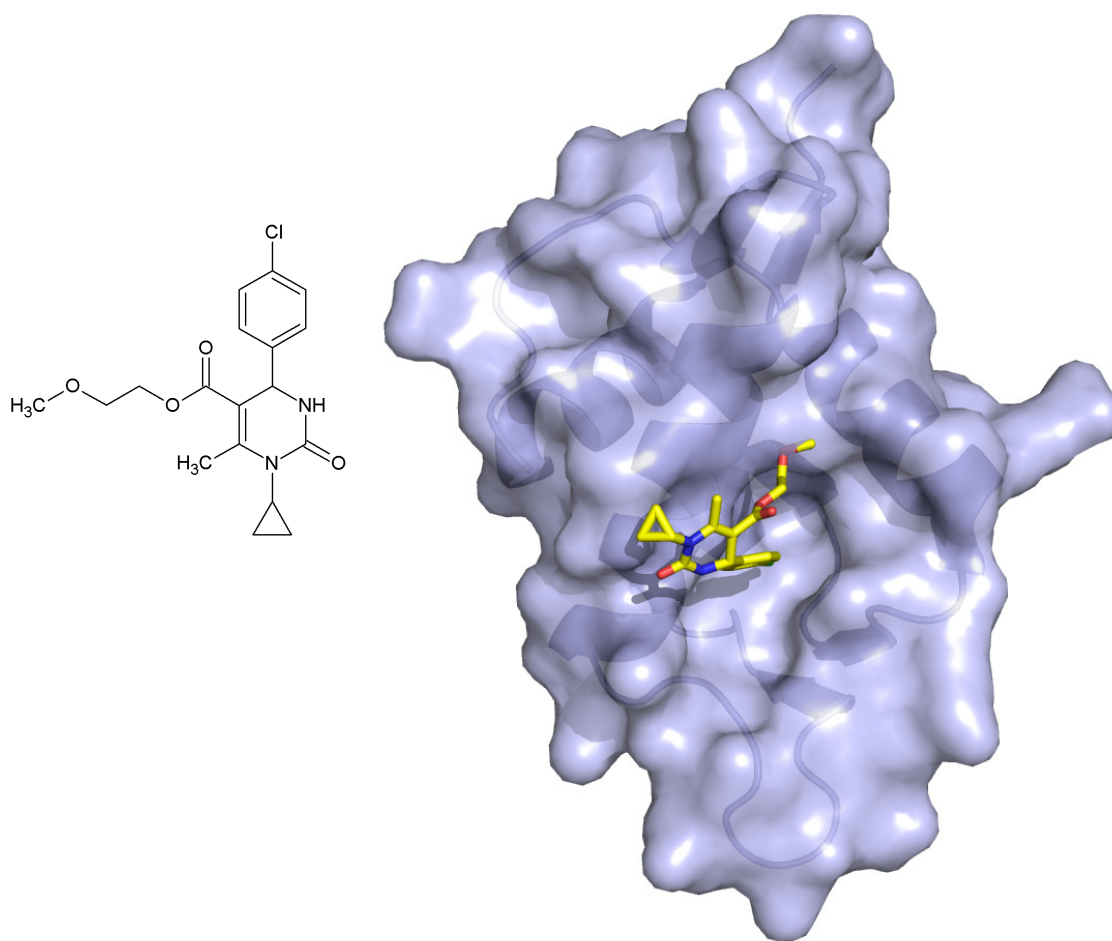


Figure 12: The formula of 3,4-dihydropyrimidin-2(1H)-one, named synt10, and the model of its interaction with Mdm2.

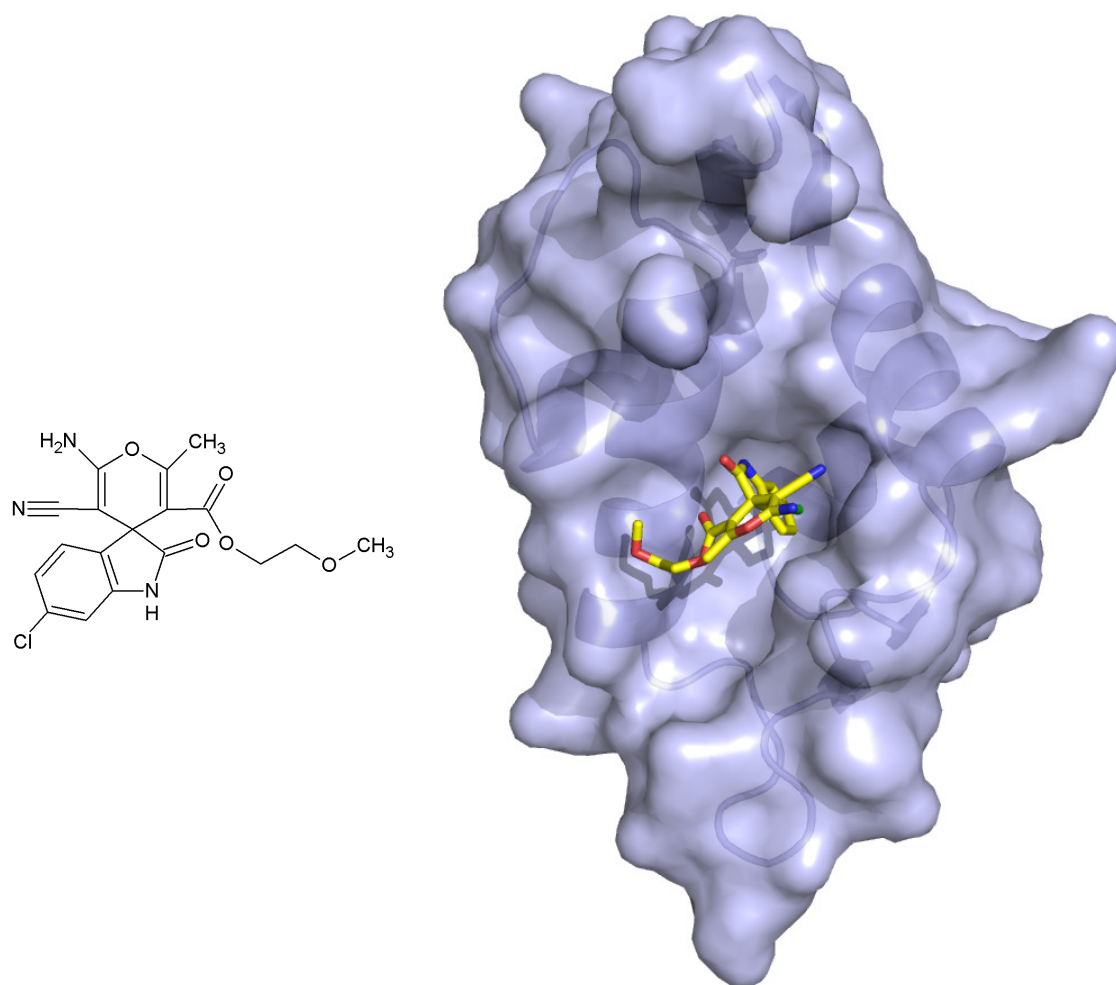
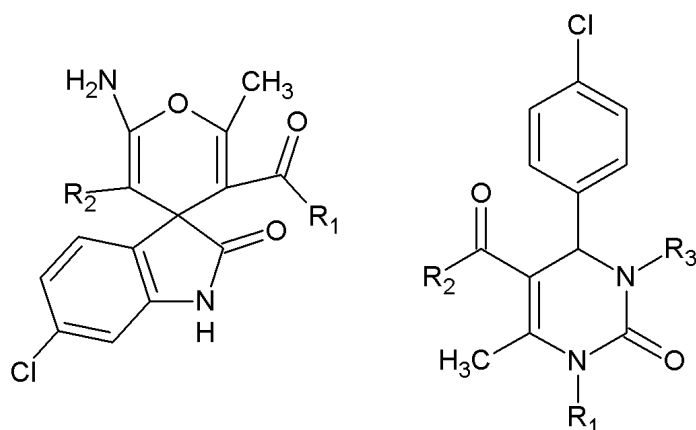


Figure 13: The formula of spiro[oxindole-3,4'-(4'*H*-pyran)], named si2, and the model of its interaction with Mdm2

Both types of compounds, spiro[oxindole-3,4'-(4'*H*-pyran)] and 3,4-dihydropyrimidin-2(1*H*)-ones, could readily be obtained by multicomponent reactions carried out at room temperature. This allowed for a large variety of compounds in parallel syntheses. All compounds were synthesized as racemic mixtures and the enantiomers were not separated.

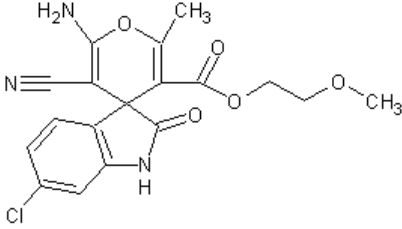
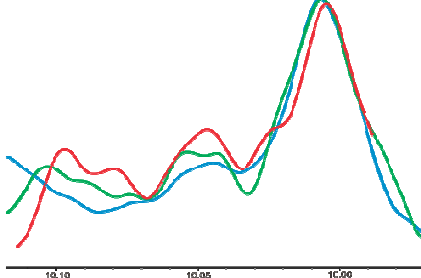
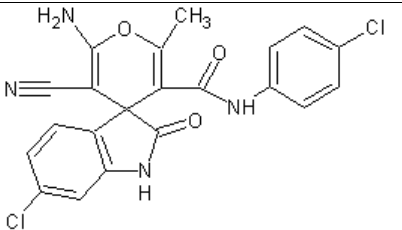
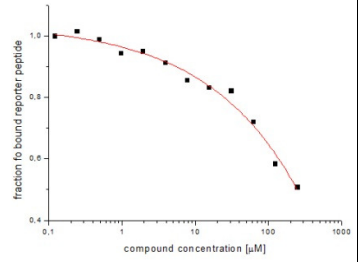
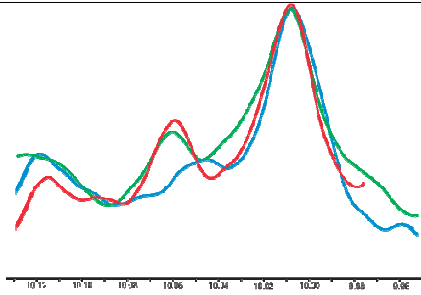
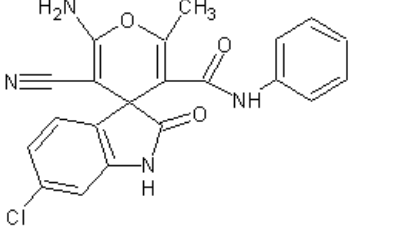
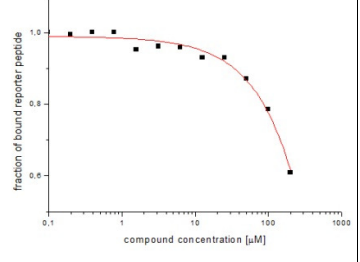


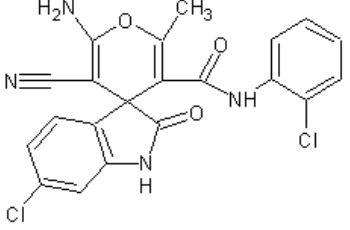
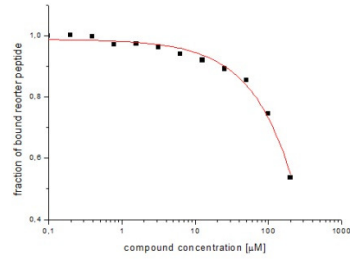
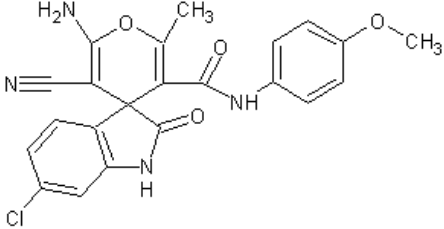
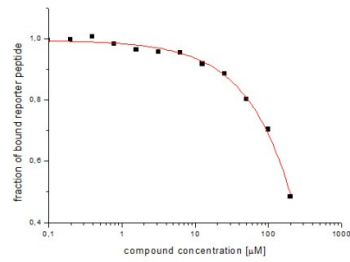
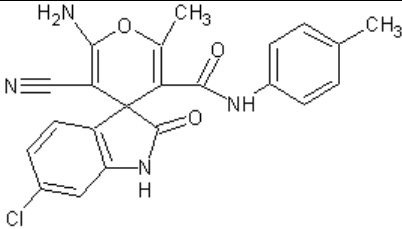
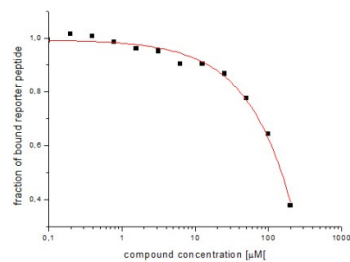
Scheme 31: Core scaffolds with substituents chosen for optimization.

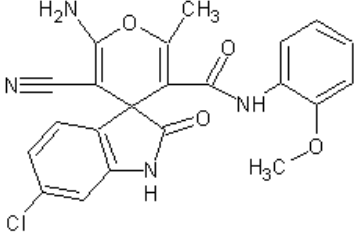
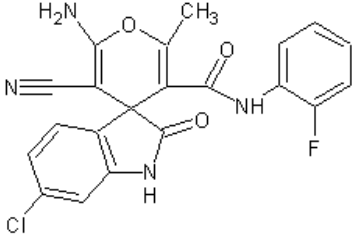
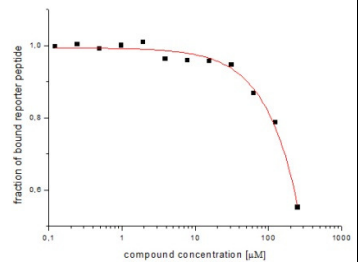
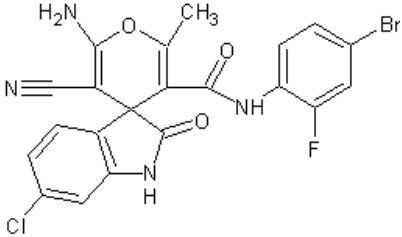
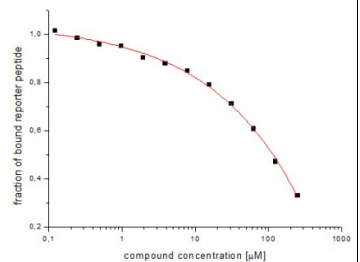
Several compounds from both of the series partially disrupted the Mdm2-p53 complex. The compound crucial structural elements, which fit well the p53-binding pocket of Mdm2, together with those substituents which place them in the “right positions were defined as core scaffolds (Scheme 31) and not changed during the optimizations, while the other substituents were changed in order to exploit the protein’s binding capacity in the most efficient way. We searched for possible extra hydrophobic interactions and hydrogen bonds.

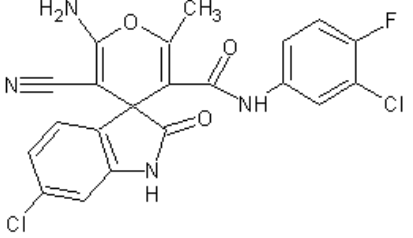
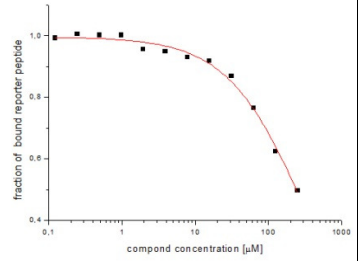
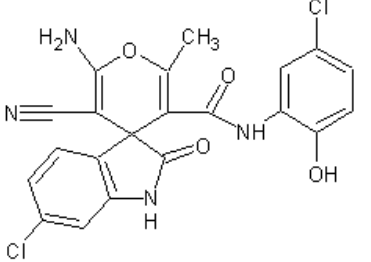
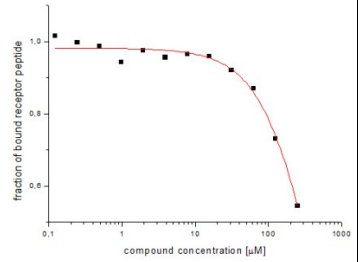
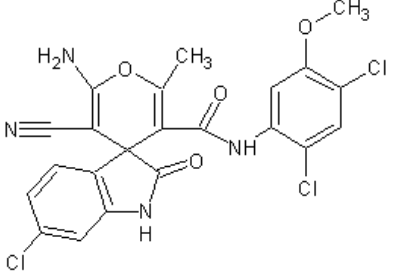
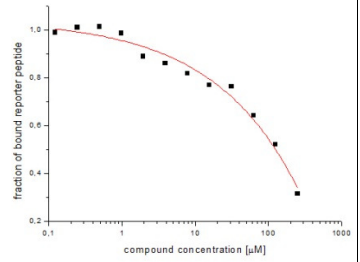
The compounds were synthesized in series, each in one position of the core scaffold. After the synthesis of each series, their ability for binding to Mdm2 was measured to fish out compounds that are able to interact with Mdm2 in the most efficient way and would inhibit the Mdm2-p53 complex. The second generation of the modified compounds were first screened by the fluorescence polarization assay for inhibition of the Mdm2-p53 interaction (Czarna et al., 2009). The interaction of compounds which gave the best results in the FP assay was orthogonally confirmed by the AIDA-NMR (Krajewski et al., 2007). The inhibitors of the Mdm2-p53 interaction which showed activities in both tests were used as references for subsequent series of syntheses. The structures of all synthesized spiro[oxindole-3,4'-(4'*H*-pyran)] and 3,4-dihydropyrimidin-2(1H)-ones and the data regarding their interaction with Mdm2 are shown in Table 1 and Table 2, the blue line in the AIDA-NMR plots is a reference spectrum of the p53-Mdm2 complex, the green one is the spectrum after addition of the compound in an equimolar concentration to the protein and the red line is the spectrum of the mixture containing the protein and the compound in the 1 : 5 molar ratio, respectively.

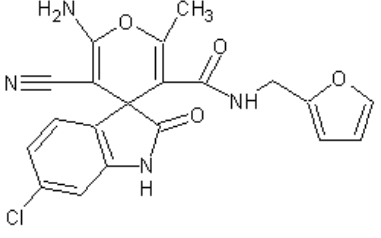
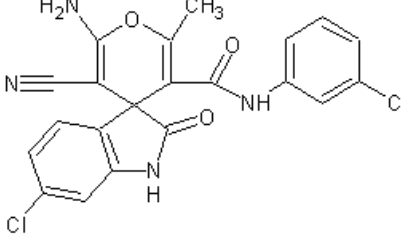
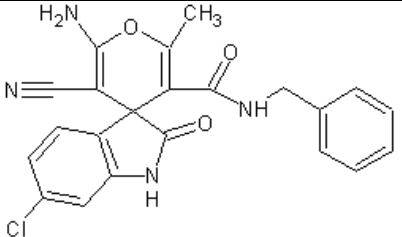
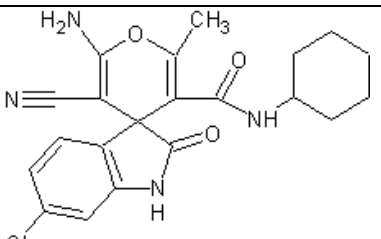
Table 1: Synthesized spiro[oxindole-3,4'-(4'-H-pyran)]es and their interaction with Mdm2.

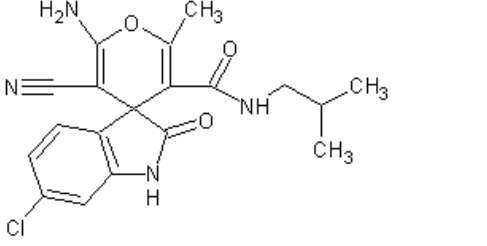
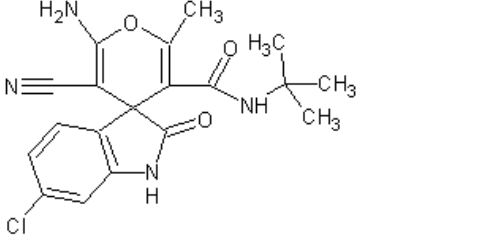
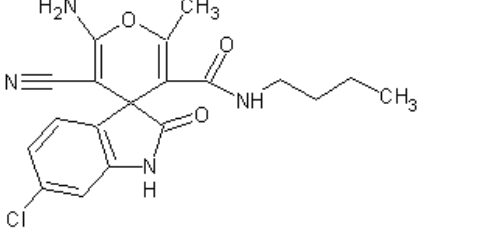
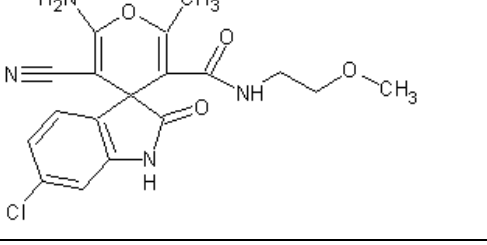
Name	Formula	MW [g/mol]	FP K _i [μM]	FP plot	AIDA K _i [μM]	AIDA plot
Si2		389			3	
Si3		441	10		1.5	
Si6		406	60			

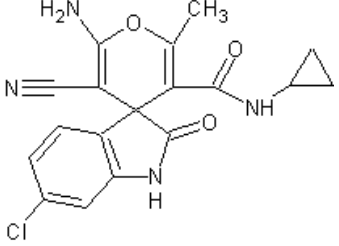
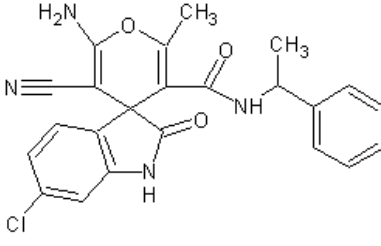
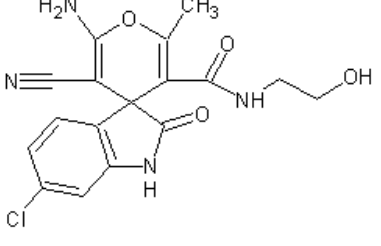
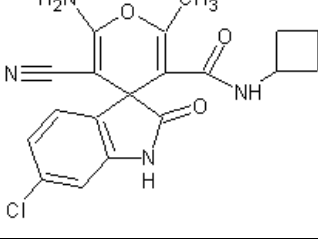
Si7		441	29			
Si8		436	25			
Si9		420	19			

Si11		436	Weak			
Si13		424	50			
Si14		503	55			

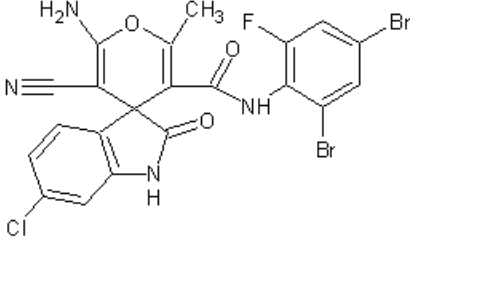
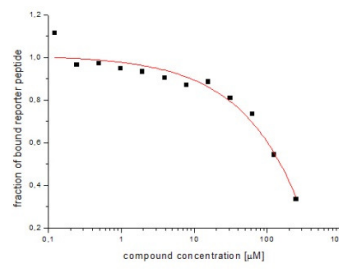
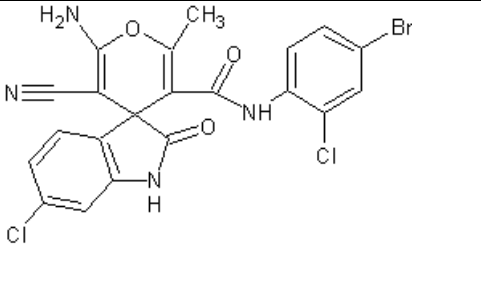
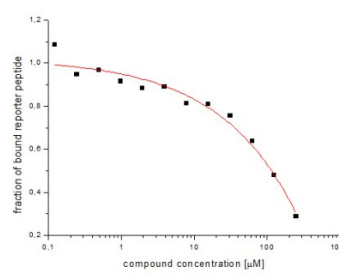
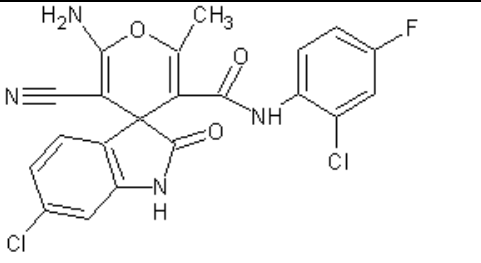
Si15		459	45			
Si17		457	50			
Si18		505	21			

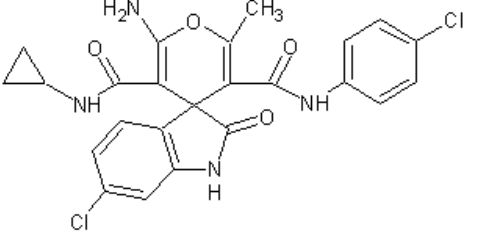
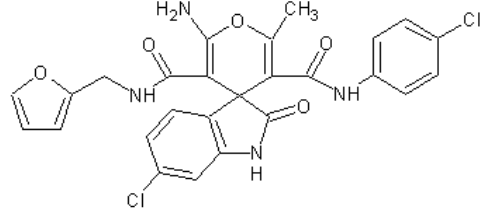
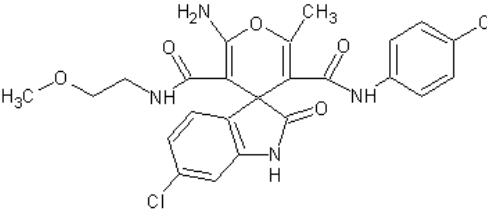
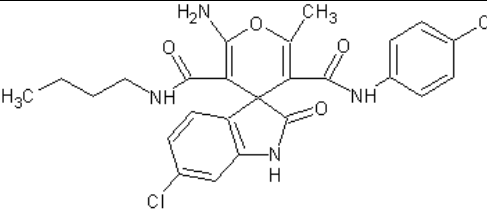
Si19		410	Weak			
Si20		441	Weak			
Si21		420	Weak			
Si22		412	Weak			

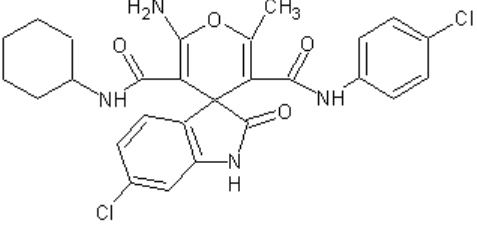
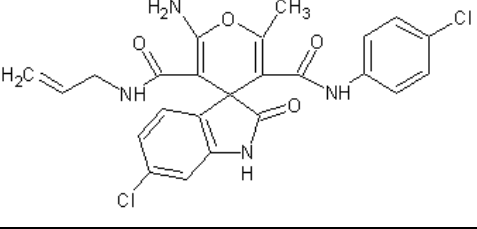
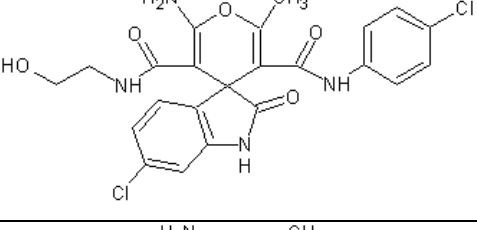
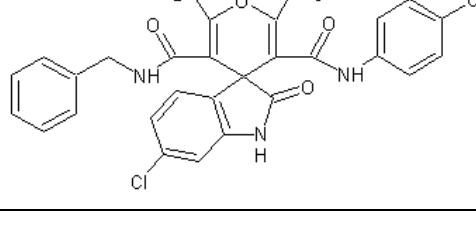
Si24		386	Weak			
Si25		386	Weak			
Si28		386	No interaction			
Si29		388	Weak			

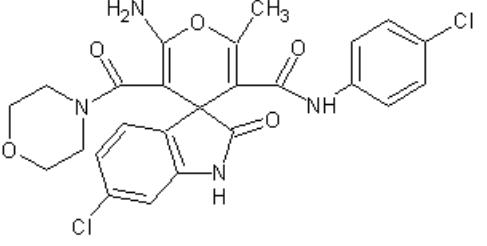
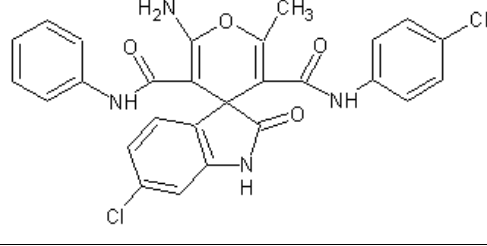
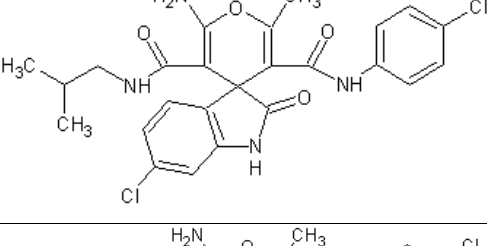
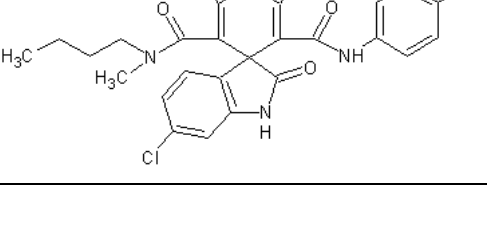
Si30		370	No interaction			
Si32		434	No interaction			
Si33		374	Weak			
Si34		384	Weak			

Si36		473	Weak			
Si38		520	Weak			
Si39		485	29			

Si40		582	33			
Si41		520	48			
Si42		459	Weak			

Si48		499	Weak			
Si50		539	No interaction			
Si51		517	No interaction			
Si52		515	No interaction			

Si53		541	No interaction			
Si54		499	No interaction			
Si55		503	No interaction			
Si56		549	No interaction			

Si57		529	Weak			
Si58		535	No interaction			
Si59		515	Weak			
Si60		529	No interaction			

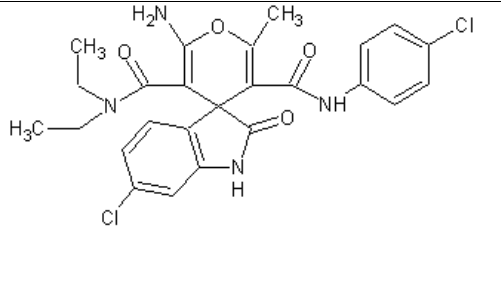
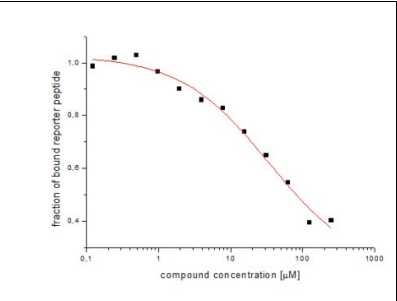
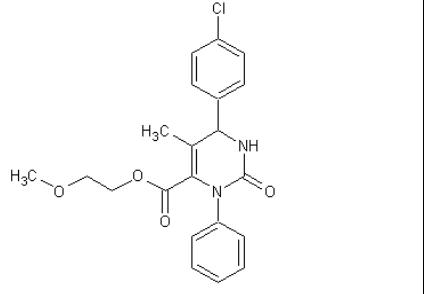
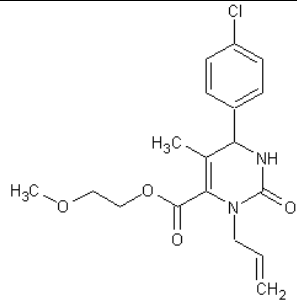
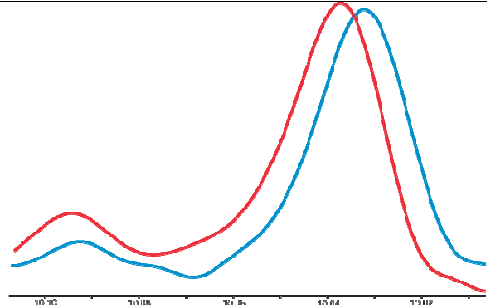
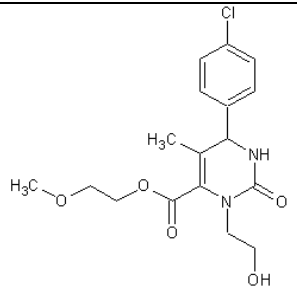
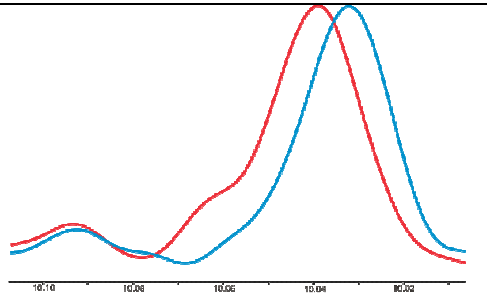
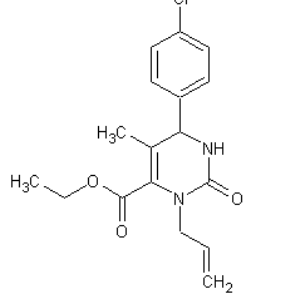
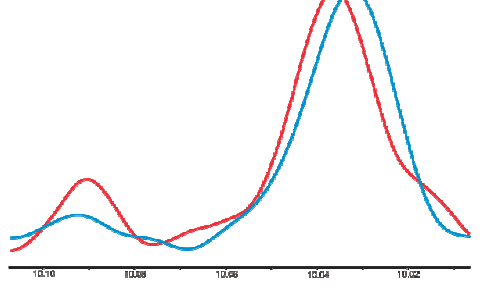
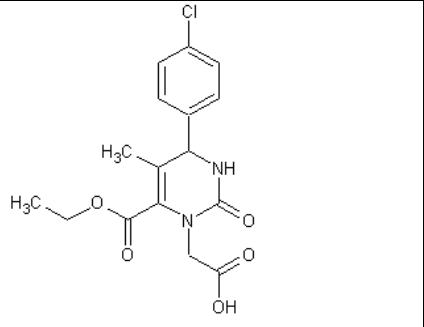
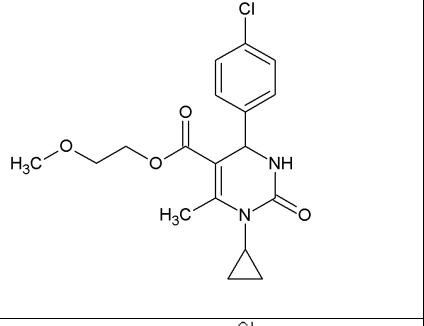
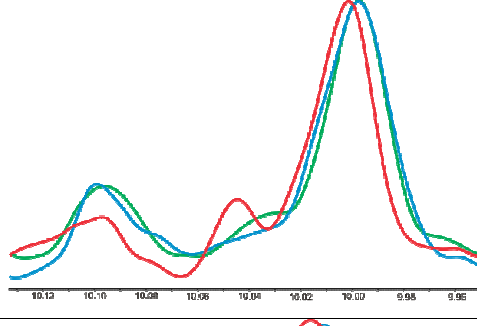
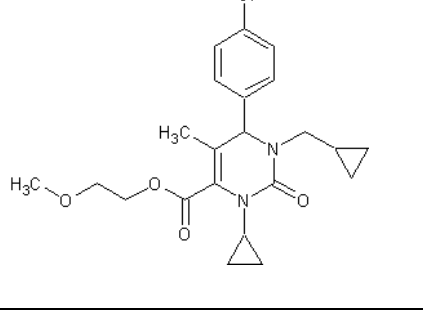
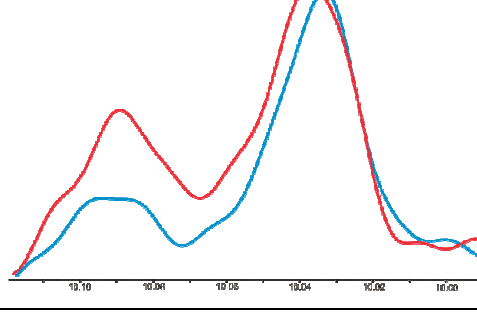
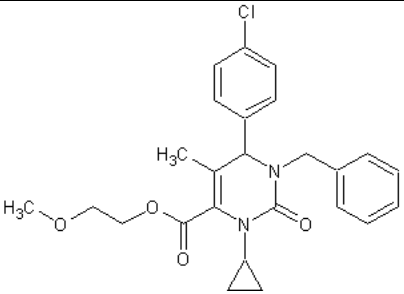
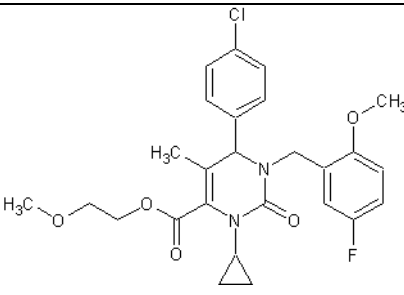
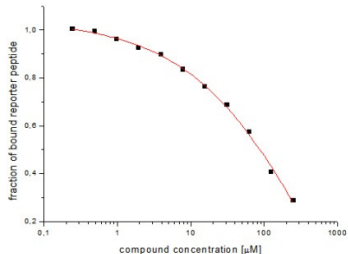
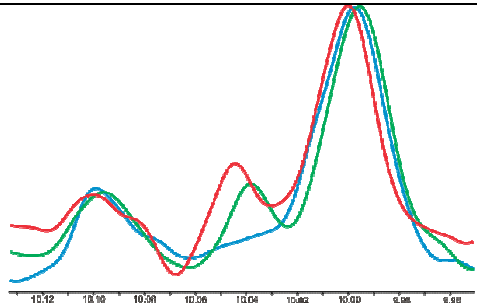
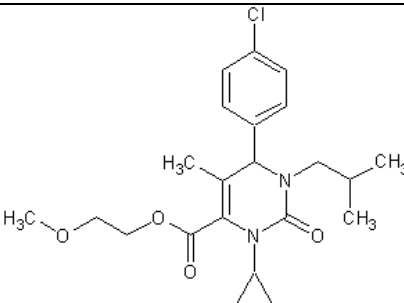
Si61		515	17			
------	---	-----	----	--	--	--

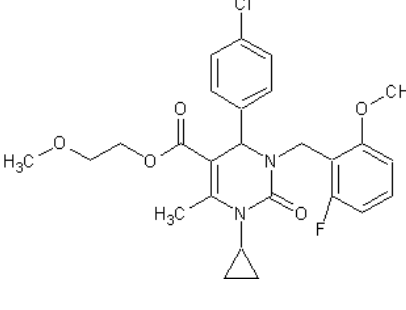
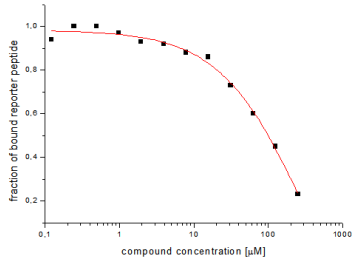
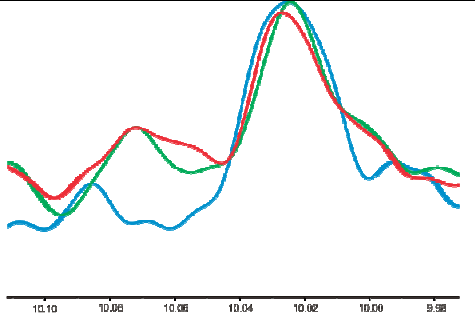
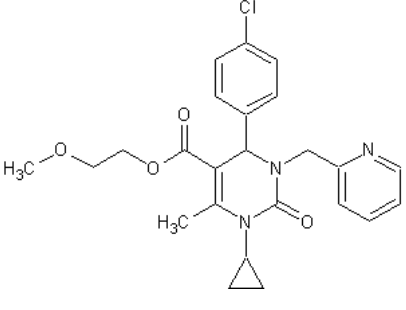
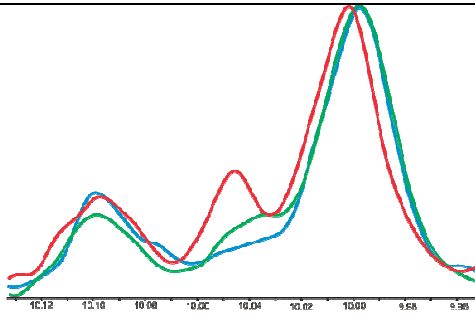
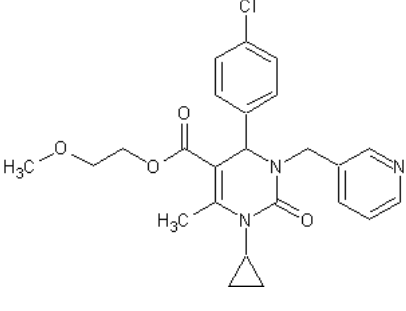
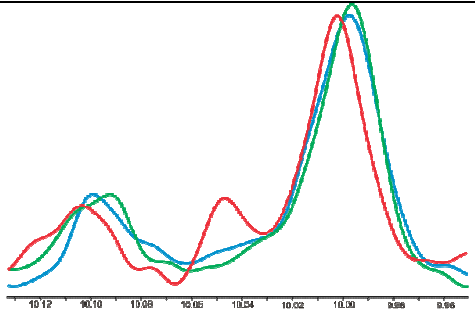
Table 2: Synthesized 3,4-dihydropyrimidin-2(1H)-ones and their interaction with Mdm2.

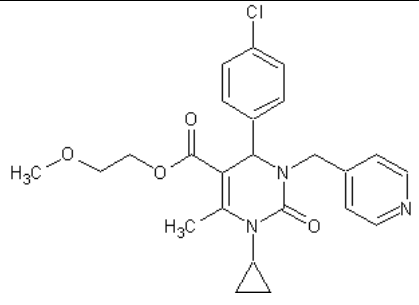
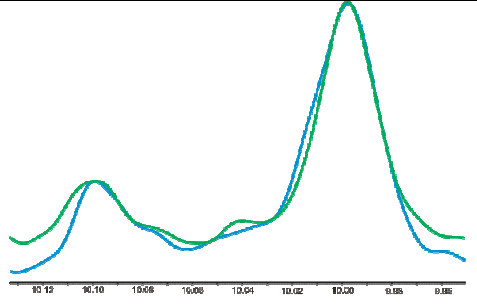
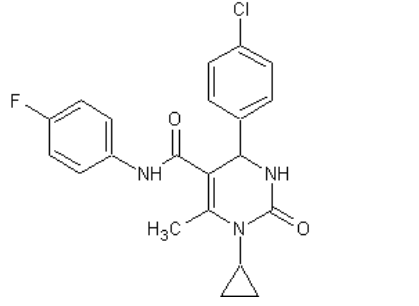
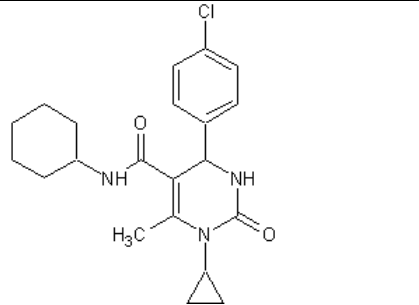
Name	Formula	MW [g/mol]	FP K_i [μ M]		AIDA K_i [μ M]	AIDA plot
Synt2		401			weak	

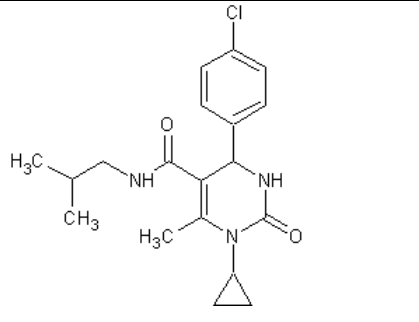
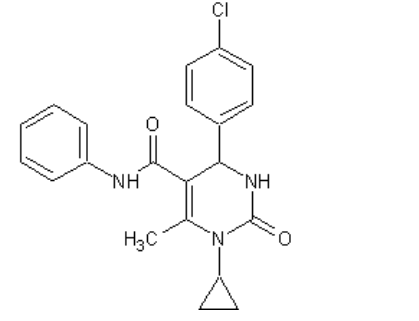
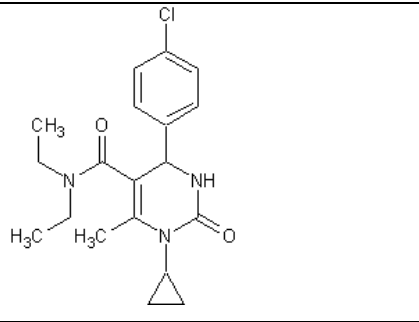
Synt3		436			weak	
Synt4		369			weak	
Synt8		334			40	

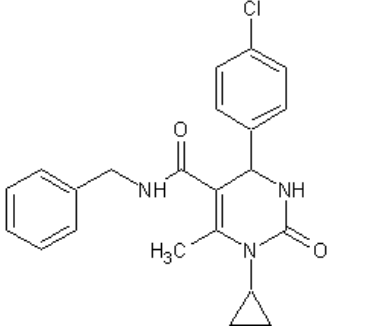
Synt9		352			No interaction	
Synt10		364			4	
Synt10A		418			20	

Synt10B		455			No interaction	
Synt10C		502	24		4	
Synt10D		456			No interaction	

Synt10G		502	13		2	
Synt13O		456			13	
Synt13M		456			13	

Synt13P		456			13	
Synt20		399			weak	
Synt40		387	weak			

Synt41		361	weak			
Synt44		381	weak			
Synt45		361	weak			

Synt48	 <chem>Cc1c(C(=O)NCC2=CC=CC=C2)c3c(c(=O)[nH]3)N1CC1c4ccc(Cl)cc4</chem>	395	weak			
--------	---	-----	------	--	--	--

The optimization lead to the stronger binding to Mdm2, which increased the compound's capability of disrupting the Mdm2-p53 complex. This was achieved by adding large chlorinated-aromatic substituents that were able to exploit the hydrophobic space inside the p53 binding pocket of Mdm2 and if possible adding structural elements able to form hydrogen bonds with Mdm2 (Figure 14 and Figure 15).

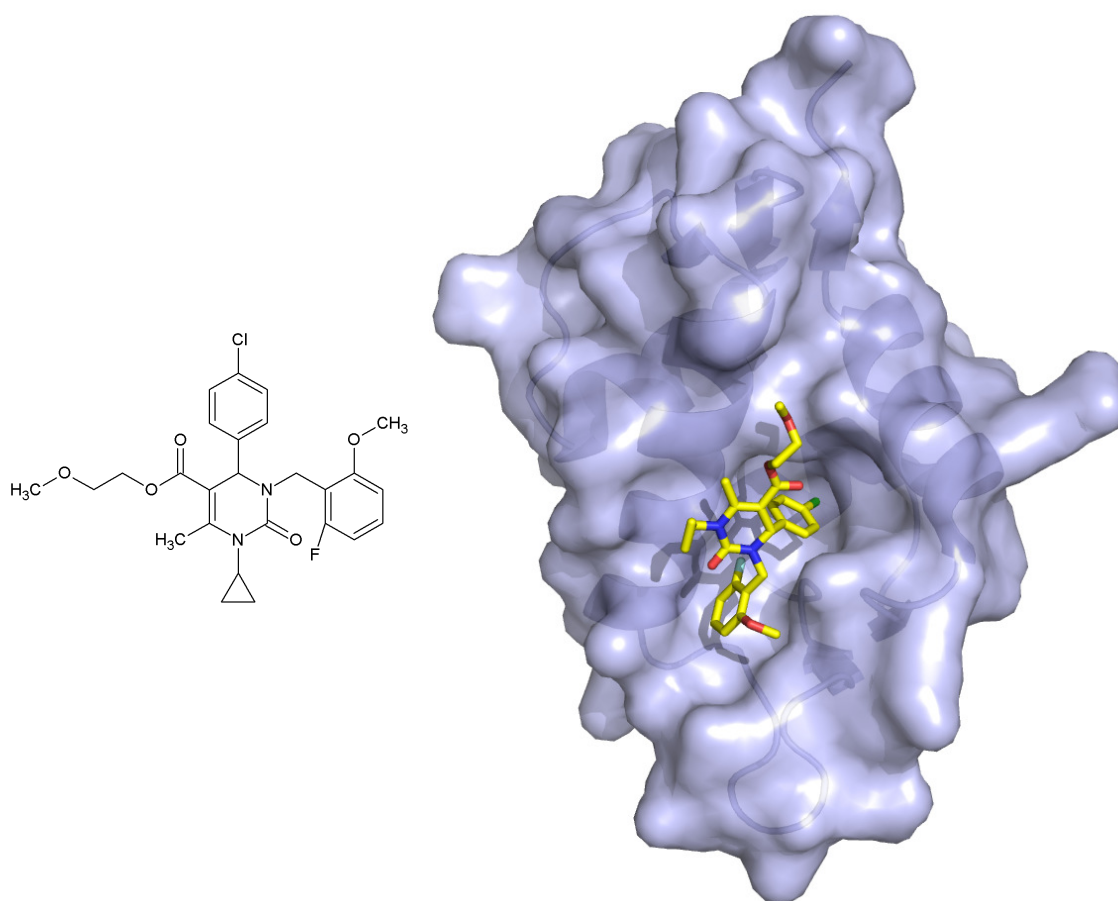


Figure 14: The formula of synt10G, the model of its interaction with Mdm2.

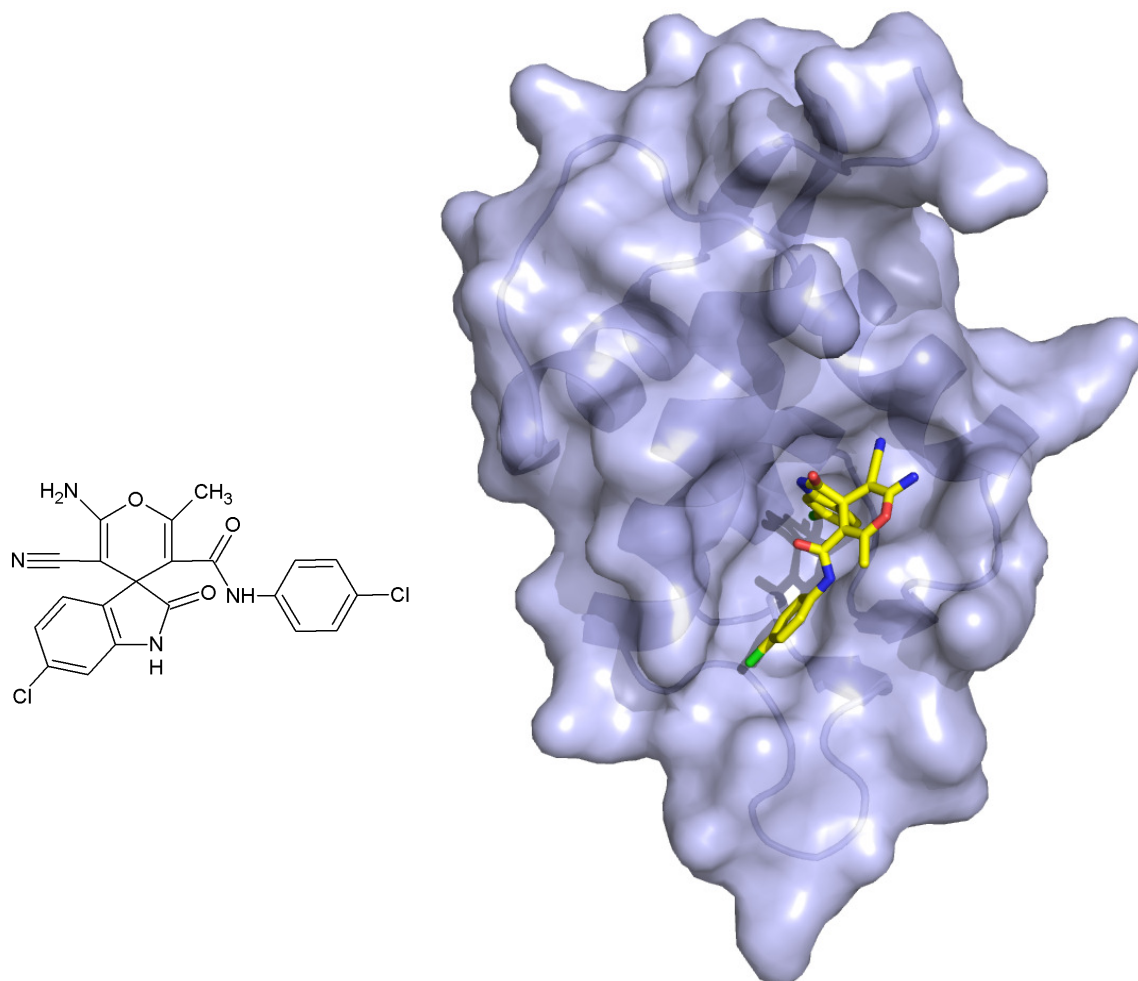


Figure 15: The formula of SI3 and the model of its interaction with Mdm2.

The fluorescence polarization assay binding curves for the strongest compounds are shown in Figure 16. Detailed binding affinities are summarized in Tables 1 and 2. Strongest-binding compounds were subjected to AIDA-NMR assays.

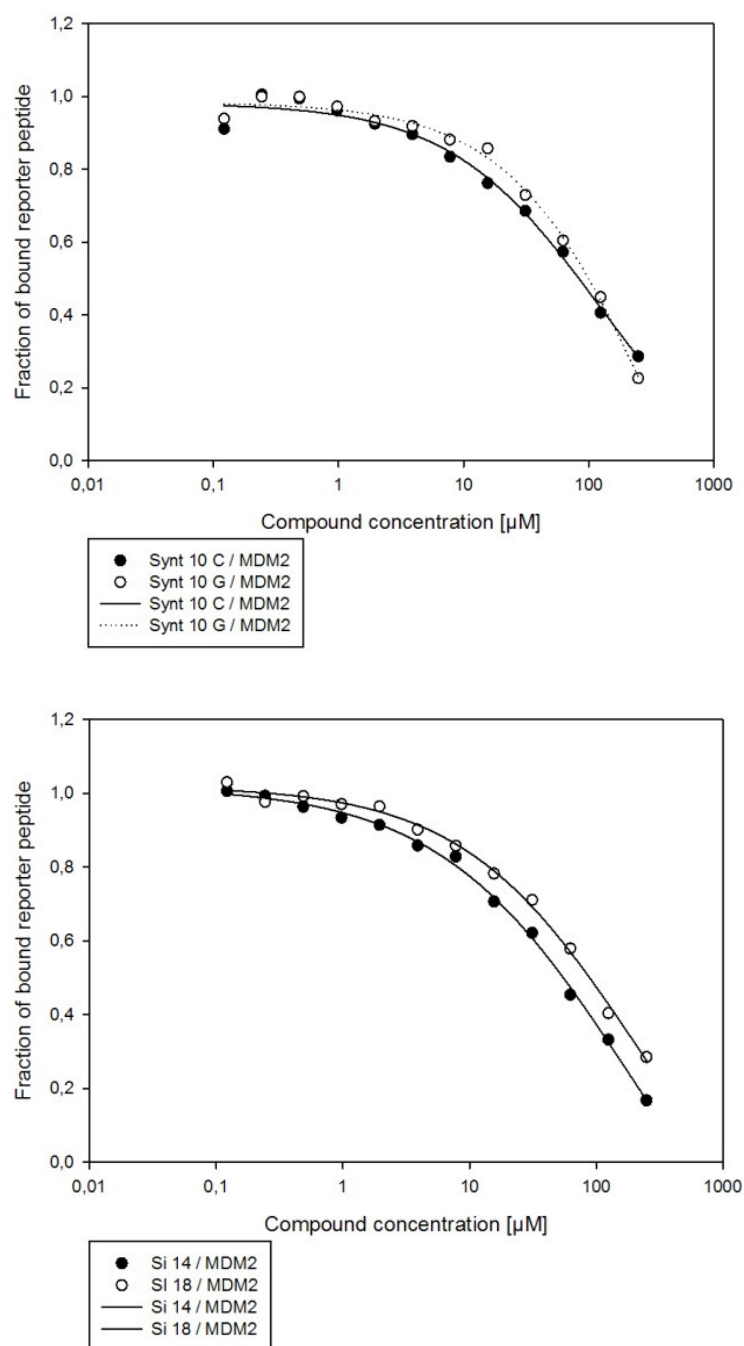


Figure 16. Fluorescence polarization graphs of the strongest ligands from (a) 3,4-dihydropyrimidin-2(1H)-one and (b) spiro[oxindole-3,4'-(4'H-pyran)] family. For Si14 $K_i = 55 \mu\text{M}$, Si18 $K_i = 21 \mu\text{M}$, Synt10C $K_i = 23 \mu\text{M}$, Synt10G $K_i = 23 \mu\text{M}$.

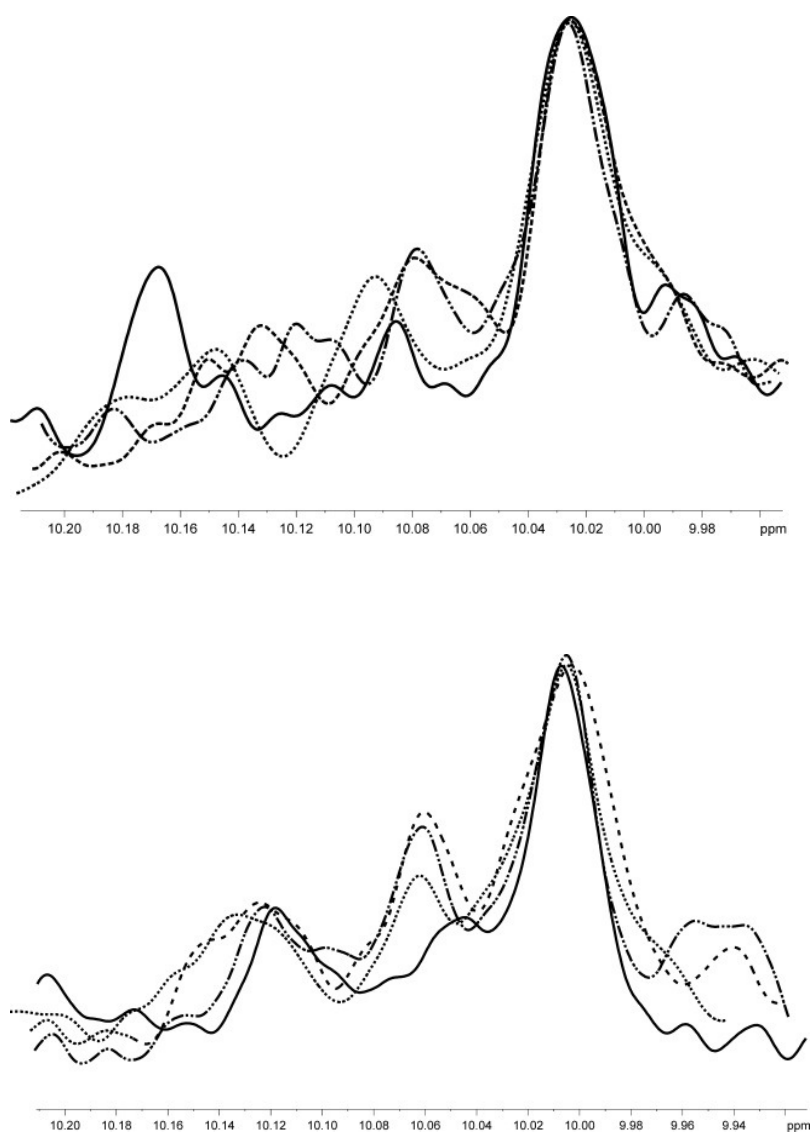


Figure 17. One-dimensional NMR-AIDA assay for synt10G (up) and si3 (down). The reference, the p53-Mdm2 complex, solid line; after addition of the compound up to concentration 1:1 dotted line, 2:1; dashed line, 5:1 dotted-dashed line. The rising peak at 10.08 ppm indicates release of p53 from Mdm2.

Based on the AIDA-NMR assay it was possible to calculate the values of K_i for the measured compounds. The percentage of the recovery of the Trp23 signal from the p53 was estimated after each step of the titration. And the K_i could be calculated from Krajewski et al. (2007) (Table 1 and Table 2). For Synt10G, the recovery after the first step of titration was estimated 20% and did not change after further addition of the compound. It can indicate that the saturation of compound in the solution has already been reached. That is why for those steps the values of K_i have not been

calculated. For compound Si3, the recovery 50% has been reached in the second step. It did not change after further titration (Figure 17). In that case the K_i has been calculated for both steps. For Synt10G $K_i = 4 \mu\text{M}$, for Si3 $K_i = 1.5 \mu\text{M}$. The collected data allowed to verify the models of interaction of 3,4-dihydropyrimidin-2(1H)-ones and spiro[oxindole-3,4'-(4'*H*-pyran)]es.

The 2-fluoro-5-methoxybenzyl of synt10G mimics Phe19 of p53 and thus increases the binding. In addition, the 2-methoxyethyl ester group is exposed into the solvent and increases the solubility of the compound, which is otherwise low. Attempts to use this position to fill in the Leu26 failed, probably due to the decreased solubility, the compounds with more hydrophobic esters or amides gave barely detectable interaction with Mdm2, even without any hydrophobic substituent at the N1 nitrogen. The function of the cyclopropyl group exposed into solvent is not well understood; replacing it with a hydrophilic substituent decreases the binding. The same is true for larger hydrophobic groups.

The potency of spiro[oxindole-3,4'-(4'*H*-pyran)]es improved after replacing the 2-methoxyethyl group with 4-chlorophenyl group, which decreased the compounds solubility, but created additional interactions with the protein in its Phe26 binding pocket. Larger chlorinated, aromatic systems in this position did not lead to any improvement, especially if there was the substitution in the ortho or meta positions of the phenyl ring, the compounds' binding was greatly decreased. The compounds with aliphatic amides showed, for the best cases, only weak interaction with Mdm2. The compounds with the nitrile group replaced by various amides were tested in order to exploit the potential interaction in the Leu26 binding pocket, though none of them was able to disrupt the Mdm2 binding. In the model of the complex of Si3 with Mdm2 in Figure 15 not much space is visible in the Leu26 pocket, which can be the reason why the compounds with large groups targeting this place may not fit into the binding cleft of Mdm2.

4.2. 2,3-dihydroquinazolin-4(1H)-ones

7-chloro-2,3-dihydroquinazolin-4(1H)-one of Figure 18 showed an interaction with Mdm2 in the fluorescence polarization assay.

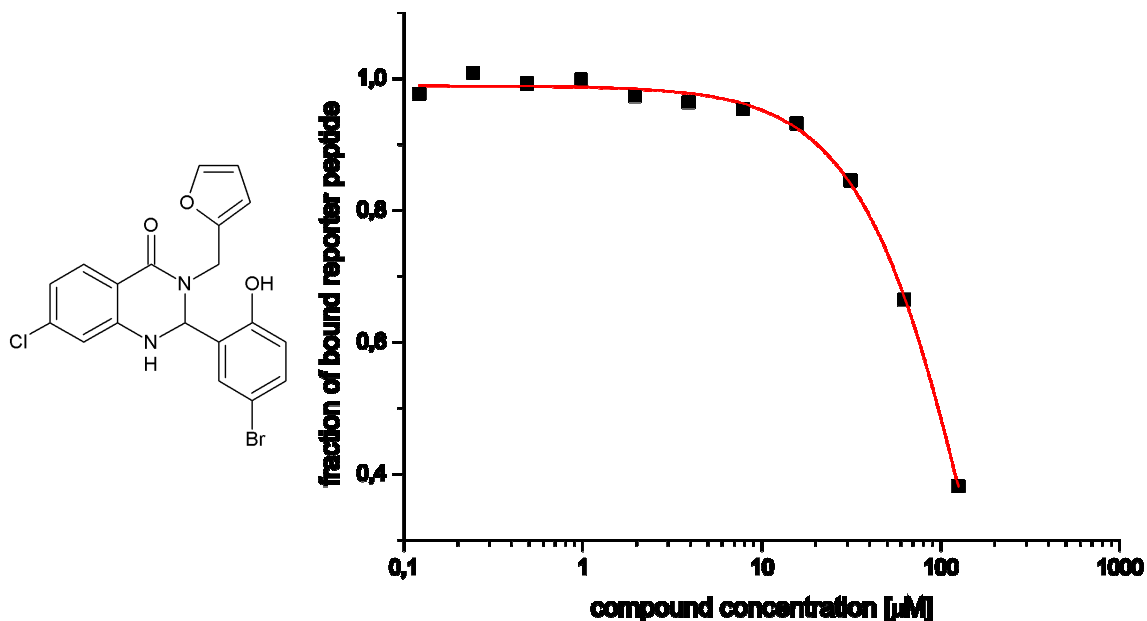
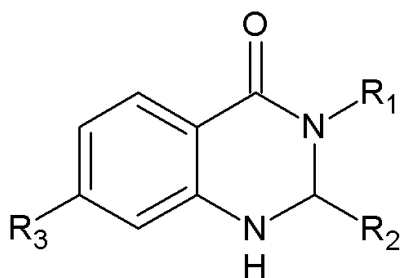


Figure 18: 7-chloro-2,3-dihydroquinazolin-4(1H)-one and the corresponding fluorescence polarization assay of its binding to Mdm2.

The calculated K_i was 20 μM , which qualified it for the optimization. The compounds were synthesized in a one step, multicomponent reaction, carried out under reflux in ethanol as a solvent. A big variety of primary amines and aldehydes are commercially available and relatively cheap, which made the optimization easy from the synthetic point of view. The use of 4-chloroisatoic anhydride caused the reaction to proceed much slower and with significantly lower yield than with the unsubstituted isatoic anhydride. The reactions with 4-chloroisatoic anhydride required much more time to complete and more care during the product purification. All the compounds were synthesized as racemic mixtures and the enantiomers were not separated.

The 2,3-dihydroquinazolin-4(1H)-one scaffold (Scheme 32) was kept the same during the optimization.

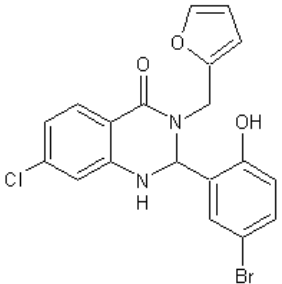
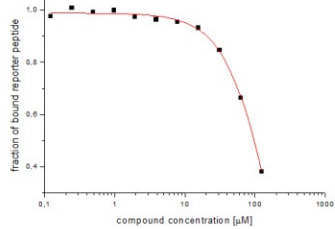
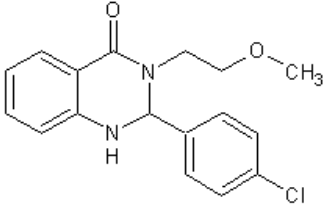
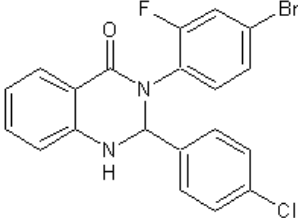


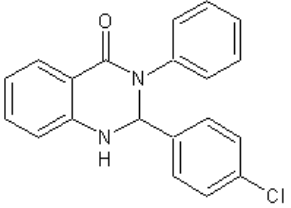
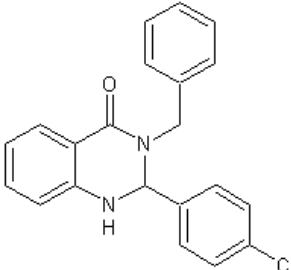
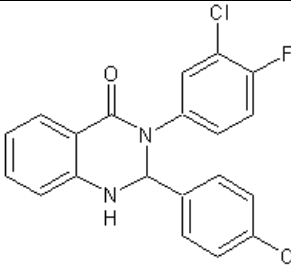
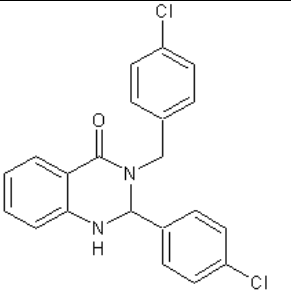
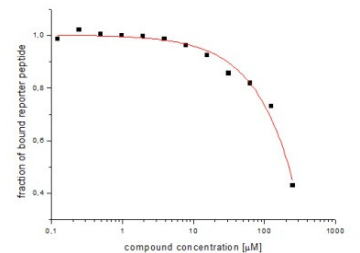
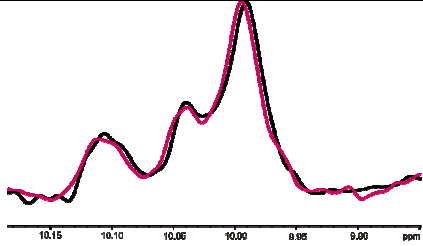
Scheme 32: The core 2,3-dihydroquinazolin-4(1H)-one scaffold of the Q type compounds.

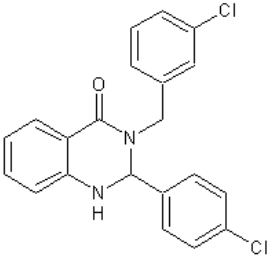
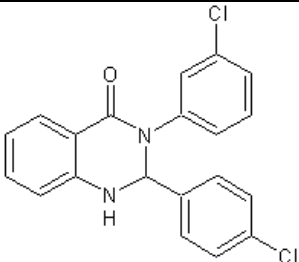
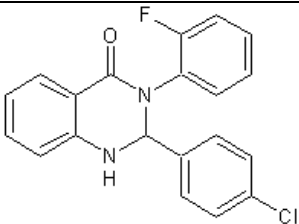
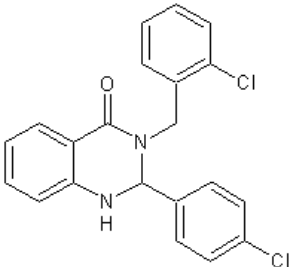
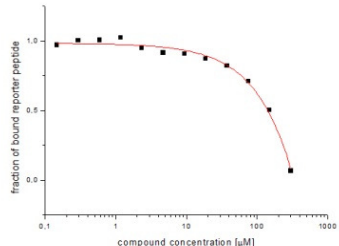
The first step of the optimization was finding the best substituent in the R_1 position, which was accomplished by using different primary amines in the synthesis. 2-hydroxy-4-bromophenyl was expected to occupy the Trp23 binding pocket of the Mdm2 protein; however, 4-chlorophenyl or 6-chloroindole are more preferred groups in this place than 2-hydroxy-4-bromophenyl. During the optimization of the R_1 substituent, R_2 was changed to 4-chlorophenyl, which was expected to fit the protein binding site better and the chlorine was removed from the position R_3 to make the synthesis easier. The synthesized compounds were screened with the fluorescence polarization assay, and for the best of them the ability to disrupt the Mdm2-p53 complex formation was confirmed by the NMR-based AIDA. The 4-chlorobenzyl and 2-chlorobenzyl substituents in the position R_1 were found to be the best.

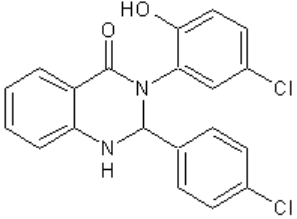
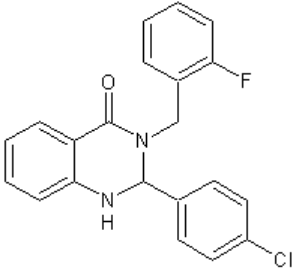
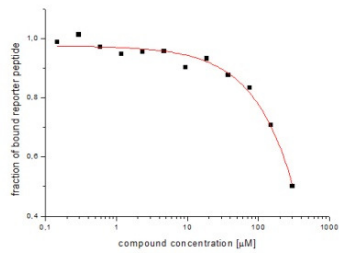
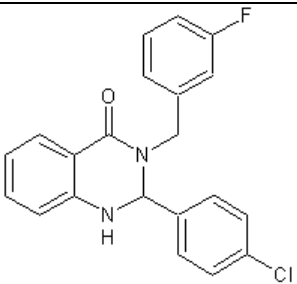
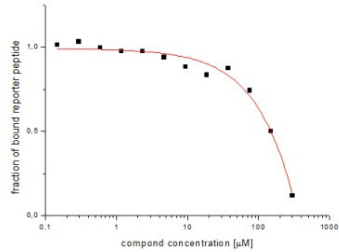
In the second step we checked whether the 4-chlorophenyl substituent in the R_2 position was a right choice and the influence of chlorine in the R_3 position was investigated. The structures of the tested compounds and the results of the binding assays are shown in Table 3. The 4-chlorophenyl in the R_2 position was indeed the right choice, even 6-chloroindole is, in this case, less optimal for the Mdm2 binding. The chlorine in the R_3 position has positive influence on the Mdm2 binding, probably because it helps to exploit more hydrophobic interactions with the protein. The structures of all synthesized 2,3-dihydroquinazolin-4(1H)-ones and the data regarding their interaction with Mdm2 is collected in Table 3; the black line in the AIDA-NMR plot is the reference spectrum of the p53-Mdm2 complex and the red one is the NMR spectrum after addition of the compound in the equimolar concentration to the protein.

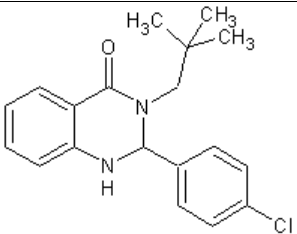
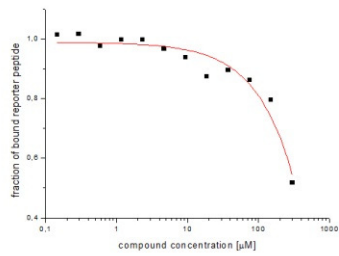
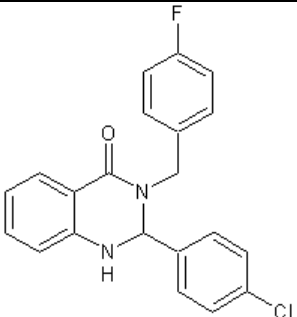
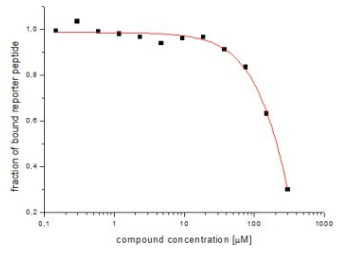
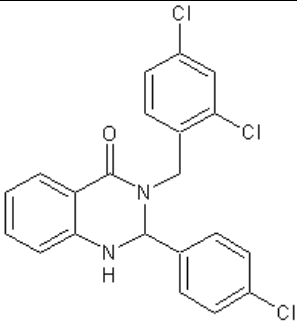
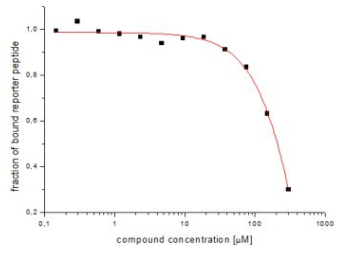
Table 3: Synthesized 2,3-dihydroquinazolin-4(1H)-ones and their interaction with Mdm2.

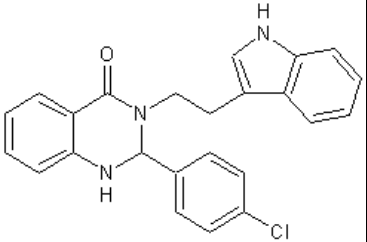
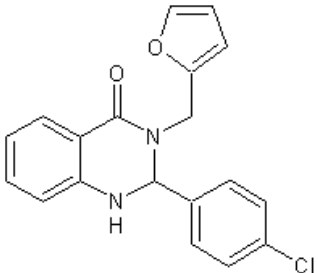
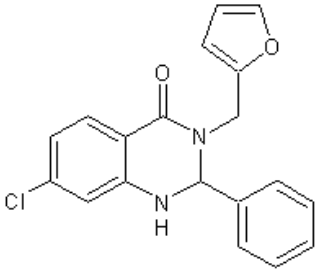
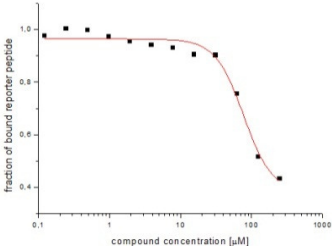
Name	Formula	M [g/mol]	FP K _i [μM]	FP plot	AIDA K _i [μM]	AIDA plot
Q0		433	20			
Q1		316	No interaction			
Q2		432	Weak			

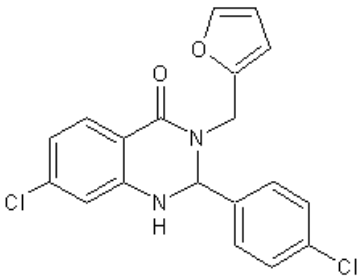
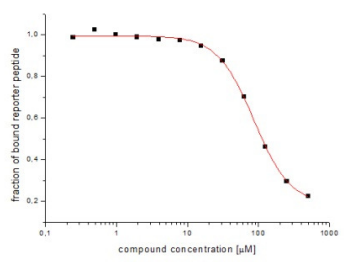
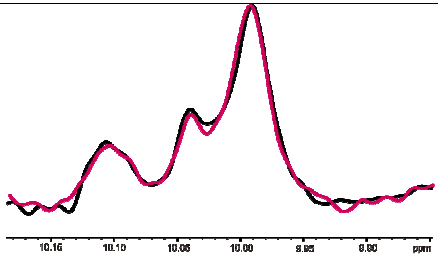
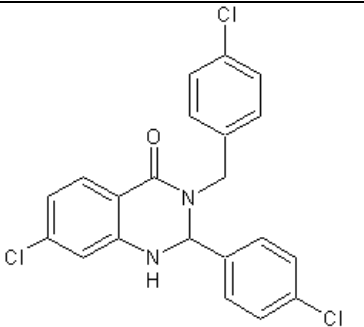
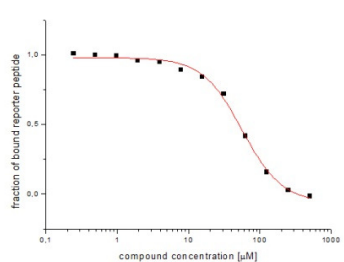
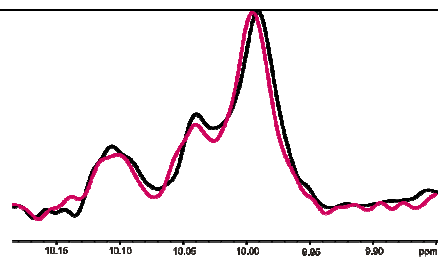
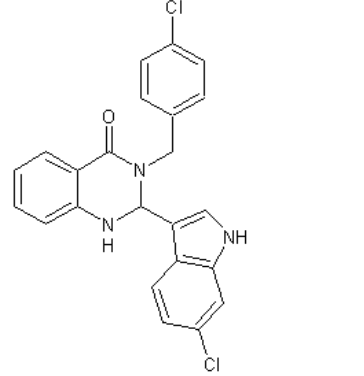
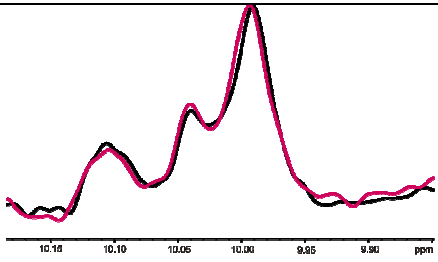
Q3		334	No interaction			
Q4		348	No interaction			
Q5		386	No interaction			
Q6		382	25		No interaction	

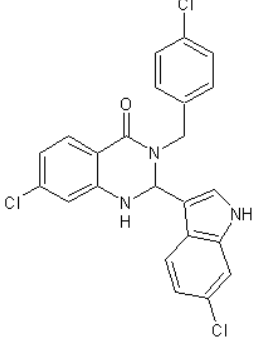
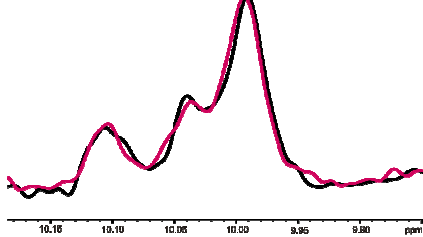
Q7		382	No interaction			
Q8		368	No interaction			
Q9		352	No interaction			
Q10		382	25			

Q11		385	No interaction			
Q12		366	66			
Q13		366	33			

Q14		328	66			
S15		366	40			
Q16		417	65			

Q17		401	No interaction				
Q19		338	No interaction				
Q20		338	24				

Q21		373	17		No interaction	
Q22		417	8		No interaction	
Q23		422	No interaction		No interaction	

Q24	 <chem>Clc1ccc(cc1)CN(Cc2ccc(Cl)cc2)C3=CNC4=CC=C(Cl)C43</chem>	455	No interaction		No interaction	
-----	---	-----	-------------------	--	-------------------	---

Among all tested 2,3-dihydroquinazolin-4(1H)-ones, compound Q22 showed the highest activity in the FP assay. It probably makes many hydrophobic interactions with the Mdm2 protein. Surprisingly, the compounds with 6-chloroindole at the R₂ position did not interact with Mdm2 at all, probably because the 6-chloroindole moiety in this position was too large for the Mdm2's binding cleft, thus 4-chlorophenyl group is the best in this position. From many tested substituents in the R₁ position, 4-chlorophenyl and 2-chlorophenyl had the most positive influence on the compounds' potency. 4-chlorination of the quinazolinone system further improved the binding to Mdm2.

The AIDA assay indicated no interaction with Mdm2-p53 complex due to low solubility of the compounds in water, despite of the addition of 10% DMSO and 0.7% of the Brij detergent, the compounds remained almost insoluble, only very low concentration of them was detectable in NMR.

4.3. 1'H-spiro[6-chloro-isoindole-1,2'-quinazoline]-3,4'(3'H)-diones

1'H-spiro[6-chloro-isoindole-1,2'-quinazoline]-3,4'(3'H)-dione of Figure 19 showed the interaction with Mdm2 in the fluorescence polarization assay as shown in the right panel of Figure 19.

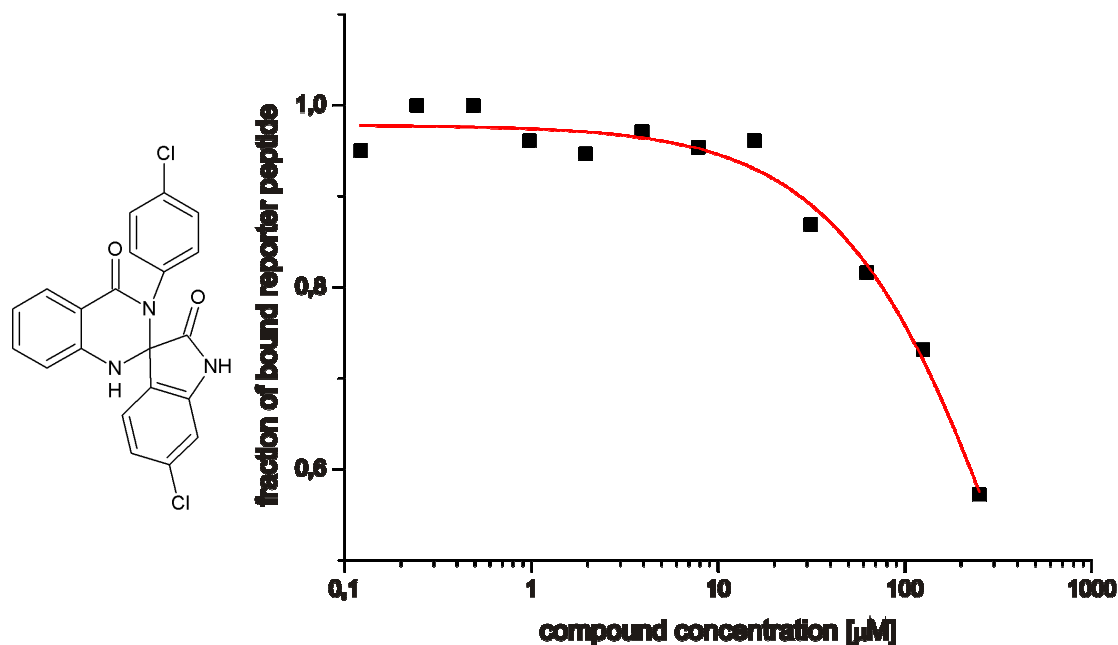


Figure 19: The structure Mdm2-binding 1'-chloro-1,2'-quinazoline]-3,4'(3'H)-dione and the corresponding fluorescence polarization assay.

The K_i calculated for this compound was 65 μM , which indicates that this compound is a weak inhibitor of the p53-Mdm2 interaction, however compounds based on a similar scaffold of 2,3-dihydroquinazolin-4(1H)-one (data shown above in chapter 3.2) shown better potency while being less rigid. It was postulated that changing the chlorophenyl in the compound shown in Figure 19 to 4-chlorobenzyl could improve the binding to Mdm2. The data from previous experiments indicated that introducing the chlorine to 1,2'-quinazoline]-3,4'(3'H)-dione system cause the potency improvement, so the influence of the 7-chloro substitution on the Mdm2 binding was investigated also in this case. In this case the heavy chlorination caused the solubility problems, some compounds with the furfuryl group instead of 4-chlorobenzyl have also been synthesized.

The compounds were synthesized in one step multicomponent reaction carried out under reflux in ethanol, described in detail in "Materials and methods" chapter. Usually the reaction was completed in 8 h or 16 h when the chlorinated isatoic anhydride was one of the substrates. The products were purified by RP HPLC. The substances were synthesized as racemic mixtures and the enantiomers were not

separated. The yields of the substances were low and they were isolated in only small amounts (2-7 mg). The purity was checked on TLC, of which the UV photo is shown in Figure 20. The compounds purity was estimated to be around 90% which was enough to make the measurements of the compounds activity for the p53-Mdm2 inhibition.

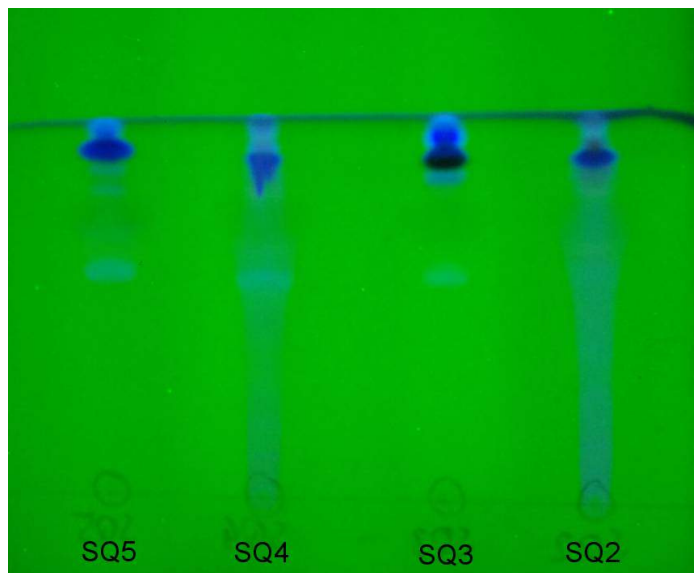
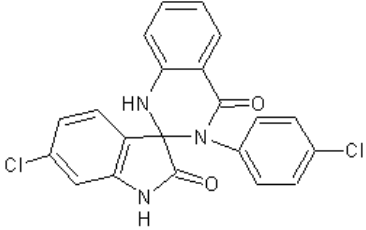
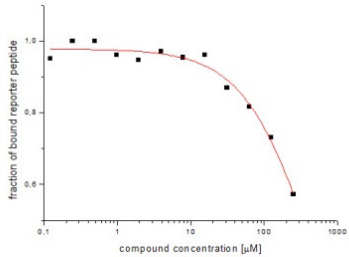
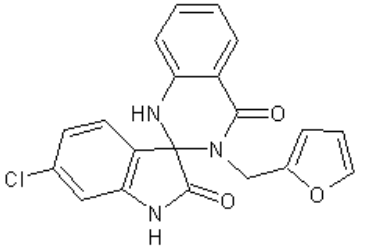
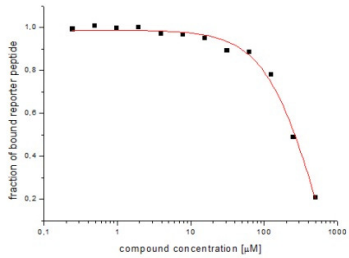
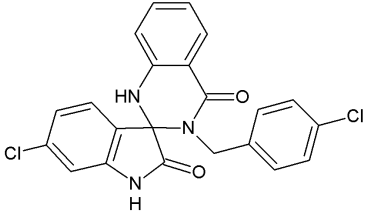
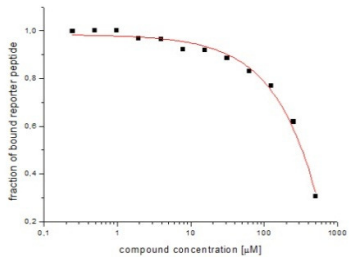
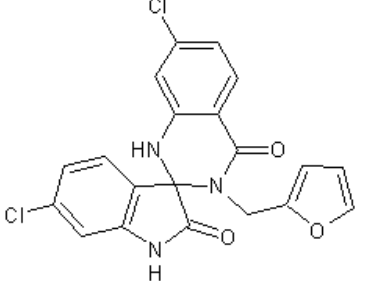
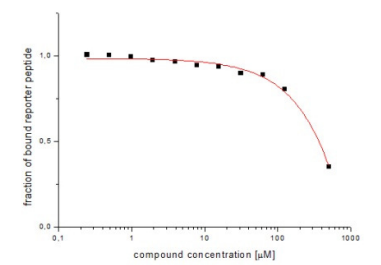
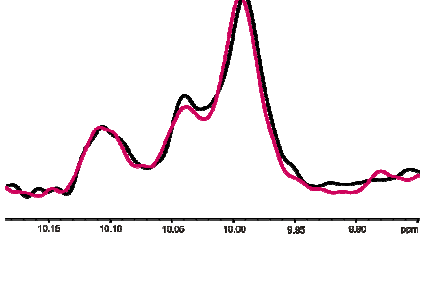
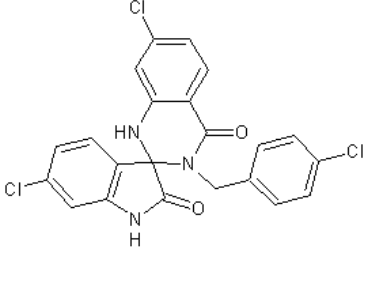
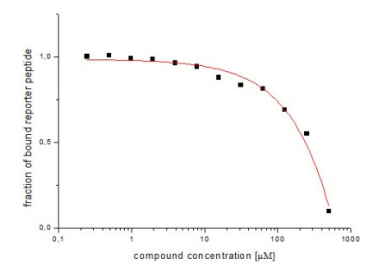
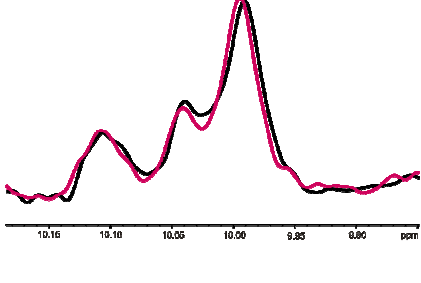


Figure 20: A photo of silica TLC plate with SQ compounds. The compounds were applied onto a plate as DMSO solutions and a running mixture was methanol/chlorophorm/water 50/20/4. The large, dark spots are the desired compounds, some minor amounts of impurities and visible.

The compounds were subjected to the FP assay and the capability of disrupting the p53-Mdm2 complex of the best of them was confirmed by the AIDA-NMR. The results of the measurements are collected in Table 4 below, the black line in the AIDA plot is the reference NMR spectrum of the p53-Mdm2 complex and the red one is the NMR spectrum after adding the compound in equimolar concentration to the protein.

Table 4: Synthesized 1'H-spiro[6-chloro-isoindole-1,2'-quinazoline]-3,4'(3'H)-diones and their interaction with Mdm2

Name	Formula	M [g/mol]	FP K_i [μ M]	FP plot	AIDA K_i [μ M]	AIDA plot
SQ1		410	65			
SQ2		379	55			
SQ3		424	63			

SQ4		413	54		No interaction	
SQ5		457	47		No interaction	

An attempt to improve the binding of 1'H-spiro[6-chloro-isoindole-1,2'-quinazoline]-3,4'(3'H)-diones did not succeed, all synthesized compounds had comparable K_i in FP assay. The connection between the quinazolinone and 6-chlorospiroindole moieties in these compounds is very rigid. Further structural analysis indicated that quinazolinone and 6-chlorospiroindole moieties are in unfavorable relative positions to each other, so if the 6-chlorospiroindole binds in the Trp23 binding pocket of Mdm2, than the quinazolinone system is placed in parallel to the surface of the protein, so it cannot interact with either the Phe19 or the Leu26 binding pockets. The AIDA assay confirmed that these compounds did not interact "well" with the Mdm2 protein.

5.1. Summary

This thesis presents my research on the discovery, design, and development of small molecule antagonists for the p53-Mdm2 interaction. The tumor suppressor protein p53, protects the organism from cancer. In order to escape the p53 mediated safeguard system, most of human cancers have either mutated the p53 or decreased effectiveness of the p53 pathway. In tumors which retain the wildtype p53, it is mostly inactivated by its negative regulators, the Mdm2 and Mdmx proteins. Mdm2, the first to gain the distinction of a principal inhibitor of p53, promotes ubiquitination of p53 followed by degradation in the proteasome.

The restoration of the impaired function of p53, by disrupting the Mdm2-p53 and Mdmx-p53 interactions, offers a new paradigm for anticancer therapy across a broad spectrum of cancers. Cancer cells are extremely sensitive to the restoration of p53.

Four groups of low molecular weight, organic compounds have been synthesized, tested and optimized in order to achieve the strongest interaction with the Mdm2 protein. The four groups comprised the scaffolds of 3,4-dihydropyrimidin-2(1H)-ones, spiro[oxindole-3,4'-(4'*H*-pyran)]es, 2,3-dihydroquinazolin-4(1H)-ones, 1'*H*-spiro[6-chloro-isoindole-1,2'-quinazoline]-3,4'(3'*H*)-diones. These structures were extended with variants that possessed an array of different substituents in order to exploit more possible interactions between the compounds and the protein. Using the multicomponent reactions a large variety of compounds with different substituents were synthesized and tested in the fluorescence polarization assay and in the NMR-based antagonist induced dissociation assay, AIDA-NMR. The best of the herein described inhibitors have single digit micromolar potency for disrupting the p53-Mdm2 interaction.

The aqueous solubility of the current derivatives of the scaffolds described in this thesis is low. This is because the protein-protein interaction of p53 and Mdm2 is highly hydrophobic and naturally results in very hydrophobic initial antagonists. In order to achieve high enough concentrations of the antagonist in the aqueous solution of the target protein for NMR measurements, we often used Tween as a solubilizer. For the future, we would need to improve water solubility of the p53-

Mdm2 antagonists discovered for this thesis. We are working toward next generations of antagonists with sufficient water solubility that will not need a solubilizing additive. In general, the proposed way to improve the potency and water solubility of the best scaffolds involves systematic variation of different substituents around their cores; for example, for the improved water solubility via introduction of a hydroxyl methyl or dialkylamino methyl groups.

5.2. Zusammenfassung

In dieser Arbeit werden die Forschungsergebnisse über die Entdeckung, Entwurf und Entwicklung von niedermolekularen Antagonisten der p53-Mdm2 Interaktion präsentiert. Der Tumorsuppressor p53 schützt den Organismus vor Krebs. Um das p53-regulierte Sicherheitssystem zu umgehen besitzen die meisten Krebsarten entweder ein mutiertes *p53* Gen oder eine verminderte Aktivität im p53-Weg. In Tumoren, die das Wildtyp-*p53* Gen exprimieren, wird p53 durch seine negativen Regulatoren Mdm2 und Mdmx inaktiviert. Mdm2, der als erstes als hauptsächlichen Inhibitor von p53 entdeckt wurde, fördert die Ubiquitinierung von p53, was die Degradierung durch das Proteosom zur Folge hat.

Die Wiederherstellung der beeinträchtigten p53-Funktion, durch die Trennung der p53-Mdm2 und p53-MdmxKomplexe, steigert die Chancen einer Krebstherapie gegen einer Vielfalt von Krebsarten. Krebszellen sind sehr sensitiv gegenüber der Restaurierung von p53.

Vier Gruppen organischer Moleküle wurden synthetisiert, getestet und optimiert, um die stärkste Interaktion mit Mdm2 zu erhalten. Diese vier Gruppen bestehen aus 3,4-dihydropyrimidin-2(1H)-on, spiro[oxindole-3,4'-(4'H-pyran)], 2,3-dihydroquinazolin-4(1H)-on und 1'H-spiro[6-chloro-isoindole-1,2'-quinazoline]-3,4'(3'H)-dion. Diese Strukturen wurden mit Varianten verschiedener Substituenten verlängert, um mögliche Interaktionen zwischen der Verbindung und dem Protein zu entdecken. Eine große Vielfalt von Verbindungen mit verschiedenen Substituenten wurden durch die Multikomponentenreaktion synthetisiert, die durch der fluoreszenz polarisations Untersuchung und der NMR basiertem „antagonistinduced dissociation“ Untersuchung getestet worden sind. Die Besten hier beschriebenen Inhibitoren sind im mikromolarem Bereich wirksam.

Die Wasserlöslichkeit der Derivaten der hier beschriebenen Verbindungsklassen ist niedrig. Der Grund hierfür ist, dass die Interaktionsfläche zwischen p53 und Mdm2 sehr hydrophob ist, wodurch zunächst auch sehr hydrophobe Antagonisten entstehen. Um für die NMR-Messungen eine genügend hohe Konzentration in wässriger Lösung des p53-Mdm2 Antagonisten zu erlangen, wurde zur Solubilisierung Tween hinzugefügt.

Wir arbeiten an der Entwicklung von Antagonisten mit ausreichender Wasserlöslichkeit, wo die Zugabe von solubilisierenden Agentien überflüssig wird. Generell verbessert man die Löslichkeit der besten Verbindungsklassen durch eine systematische Variierung verschiedener Substituenten um deren Grundkörper, z.B. wird die Wasserlöslichkeit durch die Einführung einer hydroxymethyl oder dialkylaminomethylgruppe verbessert.

6. Appendix**6.1. Abbreviations:**

1D	one-dimensional
AIDA	antagonist induced dissociation assay
bp	base pair
Da	Dalton (g/mol)
DMSO	dimethylsulfoxide
DNA	deoxyribonucleic acid
DMF	N,N-dimethylformamide
DMSO	dimethylsulfoxide
DTT	dithiothreitol
EDTA	ethylenediamine tetraacetic acid
Et	ethyl
FP	Fluorescence polarization assay
g	gravitational acceleration (9.81 m/s ²)
h	hour
HPLC	high pressure liquid chromatography
IC50	half maximal inhibitory concentration
IPTG	isopropyl- β -thiogalactopyranoside
K _i	inhibition constant
LB	lysogeny broth medium
Me	methyl
Mdm2	Murine double minute - 2

MdmX	Murine double minute – 4
min	minute
MW	molecular weight
NiNTA	nickel-nitrilotriacetic acid
NMR	nuclear magnetic resonance spectroscopy
OD	optical density
PAGE	polyacrylamide gel electrophoresis
PBS	phosphate-buffered saline
PDB	Protein Data Bank
ppm	parts per million
RNA	ribonucleic acid
RP	reversed phase
rpm	revolutions per minute
SDS	sodium dodecyl sulfate
TAE	tris – acetate – EDTA buffer
TEMED	N,N,N',N'-tetramethylethylenediamine
Tris	tris(hydroxymethyl)aminomethane
TLC	thin layer chromatography
MS	mass spectrometry
Mdm2	Murine double minute - 2
Mdmx, Mdm4	Murine double minute - 4

6.2. Protein and peptide sequences:

Mdm2 (1-125):

MCNTNMSVPT DGAVTTSQIP ASEQETLVRP KPLLLKLLKS VQAQKDTYTM
KEVLFYLGQY IMTKRLYDEK QQHIVYCSND LLGDLFGVPS FSVKEHRKIY
TMIYRNLVVV NQQESSDSGT SVSEN

p53 (1-321):

MEEPQSDPSV EPPLSQETFS DLWKLLPENN VLSPLPSQAM DDLMLSPDDI
EQWFTEDPGP DEAPRMPEAA PPVAPAPAAP TPAAPAPAPS WPLSSSVPSQ
KTYQGSYGFR LGFLHSGTAK SVTCTYSPAL NKMFCQLAKT CPVQLWVDST
PPPGTRVRAM AIYKQSQHMT EVVRRCPHHE RCSDSDGLAP PQHLIRVEGN
LRVEYLDDRN TFRHSVVVPY EPPEVGS DCT TIHYNMCNS SCMGGMNRPP
ILTIITLEDS SGNLLGRNSF EVRVCACPGR DRRTEENLR KKGEPHHELP
PGSTKRALPN NTSSSPQPKK K

High affinity Mdm2 binding peptide for FP:

LTFEHYWAQLTS

7. References

- J.G. Allen, M.P. Bourbeau, G.E. Wohlhieter, M.D. Bartberger, K. Michelsen, R. Hungate, R.C. Gadwood, R.D. Gaston, B. Evans, L.W. Mann, M.E. Matison, S. Schneider, X. Huang, D. Yu, P.S. Andrews, A. Reichelt, A.M. Long, P. Yakowec, E.Y. Yang, T.A. Lee, J.D. Oliner, *Discovery and optimization of chromenotriazolopyrimidines as potent inhibitors of the mouse double minute 2-tumor protein 53 protein-protein interaction*. J. Med. Chem. 52 (2009) 7044-7053.
- M. Bista, K. Kowalska, W. Janczyk, A. Dömling and T.A. Holak, *Robust NMR screening for lead compounds using tryptophan-containing proteins*. J. Amer. Chem. Soc. 131 (2009) 7500-7501.
- A. Boettcher, N. Buschmann, P. Furet, J. Groell, J. Kallen, L.J. Hergovich, K. Masuya, L. Mayr, A. Vaupel, *3-Imidazolyl-Indoles for the Treatment of Proliferative Diseases*. WO 2008/119741.
- P. R. Brodfuehrer, B. Chen, T. R. Sattelberg, Sr., P. R. Smith, J. P. Reddy, Derron R. Stark, S. L. Quinlan, and J. G. Reid, *An Efficient Fischer Indole Synthesis of Avitriptan, a Potent 5-HT_{1D} Receptor Agonist*. J. Org. Chem. 62 (1997) 9192-9202.
- R. J. Clemens and J. A. Hyatt, *Acetoacetylation with 2,2,6-trimethyl-4H-1,3-dioxin-4-one: A Convenient Alternative to Diketene*. J. Org. Chem. 50 (1984) 2431-2435.
- M.D. Cummings, C. Schubert, D.J. Parks, R.R. Calvo, L.V. LaFrance, J. Lattanze, K.L. Milkiewicz, T. Lu, *Substituted 1,4-benzodiazepine-2,5-diones as alpha-helix mimetic antagonists of the HDM2-p53 protein-protein interaction*. Chem. Biol. Drug. Des. 67 (2006) 201-205.
- Y.C. Chang, Y.S. Lee, T. Tejima. *Mdm2 and bax, downstream mediators of the p53 response, are degraded by the ubiquitin-proteasome pathway*. Cell Growth Differ. 9 (1998) 79-84.
- L. Chen, H. Yin, B. Farooqi, S. Sebti, A.D. Hamilton, J. Chen. *P53 alpha-helix mimetics antagonize p53/MDM2 interaction and activate p53*. Mol. Cancer. Ther. 4 (2005) 1019-1025.

- C. Cordon-Cardo, E. Latres, M. Drobnjak, M.R. Oliva, D. Pollack, J.M. Woodruff, V. Marechal, J. Chen, M.F Brennan, A.J. Levine, *Molecular Abnormalities of MDM2 and p53 Genes in Adult Soft Tissue Sarcomas*. *Cancer Res.* 54 (1994) 794-799.
- A. Czarna, G.M. Popowicz, A. Pecak, S. Wolf, G. Dubin and T.A. Holak, *High affinity interaction of the p53 peptide-analogue with human Mdm2 and MdmX*. *Cell Cycle* 8 (2009) 1174-1183.
- M. Dabiri, P. Salehi, S. Otokesh, M. Baghbanzadeh, G. Kozehgarya and A. A. Mohammadia, *Efficient synthesis of mono- and disubstituted 2,3-dihydroquinazolin-4(1H)-ones using $KAl(SO_4)_2 \cdot 12 H_2O$ as a reusable catalyst in water and ethanol*. *Tet. Lett.* 46 (2005) 6123–6126.
- W.S. El-Deiry, S.E. Kern, J.A. Pietenpol, K.W. Kinzler, B. Vogelstein. *Definition of a consensus binding site for p53*. *Nat. Genet.* 1 (1992) 45-49.
- K. Ding, Y. Lu, Z. Nikolovska-Coleska, G. Wang, S. Qiu, S. Shangary, W. Gao, D. Qin, J. Stuckey, K. Krajewski, P.P. Roller, S. Wang, *Structure-based design of spirooxindoles as potent, specific small-molecule inhibitors of theMDM2-p53 interaction*. *J. Med. Chem.* 49 (2006) 3432-3435.
- K. Ding, G. Wang, J.R. Deschamps, D.A. Parrishb, S. Wang, *Synthesis of spirooxindoles via asymmetric 1,3-dipolar cycloaddition*. *Tetrahedron Lett.* 46 (2005) 5949-5951.
- Q. Ding, B.J. Graves, N. Kong, J. Liu, A.J. Lovey, G. Pizzolato, J.L. Roberts, S. Sungsau, B.T. Vu, P.M. Wovkulich, *4,4,5,5, Tetrasubstituted Imidazolines*. US 2007/129416.
- L. D'Silva, P. Ozdowy, M. Krajewski, U. Rothweiler, M. Singh and T.A. Holak, *Monitoring the effects of antagonists on protein-protein interactions with NMR spectroscopy*. *J. Amer. Chem. Soc.* 127 (2005) 13220-13226.
- B. Elenbaas, M. Dobbstein, J. Roth, T. Shenk, and A. J. Levine. *The MDM2 oncoprotein binds specifically to RNA through its RING finger domain*. *Mol Med.* 1996 2 (1996) 439–451

- T. Ewing, I.D Kuntz, *Critical evaluation of search algorithms for automated molecular docking and database screening*. J. Comput. Chem. 18 (1997) 1175-1189.
- R. G. Fargher, *Orientation of the Nitro- and Arylazo- glyoxalines. Fission of the Glyoxalone nucleus*. J. Chem. Soc., Trans. 117 (1920) 668 – 680.
- N. Fotouhi, G.J. Haley, K.B. Simonsen, B.T. Vu, S.E. Webber. *Cis-imidazolines*. US 2007/167437.
- P.S. Galatin, D.J. Abraham. *A nonpeptidic sulfonamide inhibits the p53-Mdm2 interaction and activates p53-dependent transcription in Mdm2-overexpressing cells*. J. Med. Chem. 47 (2004) 4163-4165.
- B.L. Grasberger, T. Lu , C. Schubert, D.J. Parks, T.E. Carver, H.K. Koblish, M.D. Cummings, L.V. LaFrance, K.L. Milkiewicz, R.R. Calvo, D. Maguire, J. Lattanze, C.F. Franks, S. Zhao, K. Ramachandren, G.R. Bylebyl, M. Zhang, C.L. Manthey, E.C. Petrella, M.W. Pantoliano, I.C. Deckman, J.C. Spurlino, A.C. Maroney, B.E. Tomczuk, C.J. Molloy, R.F. Bone, *Discovery and cocrystal structure of benzodiazepinedione HDM2 antagonists that activate p53 in cells*. J. Med. Chem. 48 (2005) 909-912.
- W. Gu, Xiao-Lu Shi, R.G. Roeder. *Synergistic activation of transcription by CBP and p53*. Nature 387 (1997) 819–23.
- Y. Haupt, R. Maya, A. Kazaz, M. Oren. *Mdm2 promotes the rapid degradation of p53*. Nature 387 (1997) 296-299.
- K. Higashiyama, H. Otomasu, *Spiro Heterocyclic Compounds. III. Synthesis of Spiro[oxindole-3,4'-(4'H-pyran)] Compounds*. Chem. Pharm. Bull. 28 (1980) 648-651.
- R. Honda, H. Tanaka, H. Yasuda, *Oncoprotein is ubiquitin ligase E3 for tumor suppressor p53*. FEBS Lett. 420 (1997) 25-27.
- X. Huang. *Fluorescence Polarization Competition Assay: The Range of Resolvable Inhibitor Potency Is Limited by the Affinity of the Fluorescent Ligand*. J. Biomol. Screen. 8 (2003) 34-38.
- J.J Irwin and B.K. Shoichet, *ZINC – A Free Database of Commercially Available Compounds for Virtual Screening*. J. Chem. Inf. Model. 45(1) (2005) 177-82.

- P. N. James and H. N. Snyder, *Indole-3-aldehyde*. *Organic Syntheses* 39 (1959) 30.
- A.C. Joerger, A.R. Fersht, *Structural Biology of the Tumor Suppressor p53*. *Ann. Rev. Bioch.* 77 (2008) 557.
- T. Juven-Gershon and M. Oren *Mdm2: The Ups and Downs*. *Mol. Med.* 5 (1999) 71-83
- B.B. Kehm and C.W. Whitehead. *3-n-heptyl-5-cyanocytosine*. *Organic Syntheses*. 4 (1963) 515
- H.K. Koblish, S. Zhao, C.F. Franks, R.R. Donatelli, R.M. Tominovich, L.V. LaFrance, K.A. Leonard, J.M. Gushue, D.J. Parks, R.R. Calvo, K.L. Milkiewicz, J. JoséMarugán, P. Raboisson, M.D. Cummings, B.L. Grasberger, D.L. Johnson, T. Lu, C.J. Molloy, A.C. Maroney, *Benzodiazepinedione inhibitors of the Hdm2 : p53 complex suppress human tumor cell proliferation in vitro and sensitize tumors to doxorubicin in vivo*. *Mol. Cancer. Ther.* 5 (2006) 160-169.
- N. Kong, E.A. Liu, B.T. Vu, *Cis-imidazolines*. US 6617346 (2003).
- N. Kong, E.A. Liu, B.T. Vu, *Cis-2,4,5-triphenyl-imidazolines and their Use in the Treatment of Tumors*. WO2003/051359.
- M. Krajewski, U. Rothweiler, L. D'Silva, S. Majumdar, C. Klein and T.A Holak, An NMR-based antagonist induced dissociation assay for targeting the ligand-protein and protein-protein interactions in competition binding experiments. *J. Med. Chem.* 50 (2007) 4382-4387.
- M.H. Kubbutat, S.N. Jones, K.H. Vousden. *Regulation of p53 stability by Mdm2*. *Nature* 387 (1997) 299-303.
- S.K. Kumar, E. Hager, C. Pettit, H. Gurulingappa, N.E. Davidson, S.R. Khan, *Design, synthesis, and evaluation of novel boronic-chalcone derivatives as antitumor agents*. *J. Med. Chem.* 46 (2003) 2813-2815.
- P.H. Kussie, S. Gorina, V. Marechal, B. Elenbaas, J. Moreau, A.J. Levine, and N.P. Pavletich, *Structure of the MDM2 oncoprotein bound to the p53 tumor suppressor transactivation domain*. *Science* 274 (1996) 948-953.

- D.P. Lane, *p53, guardian of the genome*. Nature, 358 (1992) 15–16.
- J. T. Lee, W. Gu, *The multiple levels of regulation by p53 ubiquitination*. Cell Death Differ. 17 (2010) 86.
- K. Leonard, J.J. Marugan, P. Raboisson, R. Calvo, J.M. Gushue, H.K. Koblish, J. Lattanze, S. Zhao, M.D. Cummings, M.R. Player, A.C. Maroney, T. Lu, *Novel 1,4-benzodiazepine-2,5-diones as Hdm2 antagonists with improved cellular activity*. Bioorg. Med. Chem. Lett. 16 (2006)3463-3468.
- H. Lu and A.J. Levine. *Human TAFII31 is a transcriptional coactivator of the p53 protein*. Proc. Natl. Acad. Sci. USA, 92 (1995) 5154-5158.
- C.S. Marvel and G.S. Hiers, *Isatin*. Organic Syntheses 5 (1925) 71.
- J.C. Marine, G. Lozano, *p53 stabilization: the importance of nuclear import*. Cell Death Differ. 17 (2010) 93.
- J.C. Marine, A.G. Jochemsen, *MDMX and MDM2: brothers in arms?* Cell Cycle 3 (2004) 900.
- Ali A. Mohammadi, M. Dabiri, H. Qaraat, *A regioselective three-component reaction for synthesis of novel 10 H-spiro[isoindoline-1,20 -quinazoline]-3,40 (30 H)-dione derivatives*. Tet. Lett. 65 (2009) 3804–3808.
- S. S. Novikov, L. I. Khmel'nitskii, O. V. Lebedev, V. V Sevast'ianova, L. V Epishina, *Nitration of imidazoles with various nitrating agents*. Khimiya Geterotsiklicheskikh Soedinenii 6 (1970) 503 -507.
- A.L. Okorokov, M.B. Sherman, C. Plisson, V. Grinkevich, K. Sigmundsson, G. Selivanova, J. Milner and E.V. Orlova. *The structure of p53 tumour suppressor protein reveals the basis for its functional plasticity*. EMBO J. 25 (2006) 5191–200.
- J.D. Oliner, K.W. Kinler, P.S. Meltzer, D.L. George, *Amplification of a gene encoding a p53-protein in human sarcomas*. Nature 358 (1992) 80-83.
- J. D. Oliner, J.A. Pietenpol, S. Thiagalingam, J. Gyuris, K.W. Kinzler, B. Vogelstein. *Oncoprotein MDM2 conceals the activation domain of tumour suppressor p53*. Nature 362 (1993) 857-860.

- M. Oren, *Regulation of the p53 tumor suppressor protein*. 274 (1999) 36031-36034
- D.J. Parks, L.V. LaFrance, R.R. Calvo, K.L. Milkiewicz, V. Gupta, J. Lattanze, K. Ramachandren, T.E. Carver, E.C. Petrella, M.D. Cummings, D. Maguire, B.L. Grasberger, T. Lu, *1,4-benzodiazepine-2,5-diones as small molecule antagonists of the HDM2-p53 interaction: discovery and SAR*. *Bioorg. Med. Chem. Lett.* 15 (2005) 765-770.
- D.J. Parks, L.V. LaFrance, R.R. Calvo, K.L. Milkiewicz, J.J. Marugán, P. Raboisson, C. Schubert, H.K. Koblish, S. Zhao, C.F. Franks, J. Lattanze, T.E. Carver, M.D. Cummings, D. Maguire, B.L. Grasberger, A.C. Maroney, T. Lu, *Enhanced pharmacokinetic properties of 1,4-benzodiazepine-2,5-dione antagonists of the HDM2-p53 protein-protein interaction through structure-based drug design*. *Bioorg. Med. Chem. Lett.* 16 (2006) 3310-3314.
- M.E. Perry, J. Piette, J.A. Zawadzki, D. Harvey, A.J. Levine. *The mdm-2 gene is induced in response to UV light in a p53-dependent manner*. *Proc. Natl. Acad. Sci. U.S.A.* 90 (1993) 11623-11627.
- G.M. Popowicz, A. Czarna, S. Wolf, K. Wang, W. Wang, A. Dömling and T.A. Holak, *Structures of low molecular weight inhibitors bound to MDMX and MDM2 reveal new approaches for p53-MDMX/MDM2 antagonist drug discovery*. *Cell Cycle* 9 (2010) 1-8.
- P. Raboisson, J.J. Marugán, C. Schubert, H.K. Koblish, T. Lu, S. Zhao, M.R. Player, A.C. Maroney, R.L. Reed, N.D. Huebert, J. Lattanze, D.J. Parks, M.D. Cummings, *Structure-based design, synthesis, and biological evaluation of novel 1,4-diazepines as HDM2 antagonists*. *Bioorg. Med. Chem. Lett.* 15 (2005) 1857-1861.
- G. Reissenweber *Preparation of isatoic anhydrides*. US patent 4316020 (1982).
- U. Rothweiler, A. Czarna, M. Krajewski, J. Ciombor, C. Kalinski, V. Khazak, G. Ross, N. Skobeleva, L. Weber, T.A. Holak. *Isoquinolin-1-one inhibitors of the MDM2-p53 interaction*. *Chem. Med, Chem.* 3 (2008) 1118-1128.
- S.V. Ryabukhin, A.S. Plaskon, E.N. Ostapchuk, D.M. Volochnyuk, A.A. Tolmachev, *N-Substituted Ureas and Thioureas in Biginelli Reaction Promoted by*

- Chlorotrimethylsilane: Convenient Synthesis of N1-Alkyl, N1-Aryl-, and N1,N3-Dialkyl-3,4-Dihydropyrimidin-2(1H)-(thi)ones*. *Synthesis* 3 (2007) 0417–0427.
- L.J. Saucedo, B.P. Carstens, S.E. Seavey, L.D. Albee, M.E. Perry. *Regulation of transcriptional activation of Mdm2 gene by p53 in response to UV radiation*. *Cell Growth Differ.* 9 (1998) 119-130.
- H. Schagger, G. von Jagow, *Tricine-sodium dodecyl sulfate-polyacrylamide gel electrophoresis for the separation of proteins in the range from 1 to 100 kDa*. *Anal Biochem.* 1987 166, 368-79.
- R. Stoll, C. Renner, S. Hansen, S. Palme, C. Klein, A. Belling, W. Zeslawski, M. Kamionka, T. Rehm, P. Mühlhahn, R. Schumacher, F. Hesse, B. Kaluza, W. Voelter, R.A. Engh, T.A. Holak, *Chalcone derivatives antagonize interactions between the human oncoprotein MDM2 and p53*. *Biochemistry-Us* 40 (2001) 336-344.
- O.P. Suri, N.K. Satti, K.A. Suri, *Microwave induced acetoacetylation of hetaryl and aryl amines*. *Synthetic communications* 30 (2000) 3709-3718.
- P. Di Lello, L.M. Miller Jenkins, T.N. Jones, B.D. Nguyen, T. Hara, H. Yamaguchi, J.D. Dikeakos, E. Appella, P. Legault, J.G. Omichinski. *Structure of the Tfb1/p53 Complex: Insights into the Interaction between the p62/Tfb1 Subunit of TFIIH and the Activation Domain of p53*. *Mol. Cell* 22 (2006) 731–40.
- D.P. Teufel, S.M. Freund, M. Bycroft, A.R. Fersht. *Four domains of p300 each bind tightly to a sequence spanning both transactivation subdomains of p53*. *Proc. Natl. Acad. Sci. USA* 104 (2007) 7009–14.
- C.J. Thut, J.L. Chen, R. Klemm, R. Tjian. *p53 transcriptional activation mediated by coactivators TAFII40 and TAFII60*. *Science* 267 (1995) 100–4.
- C.J. Thut, J.A. Goodrich, R. Tjian. *Repression of p53-mediated transcription by MDM2: a dual mechanism*. *Genes Dev.* 11(1997) 1974-1986.
- Vassilev LT, Vu BT, Graves B, Carvajal D, Podlaski F, Filipovic Z, Kong N, Kammlott U, Lukacs C, Klein C, Fotouhi N, Liu EA. *In Vivo Activation of the p53 Pathway by Small-Molecule Antagonists of MDM2*. *Science* 303 (2004) 844-848.

- K.H. Vousden, X. Lu, *Live or let die: the cell's response to p53*. Nature Rev. Cancer 2 (2002) 594-604.
- M. Wade, Y.V. Wang, G. M. Wahl, *The p52 orchestra: MDM2 and MDMX set the tone*. Trends Cell Biol. 20 (2010) 299
- Z. Wang. An exact mathematical expression for describing competitive binding of two different ligands to a protein molecule. Z. FEBS Lett. 360 (1995) 111-114.
- S. Wang, D. Gibson, K. Duncan, K. Bailey, M. Thomas, D. Maccallun, D. Zheleva. *Bisarylsulfonamide Compounds and Their Use in Cancer Therapy*. WO 2004/005278.
- K. Wang, K. Nguyen, Y. Huang, A. Dömling, *Cyanoacetamide Multicomponent Reaction (I): Parallel Synthesis Of Cyanoacetamides*. J. Comb. Chem. 11 (2009) 920-927.
- W. Walter, *Ueber Condensationsproducte aus aromatischen Aldehyden und Malonitril*. Chem. Ber. 34 (1902) 1302.
- J. W. Williams and J. A. Krynitsky, *Acetoacetamide*. Organic Syntheses 21 (1941) 4.
- H. Yin, G. Lee, H.S. Park, G.A. Payne, J.M. Rodriguez, S.M. Sebti, A.D. Hamilton, *Terphenyl-based helical mimetics that disrupt the p53/HDM2 interaction*. Angew. Chem. Int. Edit. 44 (2005) 2704-2707.
- S. Yu, D. Qin, S. Shangary, J. Chen, G. Wang, K. Ding, D. McEachern, S. Qiu, Z. Nikolovska-Coleska, R. Miller, S. Kang, D. Yang, S. Wang. *Potent and Orally Active Small-Molecule Inhibitors of the MDM2-p53 Interaction*. J. Med. Chem. 52 (2009) 7970-7973.
- M. Zhou, L. Gu, T. Abshire, A. Homans, A. Billett, A. Yeager, H. Findley, *Incidence and prognostic significance of MDM2 oncoprotein overexpression in relapsed childhood acute lymphoblastic leukemia*. Leukemia 14 (2000) 61-67.
- Z. Zsoldos, D. Reid, A. Simon, S.B. Sadjad and A.P. Johnson *eHiTS: A new fast, exhaustive flexible ligand docking system*. J. Mol. Graph. Model. 26 (2007) 198-212.